



**Politecnico
di Torino**

Politecnico di Torino

Master's Degree in Biomedical Engineering

A.a. 2021/2022

Graduation session July 2022

Gait analysis before and after a novel personalized system for high tibial osteotomy

statistical analysis of the entire data set and definition of
parameters for biomechanical evaluation

Relatori:

Prof. Carlo Ferraresi
Claudio Belvedere, Ph. D.
Alberto Leardini, D. Phil.

Candidato:

Pierluigi Forgione

Abstract

Numerous studies have shown that knee varus is closely linked to the incidence of arthrosis of the medial compartment of the knee, as well as causing disturbances in joint mechanics and thus in locomotion. To remedy this disorder and limit further recourse to prosthesis, one of the most promising surgical techniques is the High Tibial Osteotomy (HTO). Clinical results are encouraging, but a technique that allows accurate biomechanical evaluation is still lacking. In a recent study, an innovative approach was proposed that combines gait analysis, including Ground Reaction Force (GRF) detection, and three-dimensional morphological data obtained from a weight-bearing CBCT to obtain an estimate of the load situation on the tibial plateau. The preliminary results obtained on the first patients involved in the study were very encouraging, now, the aim of this master thesis work is to corroborate these results by analysing the aggregated pre- and post-surgery data of all 25 patients involved in the study.

The selected subjects underwent instrumental examinations to collect morphological and functional data before the surgical procedure and six months after it. For the morphological data, aimed at the evaluation of the osteoarticular anatomy in order to plan the surgery and evaluate the state of the joint, weight-bearing CBCT was used, while for the functional data, a Gait Analysis (GA) was performed using a motion-capture system with 9 video cameras, wireless EMG sensors and two force platforms. The adopted protocol includes five different motor tasks: subjects were asked to walk, sit and stand up from a chair, climb and descend stairs and perform a squat, in order to have the most varied functional data possible including more complex joint movements. To link the morphological model obtained from the CT data, we used four markers placed on the patient's knees during both the CT acquisitions and the GA, which permitted the determination of a rototranslation matrix to report the GRF data on the reconstructed tibia model.

For the data analysis, we worked in the Matlab[®] calculation environment, analysing both the functional data and the ones obtained through this new approach. For the functional data, the repeatability of both intra- and inter-patient data was analysed, and by evaluating the mean and standard deviation of the data, we obtained bands describing the trend of the variables considered during the various motor tasks, after which the pre and post data were compared. To obtain a quantitative estimate of the variation in the data between the two instants considered, the correlation coefficient between pre, post and where available normality, was calculated.

For the evaluation of the loading state of the knee joint, were studied the paths of the GRF in the plane of the tibial plateau and the percentage fraction of time in which it passes internally or externally to the plateau. Were also calculated the positions in the plane of the GRF at the instants when the peaks of the various components of the joint moment are verified in order to test the effective lateralisation of the loads.

The results obtained on the functional data showed a good repeatability and an its improvement in the post-surgery time, which indicates an increase in the control of the movement and therefore greater joint stability. The Pearson's correlation coefficients in gait (for which we have a non-pathological reference) show a substantial improvement, but generally also for the other motor tasks a variation of the patterns between pre and post is evident, which judged together the other results could be interpreted as improvement. The stress state data have confirmed the lateralisation of the loads and a reduction in the stress on the medial compartment of the tibial plateau. The fraction of the cycle percentage during which the GRF pass internally to the plateau shows a significant increase and in general the peaks of the various components are at a shorter distance from the tibial plateau.

The global data then confirm what has been seen in the previous study when the first patients reached the six-month follow-up, corroborating the goodness of the proposed approach for the evaluation of the stress state of the tibial plateau.

Abstract

Numerosi studi hanno dimostrato come il varismo di ginocchio sia fortemente legato all'insorgenza di artrosi del comparto mediale di ginocchio, oltre che causa di disturbi della meccanica articolare e quindi della locomozione. Per rimediare a questo disturbo e limitare il successivo ricorso alla protesizzazione, una delle tecniche chirurgiche più promettenti è l'osteotomia tibiale alta (HTO). I risultati clinici sono incoraggianti, ma ad oggi manca ancora una tecnica che consenta una valutazione biomeccanica accurata. In un recente studio è stato proposto un approccio innovativo che combina l'analisi di gait, completa di rilevazione della forza di reazione del suolo (GRF), e dati morfologici tridimensionali ottenuti grazie ad una CBCT in carico per ottenere una stima della situazione di carico sul piatto tibiale. I risultati preliminari ottenuti sui primi pazienti coinvolti nello studio sono stati molto incoraggianti, ora, lo scopo di questo lavoro di tesi è quello di corroborare tali risultati analizzando i dati in aggregato pre- e post-operatori di tutti e 25 i pazienti coinvolti nello studio.

I soggetti selezionati sono stati sottoposti ad esami strumentali volti a raccogliere dati morfologici e funzionali prima della procedura chirurgica e a sei mesi da essa. Per i dati morfologici, volti a valutare l'anatomia osteoarticolare con lo scopo di pianificare l'intervento e valutare lo stato dell'articolazione, si è sfruttata la CBCT in carico, mentre per quelli funzionali è stata eseguita una analisi di gait grazie ad un sistema di motion-capture che sfrutta 9 videocamere, dei sensori EMG wireless e due pedane di forza. Il protocollo adottato prevede cinque diversi compiti motori: ai soggetti è stato chiesto di camminare, sedersi e alzarsi da una sedia, salire e scendere delle scale ed eseguire uno squat, in modo da avere dati funzionali più vari che coinvolgano movimenti articolari più complessi. Per poter collegare il modello morfologico ottenuto partendo dai dati TC sono stati sfruttati 4 marker posizionati sul ginocchio del paziente sia durante le acquisizioni TC che durante l'analisi gait che hanno consentito di calcolare una matrice di rototraslazione per riportare i dati della GRF sul modello ricostruito di tibia.

Per l'analisi dei dati si è lavorato in ambiente di calcolo Matlab®, analizzando sia i dati funzionali che quelli ottenuti mediante questo nuovo approccio. Per i dati funzionali si è valutata la ripetibilità sia intra- che inter-paziente, e valutando media e deviazione standard abbiamo ottenuto delle fasce che descrivano l'andamento delle variabili considerate durante i vari compiti motori, dopodiché si è proceduto ad una comparazione tra i dati pre e post. Per avere una stima quantitativa della variazione tra i due istanti considerati si è calcolato il coefficiente di correlazione di Pearson tra pre,

post e dove disponibile normalità. Per la valutazione dello stato di carico dell'articolazione di ginocchio sono stati studiati gli andamenti della GRF nel piano del piatto tibiale e si è calcolata la frazione percentuale di tempo in cui essa passi internamente o esternamente al piatto. Sono state inoltre valutate le posizioni nel piano della GRF negli istanti in cui si verificano i picchi delle varie componenti del momento articolare per verificare l'effettiva lateralizzazione dei carichi.

I risultati ottenuti sui dati funzionali hanno mostrato una buona ripetibilità e un miglioramento della stessa nel post-operatorio, il che indica un aumento del controllo del movimento e quindi una maggior stabilità articolare. I coefficienti di correlazione nella gait (per la quale si ha un riferimento non patologico) dimostrano un sostanziale miglioramento, ma in generale anche per gli altri compiti motori è evidente una variazione dei pattern tra pre e post, che valutata nel complesso può essere interpretata come miglioramento. I dati sullo stato di sollecitazione hanno confermato la lateralizzazione dei carichi e quindi una diminuzione della sollecitazione del comparto mediale del piatto tibiale. La frazione di percentuale di ciclo durante la quale la GRF passa internamente al piatto mostra un notevole aumento e in generale i picchi delle varie componenti si attestano ad una distanza minore dal piatto tibiale.

I dati complessivi confermano quindi quanto visto nello studio precedente sui primi pazienti arrivati al follow-up a sei mesi, corroborando quindi la bontà dell'approccio proposto per la valutazione dello stato di sollecitazione del piatto tibiale.

Summary

INTRODUCTION	8
1 BASIC PRINCIPLES.....	10
1.1 Anatomical Plane.....	10
1.2 Knee anatomy.....	13
1.2.1 Articular Surfaces	13
1.2.2 Joint capsule.....	14
1.2.3 Ligaments.....	15
1.2.4 Menisci.....	17
1.2.5 Muscles and movements	17
1.3 Knee biomechanics.....	18
1.3.1 Anatomical frames	18
1.3.2 Grood and Suntay convention	21
1.3.3 Knee biomechanics	23
2 PATHOLOGY AND TREATMENTS.....	26
2.1 Degenerative pathologies	26
2.1.1 Osteoarthritis	26
2.1.2 Rheumatoid arthritis.....	26
2.1.3 Avascular necrosis.....	27
2.1.4 Post-traumatic arthritis.....	27
2.2 Varus and valgus knee.....	27
2.2.1 Biomechanical evaluations	27
2.2.2 Varus and osteoarthritis	29
2.3 Surgical treatments	31
2.3.1 TKA	31

2.3.2	UKA.....	32
2.3.3	HTO.....	33
2.4	Standard HTO	33
2.4.1	Open or closed wedge	33
2.4.2	Accuracy of 3D-planned patient specific instrumentation	35
3	GAIT ANALYSIS	36
3.1	Gait cycle	37
3.2	Variables of interest	39
3.2.1	Rotation angles	40
3.2.2	GRF	41
3.2.3	Torque	41
3.2.4	EMG signals.....	42
4	STUDY PROTOCOL.....	43
4.1	TomoFix® HTO	43
4.2	Ethical considerations	45
4.3	Obtaining participant consent.....	45
4.4	Pre-clinical trials	45
4.4.1	In silico virtual trials	46
4.5	Clinical investigation information	47
4.5.1	Outcome.....	48
4.5.2	Inclusion and exclusion criteria.....	48
4.5.3	Study population	49
5	MATERIAL AND METHOD	50
5.1	Acquisition system.....	50
5.1.1	Weight bearing CBCT	50
5.1.2	Gait laboratory and protocol	52

5.2	Data processing	60
5.2.1	Morphologic data.....	61
5.2.2	Functional data	62
5.2.3	Matching	62
5.3	TomoFix® HTO.....	63
5.3.1	Fixation plate.....	63
6	RESULTS	65
6.1	Functional data: rotations and moments.....	65
6.1.1	Repeatability	65
6.1.2	Correlations.....	93
6.2	Merging morphological and functional data: assessment of GRF in the tibial plateau plane 103	
7	DISCUSSION	115
7.1	Intra-patients repeatability	115
7.2	Inter-patients repeatability	116
7.3	Correlation.....	116
7.4	Superimposition of ground reaction force on tibial-plateau	117
8	CONCLUSIONS AND FURURE DEVELOPMENTS.....	120
	LIST OF FIGURES	123
	Bibliography	128

INTRODUCTION

The following Master's Thesis work is part of an interdisciplinary research project carried out at the Movement Analysis and Functional-Clinical Evaluation of Prostheses Laboratory of the IRCCS, Rizzoli Orthopaedic Institute, with the collaboration of the Turin Polytechnic and the University of Bath. Due to its interdisciplinary nature, the study was carried out with the collaboration of numerous professionals, such as engineers, orthopaedic surgeons, radiologists and laboratory technicians, and given the nature of clinical research, it was submitted to the ethics committee, which gave its approval, in addition to all the patients involved, whom we thank for having kindly granted permission to process and publish their clinical data, without which this research could not have taken place. We would also like to specify that all protective measures for the management of the COVID-19 emergency have been taken to ensure the health of the patients, as well as all other personnel involved.

The knee is one of the three joints of the lower limb of our body, and with hip and ankle it carries out two main tasks: providing stability and support for the body weight and permitting movement. Considering the importance of the role it plays and its complexity, its study, and therefore the understanding of its biomechanical behaviour, is of fundamental importance. Given the magnitude of the loads it has to withstand and the wide range of movement it allows, it is not surprising that the knee joint is particularly affected by numerous pathologies and injuries. One of the most common problems is knee arthrosis, or gonarthrosis, a chronic degenerative disease that affects the joint tissue, causing it to become progressively thinner, until the point of direct contact between bone components, thus causing pain and partial loss of joint mobility. Numerous studies have shown that the onset of this pathology, especially in the medial compartment, is related to an imperfect alignment of the knee axis that causes an incorrect position of the mechanical axis, varus. Varus is the orthopaedic term that refers to all those limb deformities in which, due to an abnormal relationship between two adjacent skeletal segments, the more distal of these presents a medial deviation. In the case of the knee, there is a misalignment between the axes of the femur and tibia; at a mechanical level, it causes a deviation of the load axis, that cause an over compression of the medial compartment. This overstress, in particular, seems to be the cause of the arthrosis onset. To remedy this misalignment and restore normal joint biomechanics, there are numerous surgical solutions, the most promising of which, given its low invasiveness and the high level of correction it allows, is HTO. This treatment consists of operating a wedge-shaped opening under the tibial

plateau in a medial position, hold open using a fixation plate, in order to correct its inclination and lateralise the mechanical axis. This technique requires considerable surgical precision, and to reach it, there is an increasing move towards a customised approach that employs emerging 3D technologies at all stages of the process: from planning, to surgery, to anatomical and functional assessment. This study proposes for the first time the use of a custom-made fixation plate, made by 3D Metal Printing (UK), which allows a high degree of correction and greater stability with a reduced plaque size. In the context of the pre/post-operative anatomical-functional evaluation of this study, in addition to the traditional techniques based on a parallel study of morphological and functional data (by using CT and gait analysis), an innovative method was proposed that allows an assessment of the stress state of the tibial plateau by combining these two types of information. The very promising preliminary results from the follow-up of the first four patients involved in the study resulted in the publication in 2022 of a highly successful research article 'Superimposition of ground reaction force on tibial-plateau supporting diagnostics and post-operative evaluations in high-tibial osteotomy. A novel methodology' by Ruggeri et al.

The aim of this thesis work, having reached the final stages of the study and having at our disposal the entire data set including pre- and post-operative data of the 25 patients, is therefore to extend the evaluation protocol introduced and carry out a statistical analysis of the functional data, combined with those resulting from the new proposed technique, in order to highlight the goodness of the surgical technique used in the clinical study and at the same time corroborate the results obtained in the preliminary studies using this innovative methodology.

Before evaluating the results obtained, which are reported in Chapter 6 of this paper, it was considered appropriate to recall some concepts and information useful for better understand them. To this end, a few basic concepts, such as geometric and anatomical conventions, as well as general information on the anatomy of the knee and its mechanics, were briefly outlined in Chapter 1. The second chapter summarises the main pathologies involving this joint and the surgical techniques available, with particular reference to knee varus and HTO. This is followed, in Chapters 3 and 4, by the basic principles of gait analysis and the study protocol used in the TOKA project, while Chapter 5 summarises the materials and methods used in this thesis work. Finally, in Chapter 7, some concluding considerations are given, summarising the results obtained in this work.

1 BASIC PRINCIPLES

In this chapter are reported some of the main principles to help the reader to better understand the current work and fix a few concepts concerning the anatomy of the knee and most of all its biomechanics.

1.1 Anatomical Plane

Before moving on to the description of anatomy and biomechanics of knee joint, it is helpful to define conventions regarding anatomical planes and directions used in the current work. The anatomic position is useful for establish the relationship and the movement between different segment or anatomical parts. Starting from a standard position with erect position, joined hills, arms stretched along the sides and palms facing forward, we define the following planes:

- a. Frontal plane which divides the body into anterior and posterior part
- b. Sagittal plane which divides the body into right left side
- c. Transversal plane which divides the body into upper and lower part

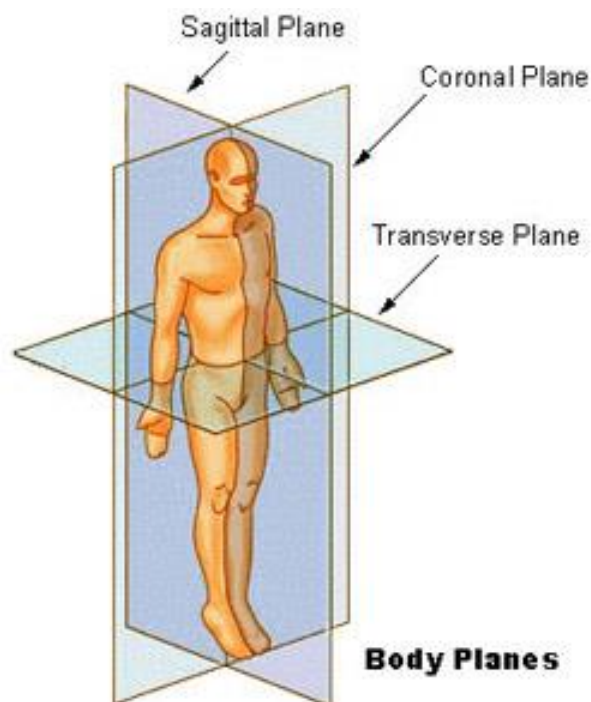


Figure 1-1: Anatomical planes of the human body[1]

and for each plane we define an axis perpendicular to it:

- a. Anteroposterior axis, perpendicular to the frontal plane
- b. Transversal axis, perpendicular to the sagittal plane
- c. Longitudinal axis, perpendicular to the transversal plane

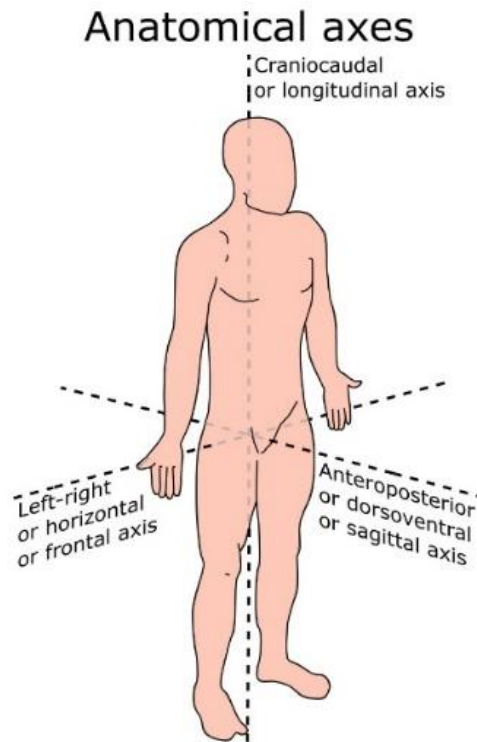


Figure 1-2: Anatomical axes of the human body[2]

In addition, we define three couple of terms to describe the relative location of different body structures:

- a. Anterior – Posterior, respectively in front and behind the frontal plane
- b. Medial – Lateral, respectively towards the center of the body or laterally
- c. Proximal – Distal, used on limbs to indicate if the point is closer or farther away from the centre of the body

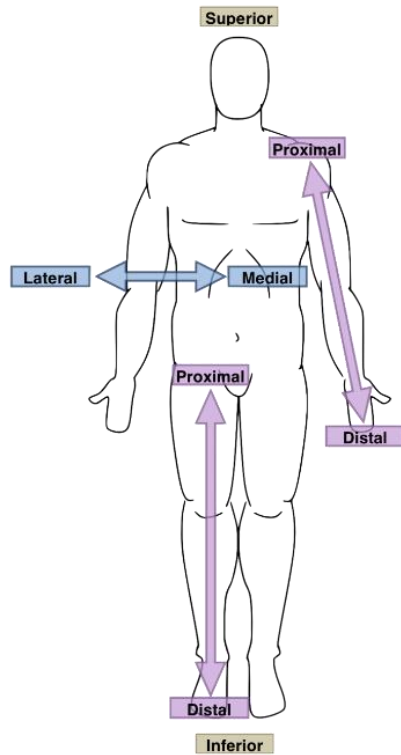


Figure 1-3: Relative location for the anatomical parts[3]

In accordance with the main theme of this thesis we can redefine a similar convention for the knee joint centering the origin of the axes in the anatomical center of the joint and redefining the directions, and therefore the rotation with respect to the knee. In the following images are shown the conventions to which we will refer in the following work

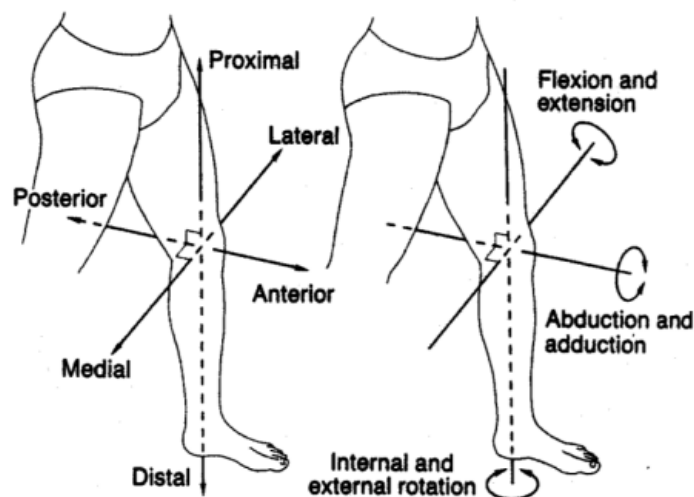


Figure 1-4: Anatomical axes of the knee and relative rotation[2]

1.2 Knee anatomy

The knee is the largest joint in the human body, it is a synovial joint that connects three bones: the femur, tibia and patella; It is a complex hinge joint composed of two articulations, the tibiofemoral joint and patellofemoral joint. The tibiofemoral joint is an articulation between the tibia and the femur, while the patellofemoral joint is an articulation between the patella and the femur. The knee is responsible for weight-bearing and movement, and evaluating the loads which it is subjected, it results one of the most stressed articular surface and for this reason is the joint most commonly affected by arthritis[4]. It requires a harmonious combination of muscles and ligaments, as well as bones, to function efficiently and maintain stability under various conditions. The ligament alone without the action of muscles cannot maintain the stability and the normal configuration of a joint for a long time[5].

1.2.1 Articular Surfaces

The knee joint consists of two articulations, tibiofemoral (TFJ) and patellofemoral (PFJ). The joint surfaces are lined with hyaline cartilage and are enclosed within a single joint cavity.

- The **tibiofemoral joint** is an articulation between the lateral and medial condyles of the distal end of the femur and the tibial plateaus, both of which are covered by a thick layer of hyaline cartilage. The lateral and medial condyles are two bony projections located at the distal end of the femur, which have a smooth convex surface, and are separated posteriorly by a deep groove known as the intercondylar fossa. The medial condyle is larger, narrower and further projected than its lateral counterpart, which accounts for the angle between the femur and the tibia. The roughened outer surfaces of the medial and lateral condyles are defined as medial and lateral epicondyles, respectively. The tibial plateaus are the two slightly concave superior surfaces of the condyles located at the proximal end of the tibia, and are separated by a bony protuberance known as the intercondylar eminence. The medial tibial articular surface is somewhat oval shaped along its anteroposterior length, while the lateral articular surface is more circular in shape

The articular surfaces of the tibiofemoral joint are generally incongruent, so compatibility is provided by the medial and lateral meniscus. These are crescent-shaped fibrocartilaginous structures that allow a more even distribution of the femoral pressure on the tibia.

- The **patellofemoral joint** is a saddle joint formed by the articulation of the patellar surface of femur (also known as the trochlear groove of femur) and the posterior surface of patella.

The patellar surface of femur is a groove on the anterior side of the distal femur, which extends posteriorly into the intercondylar fossa. The patella is a triangular shaped bone, with a curved proximal base and a pointed distal apex. Its articular surface is defined by medial and lateral facets which are concave articular surfaces covered with a thick layer of hyaline cartilage and separated by a vertical ridge. Medial to the medial facet is a third minor facet, known as the 'odd' facet which lacks hyaline cartilage. Being a sesamoid bone, the patella is tightly embedded and held in place by the tendon of the quadriceps femoris muscle. On the distal part of the patella, an extension of the quadriceps femoris tendon forms a central band called the patellar ligament. It is a strong, thick ligament that extends from the patellar apex to the superior area of the tibial tuberosity [6][7].

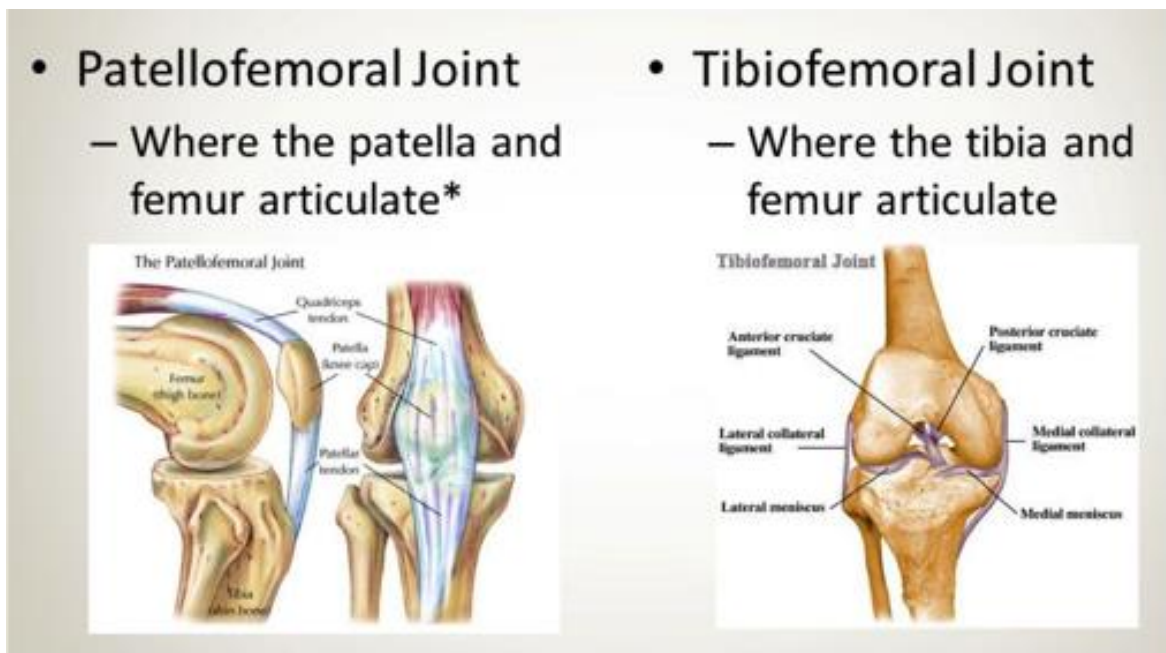


Figure 1-5: Articular Surfaces: patellofemoral (left side), tibiofemoral (right side)[8]

1.2.2 Joint capsule

The joint capsule of the knee joint is of a composite nature, mainly formed by muscle tendons and their expansions, forming a thick ligamentous sheath around the joint. The capsule is relatively weak and attached to the margins of the femoral and tibial articular surfaces. The anterior portion of the capsule features an opening, whose margins attach to the borders of the patella. A second gap is also present in the lateroposterior portion of the capsule to give passage to the tendon of the popliteus muscle. The capsule is formed from an outer fibrous layer (which is continuous with adjacent tendons) and an inner synovial membrane that lubricates the articular surfaces, reducing

friction in addition to providing nourishment to the cartilage. The joint capsule forms several fluids filled pouches called bursae, that reduce friction within the knee joint.

1.2.3 Ligaments

The ligaments of the knee joint can be divided into two groups: extracapsular ligaments and intracapsular ligaments. These ligaments connect the femur and tibia, holding them in place, providing stability, and preventing dislocation. Extracapsular ligaments are found outside the joint capsule and include the patellar ligament, fibular (lateral) and tibial (medial) collateral ligaments, and oblique and arcuate popliteal ligaments. Intracapsular ligaments are found inside the joint capsule, with the cruciate ligaments being the most well-known of this subgroup.

- The **patellar ligament** is a strong, thick fibrous band that is a distal continuation of the quadriceps femoris tendon. It is found superficial/anterior to the infrapatellar bursa and extends from the apex of patella to the tibial tuberosity. Along its outer margins, the patellar ligament blends with the medial and lateral patellar retinacula, which are extensions of the vastus medialis and lateralis muscles, respectively, as well as the overlying fascia. The patellar ligament plays a major role in stabilizing the patella and preventing its displacement.
- The **fibular collateral ligament** is a strong ligament that originates from the lateral epicondyle of the femur, just posterior to the proximal attachment of the popliteus, and extends distally to attach on the lateral surface of the fibular head. As it attaches to the fibular head, the ligament splits the tendon of biceps femoris muscle in two. The fibular collateral ligament is found deep to the lateral patellar retinaculum, and superficial to the tendon of popliteus muscle, which separates the ligament from the lateral meniscus.
- The **tibial collateral ligament** is the strong, flat ligament of the medial aspect of the knee joint. The tibial collateral ligament, in addition to its fibular counterpart, acts to secure the knee joint and prevent excessive sideways movement by restricting external and internal rotation of the extended knee. The tibial collateral ligament is sometimes divided the literature into superficial and deep parts: superficial and deep part.
- The **oblique popliteal ligament** (Bourgerie ligament) is an expansion of the semimembranosus tendon which originates posterior to the medial tibial condyle and reflects superiorly and laterally to attach on the lateral condyle of the femur. As it spans the intercondylar fossa, the oblique popliteal ligament reinforces the posterior part of the joint capsule and blends with its central portion.

- **Arcuate popliteal ligament** is a thick, fibrous band that arises on the posterior aspect of the fibular head and arches superiorly and medially to attach on the posterior side of the joint capsule of the knee. The arcuate popliteal ligament reinforces the posterolateral part of the joint capsule, and together with the oblique popliteal ligament, prevents overextension of the knee joint.
- The **cruciate ligaments** got their name due to the fact that they cross each other obliquely within the joint in a way that resembles a cross, or a letter X. They cross within the joint capsule, however remain external to the synovial cavity. The cruciate ligaments are divided as follows:
 - Anterior cruciate ligament arises from the anterior intercondylar area of the tibia just behind the attachment of the medial meniscus, and extends posterolaterally and proximally to attach on the posterior part of the medial surface of the lateral femoral condyle. As it crosses to the other side of the knee joint, the ligament passes underneath the transverse ligament and blends with the anterior horn of the lateral meniscus. The anterior cruciate ligament is important to prevent posterior rolling and displacement of the femoral condyle during flexion, as well as to prevent hyperextension of the knee joint.
 - Posterior cruciate ligament arises from the posterior intercondylar area of the tibia and extends anteromedially and proximally to attach on the anterior part of the lateral surface of the medial femoral condyle. This ligament is almost twice as strong and has better blood supply than the anterior cruciate ligament. The posterior cruciate ligament has the opposite function of the anterior cruciate ligament, serving to prevent anterior rolling and displacement of the femoral condyle during extension, as well as to prevent hyperflexion of the knee joint.

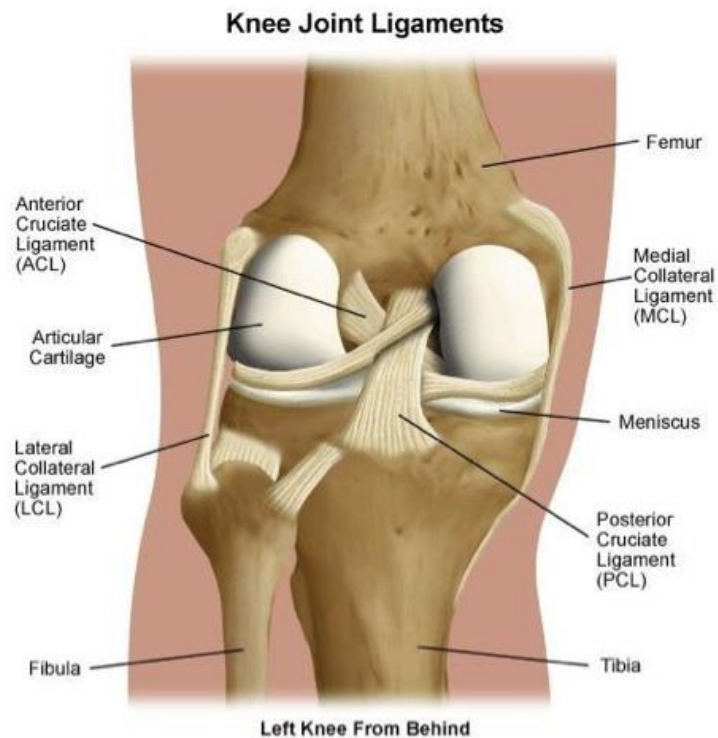


Figure 1-6: Knee ligaments [9]

1.2.4 Menisci

The menisci are fibrocartilaginous crescent-shaped plates found between the articular surfaces of the femur and tibia and serve to provide their congruence and shock absorption. The menisci are thick and vascularized in their outer one third, while their inner two thirds are thinner and avascular. Additionally, the inner two thirds contain radially organized collagen bundles, whereas the outer third contains larger circumferentially arranged bundles. Thus, it is believed that the inner portion is more adapted for weight-bearing and resisting compressive forces, while the outer portions are suited for resisting tensional forces.

1.2.5 Muscles and movements

In addition to producing motion, the muscles in the knee have the role of assisting the ligaments in stabilizing the joint, acting especially as dynamic stabilizers. The main muscles are listed below, subdivided according to the movement they perform:

- Flexion - the prime flexors of the knee joint are biceps femoris, semitendinosus and semimembranosus, whereas popliteus initiates flexion of the “locked knee” and gracilis and sartorius assist as weak flexors.

- Extension - the primary extensor of the knee joint is quadriceps femoris, assisted by the tensor fasciae latae. Quadriceps femoris of four muscle bellies: rectus femoris, vastus lateralis, vastus medialis and vastus intermedius, all innervated by the femoral nerve.
- Rotation - medial rotation occurs when the knee is in the last stage of extension, with some also occurring when the knee is flexed. It is primarily produced by the actions of popliteus, semimembranosus and semitendinosus, which are assisted by sartorius and gracilis. Lateral rotation is produced by biceps femoris and also occurs when the knee is flexed.

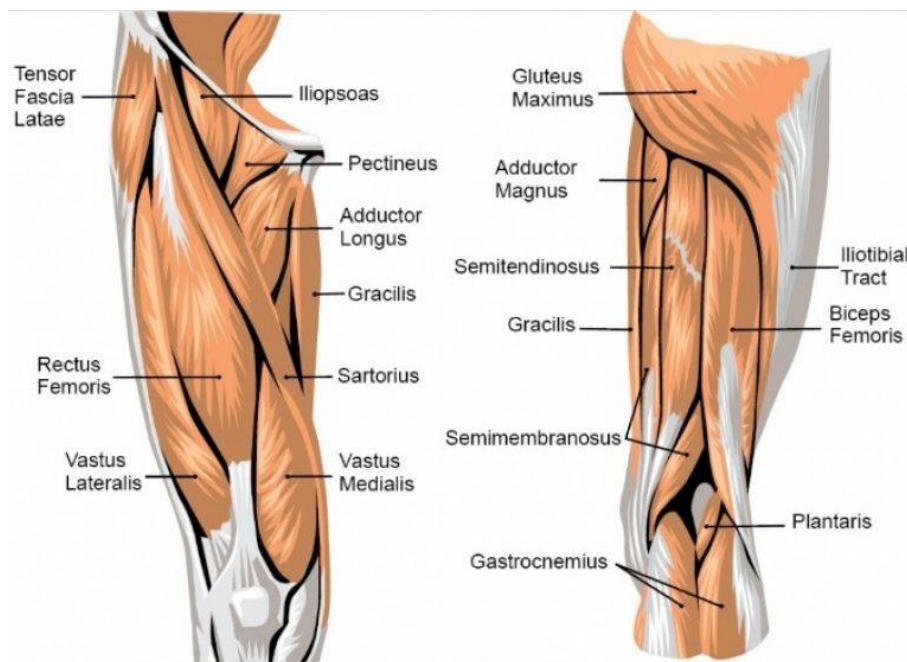


Figure 1-7: knee muscles anatomy, frontal and back view [10]

1.3 Knee biomechanics

1.3.1 Anatomical frames

For a correct biomechanical evaluation of joint movements during locomotion, it is essential to define a series of reference systems, each of which remains attached to a specific bone segment in order to evaluate relative positions and movements: a bone-embedded anatomical reference frame[11]. Once these reference systems have been defined, it will be possible to derive kinematic and dynamic parameters useful for the mechanical and clinical evaluation of the joint. Basically, this requires two sets of data:

- 1) the musculoskeletal geometry and musculotendon parameters;

- 2) the three-dimensional (3-D) instantaneous position and orientation of the bones and soft tissues, and the external forces and couples acting on the relevant body segments during the execution of the physical exercise under analysis.

The accuracy of the data will depend on the data set chosen. One of the most critical points in the procedure of defining these positions and orientations is the identification of specific landmarks (derived from the literature) which is done by palpation or derived from these and/or other measurements, for this reason it is inherently affected by skin artifacts during movement. Both positions and orientations of anatomical frames should be defined, whenever possible, using observable anatomical landmarks.

In accordance with what has been established we define the following anatomical frames:

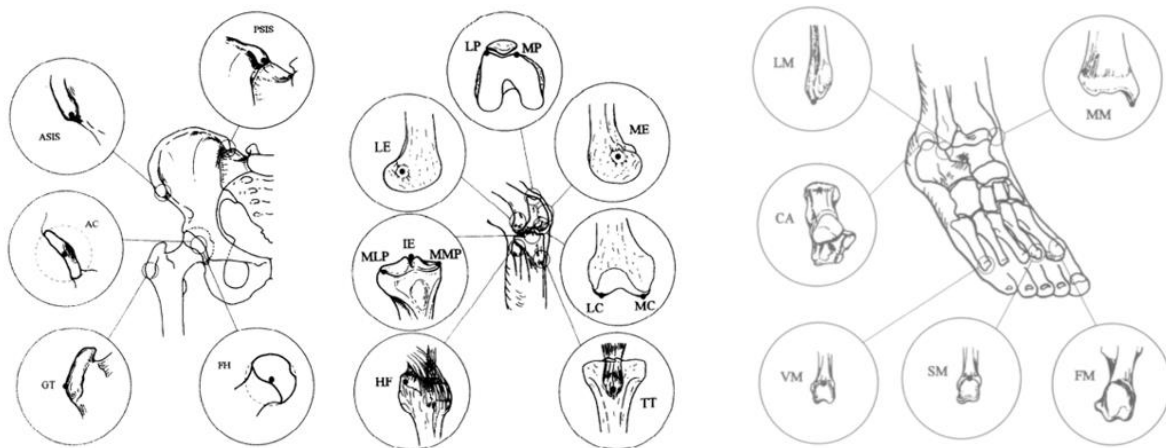


Figure 1-8: anatomical landmark in the pelvis and proximal femur (on the left), in the distal femur and proximal tibia and fibula (in the centre) and in the distal tibia and fibula, and in the foot (on the right) [11]

- **Pelvis (right and left hip bones and sacrum)**
 - O_p - The origin is in the midpoint between the anterior superior spines (right and left ASIS);
 - z_p - The z axis is oriented as the line passing through the ASISs with its positive direction from left to right;
 - x_p - The x axis lies in the quasi-transverse plane defined by the ASISs and the midpoint between the posterior superior iliac spines (right and left PSIS) and with its positive direction forwards;
 - y_p - The y axis is orthogonal to the xz plane, and its positive direction is proximal;
- Right and left thigh

- O_t - The origin is in the midpoint between the lateral and medial epicondyles (LE and ME);
- y_t - The y axis joins the origin with the centre of the femoral head (FH) and its positive direction is proximal;
- z_t - The z axis lies in the quasi frontal plane defined by the y axis and by the epicondyles with its positive direction from left to right;
- x_t - The x axis is orthogonal to the yz plane with its positive direction forwards;
- Right and left shank
 - O_s - The origin is located at the midpoint of the line joining the lower ends of the medial and lateral malleoli (MM and LM);
 - y_s - The malleoli and the head of the fibula landmarks (HF) define a plane which is quasi-frontal. A quasi-sagittal plane, orthogonal to the quasi-frontal plane, is defined by the midpoint between the malleoli and the tibial tuberosity (TT). The y axis is defined by the intersection between the above-mentioned planes with its positive direction proximal;
 - z_s - The z axis lies in the quasi-frontal plane with its positive direction from left to right;
 - x_s - The x axis is orthogonal to the yz plane with its positive direction forwards;
- Right and left foot (talus + calcaneus + cuboid + navicular + lateral, medial, intermediate cuneiform + metatarsals)
 - O_f - The origin is located at the calcaneus landmark (CA);
 - y_f - The calcaneus and the first and fifth metatarsal heads (FM and VM) define a plane which is quasi-transverse. A quasi-sagittal plane, orthogonal to this latter plane, is defined by the calcaneus landmark and the second metatarsal head (SM). The y axis is defined by the intersection of these two planes and its positive direction is proximal;
 - z_f - The z axis lies in the quasi-transverse plane and its positive direction is from left to right;
 - x_f - The x axis is orthogonal to the yz plane and its positive direction is dorsal;

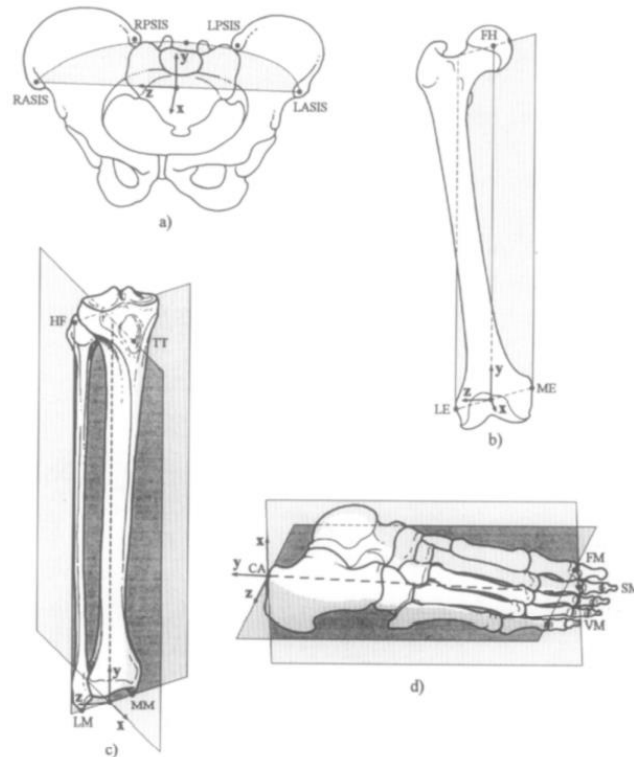


Figure 1-9: Bone embedded anatomical frames [11]

1.3.2 Grood and Suntay convention

The convention devised by Grood and Suntay represents a reference in the description of three-dimensional motion[12]. In their work, the researcher illustrated a joint coordinate model that provides a simple geometric description of rotations, translations, and motion in 3 dimensions between two rigid bodies. The motion which occurs in most anatomical joints involves three-dimensional movement which is described by six independent coordinates or degrees of freedom, three translations and three rotations. In the past Euler angles were used to describe this motion but this description is not readily understood by clinicians, the Grood and Suntay convention had, among its objectives, to describe joint motion in a way in which facilitates the communication between biomechanician and physician. The proposed approach is based on a non-orthogonal tern e_1, e_2, e_3 , through which all relative motions between the two rigid segments under consideration will be described. Two of the axes (e_1 and e_3), called body fixed axes, are embedded in the two bodies whose relative motion is to be described, the third axis (F), is the common perpendicular to the body fixed axes and, its orientation is given by the cross product of the unit base vectors which define the orientation of the fixed axes, $e_2 = e_3 \times e_1 / |e_3 \times e_1|$. We refer to the common perpendicular as the floating axis because it is not fixed in either body and moves in relation to both.

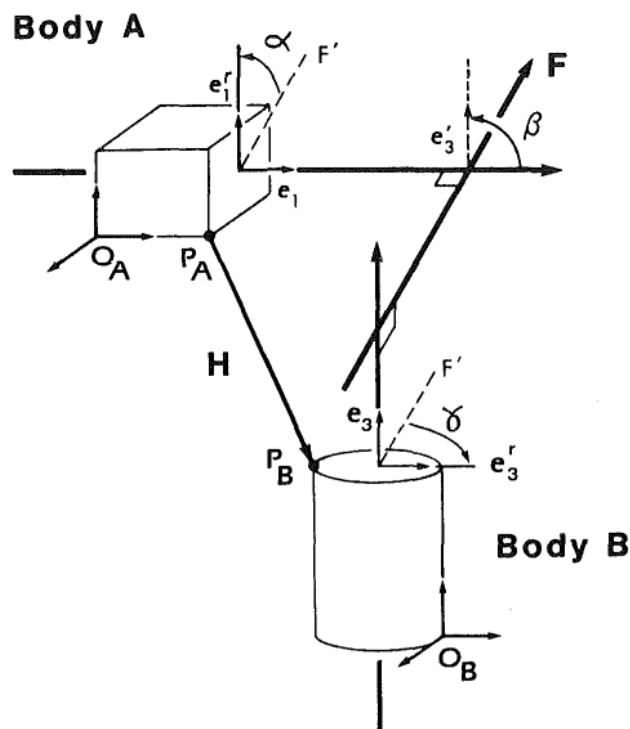


Figure 1-10: The generalized joint coordinate system composed of three axes e_1, e_2, e_3 [12]

Moving on to the specific case of the knee joint, the two segments that will be assimilated to rigid bodies are femur and tibia, and to define a coordinate system it is necessary to specify:

- The cartesian coordinate systems fixed in each bone used to describe its shape;
- The body fixed axes of the joint coordinate system (e_1 and e_3) and the reference axes of the joint coordinate system used to describe the relative motion between the two bones;
- The location of the translation reference point.

It is convenient to establish the cartesian systems located in each bone so that two of their axes correspond to the body fixed and reference axes of the joint coordinate system and to locate the origin of the cartesian system, so it is coincident with the translation reference point.

To denote the femoral cartesian coordinate system we use capital letters X, Y, Z with I, J, K as the respective base vectors, while for the tibial cartesian coordinate system we use lower case letters x, y, z with i, j, k as their respective base vectors. One clinical motion of interest is the internal-external rotation of the tibia about its mechanical axis. This axis, labelled as the z-axis in Fig. 1-11, is therefore selected as the tibial body fixed axis ($e_3 = k$). It is located so it passes midway between the two intercondylar eminences proximally and through the center of the ankle distally. In the femur, the body fixed axis is chosen so that rotations about it correspond to the clinical motion of

flexion-extension. This is accomplished by choosing the fixed axis, so it is perpendicular to the femoral sagittal plane, corresponding to the femoral Y-axis in Fig. 1-11 ($e_1 = l$). Then by construction we can get the vector e_2 (having to be orthogonal to both) around which we will have the abduction movement.

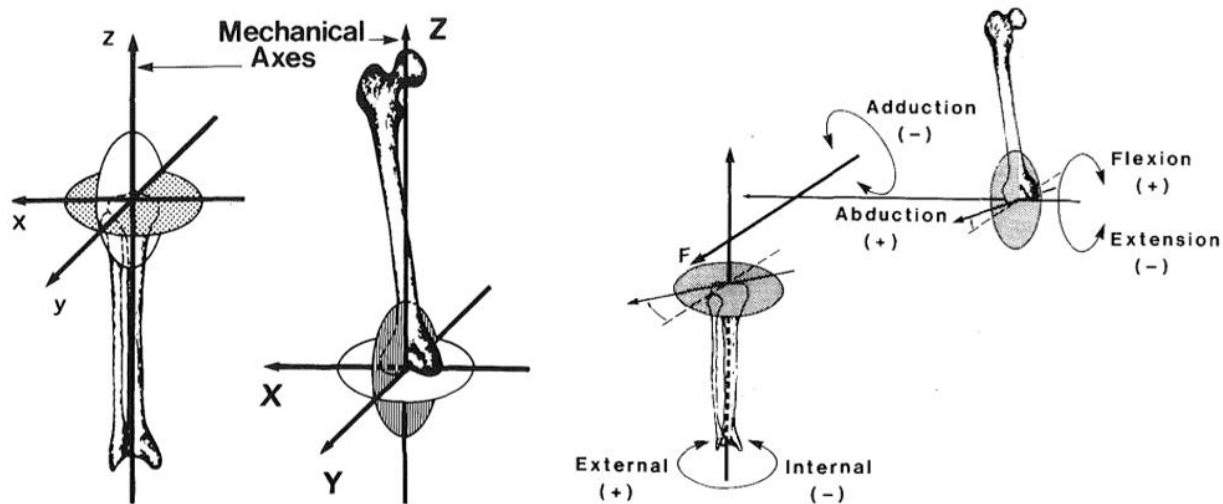


Figure 1-11: Cartesian coordinate systems defined in each bone (on the left) and joint angles defined by the rotations that occur around the three joint coordinate axes (on the right) [12]

1.3.3 Knee biomechanics

The analysis of motion applied to a joint requires the use of both kinematics and kinetics data. In biomechanics, kinematics describes the motion of multi-link systems, such as the human skeleton, without reference to the causes of motion, while kinetics is the study of the relationship between the motion of bodies and its causes, from both a static and dynamic point of view. Understanding joint kinematics is very important, in fact, it is used to make better diagnoses of some pathologies, providing a quantitative evaluation of the treatment and improve the development of prosthetic devices. The knee is one of the most complex joints of the human body, both from an anatomical and a functional point of view and the functions that characterize the biomechanics are complex, due to the necessity to simultaneously guarantee mobility and stability. The knee joint offers a wide range of motion together with high resistance to external stress, thanks to passive and active stabilizers.

- **Kinematics:** correct joint kinematics is fundamental to protect articular functionality. An alteration may change the transmission of physiological loads. Compartmental overload can be a consequence that may lead to degenerative arthrosis. In the knee the three translations

are significantly restricted by the fibrous capsule, ligaments and muscles. Instead, the rotation with the greatest range of motion is around the sagittal plane (flexion and extension), while the ab/adduction and the intra/extra rotation around the frontal and transverse are also more restricted. Flexion is the movement when the calf touches the posterior thigh, so the range of motion from full extension to full flexion is from 0 ° to 140 ° [13]. This range changes in relation to the activity. During walking, the flexion/extension ranges from 0 ° to 67 ° [14] while for climbing and descending stairs and sitting down it ranges from 0 ° to about 90 °. The mechanism of knee flexion implies a combined movement of rolling and sliding of the femoral condyles over the tibial plate. Only this combined motion, also called rollback, allows a wide rotation on the sagittal plane Fig. 1-12, and for this reason, the centre of rotation is not fixed during the flexion/extension movement, O'Connor et al. suggest that the cruciate ligaments are responsible for the translation of the instant centre of rotation. Internal rotation moves the foot inward, and external rotation moves the foot outward. The rotations occur in the transverse plane and they are influenced by the position of the joint in the sagittal plane, this phenomenon is called 'screwhome' and rotation depends on the degree of flexion. Joint flexion is also associated with motion in the frontal plane, known as abduction and adduction. These movements are passive and increase with knee flexion upto 30 °. Normally they involve only a few degrees, because the surrounding soft tissue limits excessive motion.

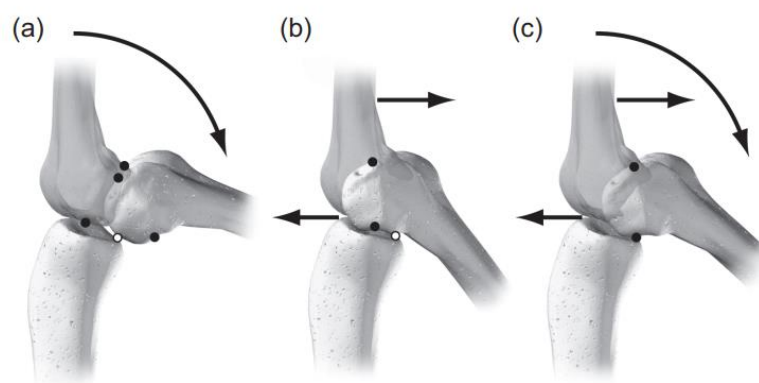


Figure 1-12: mechanism of knee flexion (a) rolling, (b) sliding, and (c) rolling and sliding of the femoral condyles over the tibial plate.

- **Statics:** static analysis is used to determine forces and moments acting on a joint when there is no motion. A simplified technique for this analysis considers a free body diagram, limiting the study to only one plane and the main forces and moments acting on the joint.

- **Dynamics:** dynamic analyses are very useful because most of our activities are generally of a dynamic nature rather than static. The dynamic study is similar to the static one, considering the same main forces produced for example by: body weight, muscles, soft tissues and applied loads. Two additional factors are required: the acceleration and the inertial body mass of the body part in question, in particular, body part acceleration involves a change in joint angle.

2 PATHOLOGY AND TREATMENTS

The knee joint, also because of the heavy loads to which it is subjected, encounters many degenerative and or traumatic pathologies. In this chapter we will look at some general aspects of the pathologies affecting this joint, in particular the joint degeneration caused by knee varus and the related treatments.

2.1 Degenerative pathologies

A prolonged lack or imbalance in muscle forces or joint congruence can result in damaging or degenerative situations for the anatomical structures of the knee. The smooth, protective layer of cartilage that covers the bones at the points of contact can eventually wear away, resulting in increased damage to the underlying bone. This can cause pain, swelling and stiffness, decreasing the function of the joint.

2.1.1 Osteoarthritis

Osteoarthritis (OA) is a painful chronic joint disease. It affects the whole joint and in particular the articular cartilage. It is generally associated with decreasing mobility, pain, instability and abnormal interaction between bone, ligaments and muscles. It is also related to the development of osteophytes, synovial inflammation, subchondral bone changes and meniscal damage [15]. It is caused by wear phenomena and is the most common reason individuals need to undergo knee replacement surgery. This condition may be due to an old injury or infection in the knee joint but mostly there are no obvious causes. It results from a complex interplay of genetic, metabolic, biomechanical and biochemical factors [15]. This results in narrowing of the joint space, with the development of cysts and erosions in the bone ends. As a result, bone comes directly into contact with bone, which is painful. All of these changes ultimately lead to increasing pain and stiffness in the joint.

2.1.2 Rheumatoid arthritis

Rheumatoid arthritis (RA) involves deterioration of cartilage and other parts of the joint, and results in the need for knee joint replacement. It is one of the inflammatory types of arthritis which affects the tissue surrounding the joints. It can also affect other organs. The cause of RA is unknown. It is an auto-immune disease that can occur at any age and affects women more often than men.

2.1.3 Avascular necrosis

Avascular necrosis (AVN) is defined as cellular death of bone due to an inadequate blood supply inside the joint. As a result, articular cartilage wears away. The bone structures risk collapse and destruction, with consequent pain and loss of joint function. Normally, AVN involves the epiphysis of the long bone as femoral and humeral heads or femoral condyles. The process is progressive, leading to joint destruction in about 5 years. The eventual solution is joint replacement.

2.1.4 Post-traumatic arthritis

Post-traumatic arthritis is a joint disease following an injury to the joint cartilage or through damage to the ligaments leading to an unstable knee. It is a particular problem in young, active patients. In general, any abnormalities causing excessive wear within the joint (from fractures of the knee, torn cartilage and torn ligaments) can lead to degeneration long after the original injury. The final solution is a knee replacement.

2.2 Varus and valgus knee

Perfect alignment between the two main bony segments of the lower limb is essential for proper distribution of the loads the joint must cope with. When this alignment undergoes changes due to congenital problems, traumatic events, incorrect posture or other, two main anatomical morphological conditions may occur: knee varus or valgus. We speak of misalignment of the knee in valgus, or knock knee, when morphologically the knees, in upright position, are in contact while the feet are at a significant distance, in varus, or bow-legged, when the knees remain distant even when the feet are side by side.

2.2.1 Biomechanical evaluations

From a biomechanical point of view, both anatomical conditions cause a misalignment of the load axes in addition to the anatomical ones, leading to their incorrect distribution at the joint level, which in some cases, as we will see later, can lead to the onset of arthrosis problems. In a normal anatomic condition, the mechanical axis of the entire leg, defined as the axis intersecting the center of the femoral head and the center of the tibiotalar joint, passes approximately through the center of the tibial plateau, resulting in adequate load distribution across the entire joint surface. In a normal anatomic condition, the mechanical axis of the entire leg, defined as the axis intersecting the center of the femoral head and the center of the tibiotalar joint, passes approximately through the center of the tibial plateau, resulting in adequate load distribution across the entire joint surface Fig. 2-1.



Figure 2-1: mechanical axis on a full-length, standing anteroposterior radiograph [16]

On the other hand, going to analyse altered anatomical situations in one of the two seen conformations, we can notice how the mechanical axis of the leg is displaced. In particular, analysing the case of valgus knee, we can see how the mechanical axis is lateralized, while in the case of varus it undergoes a medialization.

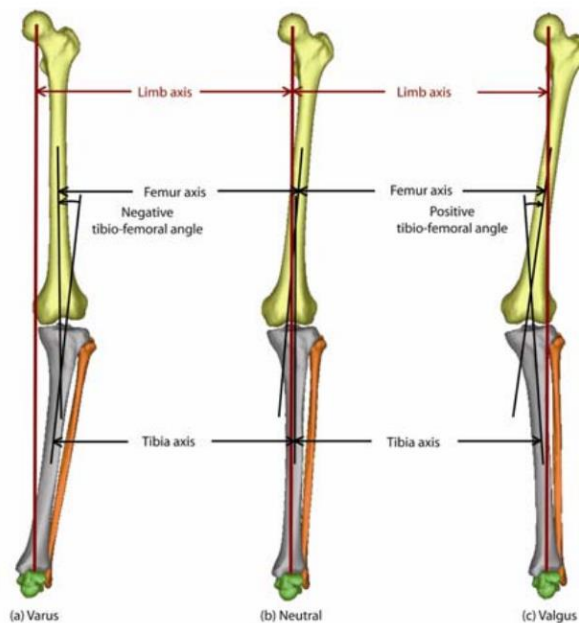


Figure 2-2: Illustrations of (a) varus, (b) neutral, and (c) valgus alignments [17]

Traditionally, radiographic images of the entire lower limb in frontal view are used to evaluate the possible presence of these anatomical disorders and at the same time verify the degree of deformity. In addition to evaluating the point of intersection of the mechanical axis with the frontal section of the tibial plateau, also in order to provide a measure of any deformity that can be easily understood and extrapolated, the anatomical and mechanical axes of the femur and tibia are defined. The mechanical axis for each segment corresponds to the diaphyseal axis: for the femur it

passes through the diaphysis and the center of the intercondylar fossa of the distal epiphysis (red line in the femur in Fig. 2-3), while for the tibia it crosses the diaphysis and connects the spine of the tibial plateau with the center of the tibiotalar joint (red line in the tibia in Fig. 2-3). Between the mechanical axis of the lower limb and the anatomical axis of the femur, even in a non-pathological condition, there is an angle of about 5° - 7° [18]. Therefore, it is possible to define an angle between the anatomical axes that intersect in the knee joint and from the value of this angle it is possible to evaluate the degree of deformity as well as calculate the angle of correction necessary as we will see in the chapter dedicated to the surgical technique of knee varus correction.



Figure 2-3: anatomical and mechanical axis [18]

2.2.2 Varus and osteoarthritis

As anticipated in the previous section, both anatomical conditions cause improper load distribution in the tibial plateau by increasing loads on the medial (in the case of varus) or lateral (in the case of valgus) compartment of the tibial plateau. Alignment of the mechanical axis has been associated with the progression of osteoarthritic pathology [17]. A kind of loop is observed to be triggered between the mechanical-anatomical disorder and arthrosis: in a nonpathological situation of the knee joint, the distance between the femur and tibia bone segments in the medial and lateral sectors is almost comparable, but damage to the tibial plateau joint leads to mechanical disturbance

in the joint and thus to an incorrect loading situation, which in turn goes to increase joint damage and thus to reduce joint spacing.

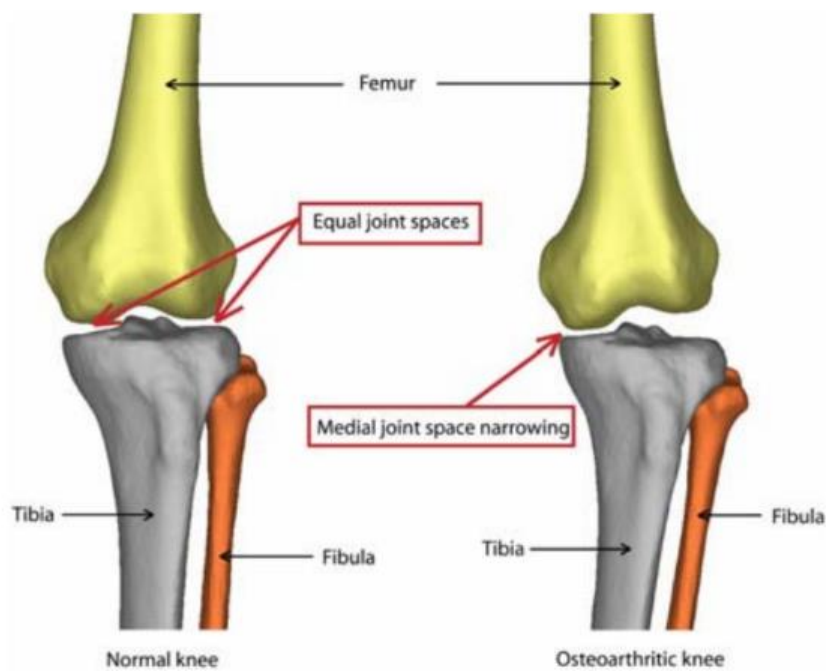


Figure 2-4: illustration of normal and osteoarthritic knee joint [17]

In engineering terms, joint damage can be considered as progressive failure, precisely because of this self-feeding mechanism between joint thinning and misalignment. This issue, in addition to a possible genetic condition is possible to be triggered by numerous factors, such as obesity, physical activity, incorrect posture or traumatic event that generates a greater than normal initial stress situation in a joint compartment. To corroborate this link between mechanical and pathological knee condition, numerous studies have been conducted on load distribution in pathological and non-pathological knees. Thus, numerous cadaver simulations have been performed by examining the three conformations, varus, valgus, and normal. The higher incidence of this pathology on the medial compartment of the joint suggested how the two anatomical conditions did not have the same weight and influence on the occurrence of osteoarthritis. These considerations led a group of researchers to conduct a large study of a statistically relevant sample of participants [19]. Indeed, 1752 participants (2958 knees) who did not have osteoarthritis in the early stage were involved in the study. Among them, the three control groups were defined according to the alignment assessed by tibiofemoral radiography: neutral, varus, and valgus. From a 30-month follow-up, it was possible to confirm that varus, but not valgus, is associated with osteoarthritis, confirming that varus alignment is associated with the onset and progress of joint pathology leading to progressive

deterioration of the medial knee joint compartment. In light of these results, some surgical techniques have been proposed and implemented in recent years that permit intervention in the preliminary stages of the disease, allowing to delay, or in some cases even avoid, the need for joint replacement surgery. Among those proposed, as we will see in the following paragraphs, the high tibial osteotomy (HTO) is of particular importance, it is a surgical technique that allows to completely safeguard the articular surfaces by intervening on the joint alignment and not directly on the knee joint.

2.3 Surgical treatments

In this section we are going to analyse what are the main surgical treatments that are resorted to in cases of knee osteoarthritis. It should be noted that these techniques, which differ greatly in invasiveness, level of prosthesis and recovery time, are not alternatives, the choice depending on several criteria such as: degree of pathology, age of the patient, level of mobility required and state of the joint compartment. We therefore report on the different procedures from the most invasive to the most conservative.

2.3.1 TKA

Total knee arthroplasty (TKA), also known as total knee replacement, is one of the most commonly performed orthopedic procedures. As of 2010, over 600,000 TKAs were being performed annually in the United States and were increasingly common [20]. It is the least conservative and most invasive surgical technique for the treatment of knee arthrosis, TKA consists of resection of the diseased articular surfaces of the knee, followed by resurfacing with metal and polyethylene prosthetic components. For the properly selected patient, the procedure results in significant pain relief, as well as improved function and quality of life. In spite of the potential benefits of TKA, precisely because of its invasiveness, TKA is usually performed on an elective basis and should only be considered after exhaustion of appropriate nonsurgical therapies and extensive discussion of the risks, benefits, and alternatives. This is the technique of choice for patients with a largely and extensively deteriorated joint condition, as well as for patients requiring revision prostheses due to the failure of a previously installed prosthesis [21].

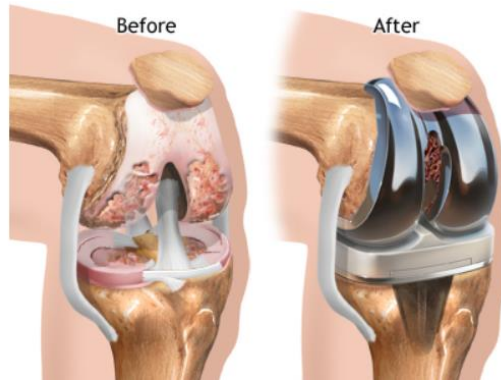


Figure 2-5: Total Knee Arthroplasty before and after surgery [22]

2.3.2 UKA

In the case of patients with joint pathology localised to a specific compartment, it is preferable to operate on that compartment and preserve the remaining joint surfaces as much as possible, which allows for a good recovery but with a much reduced bone resection and reduced surgical access, which leads to a faster recovery and less stress on the bone-articular segments. The use of conservative surgical techniques is particularly important in the case of young and/or active individuals who require extensive mobility. Another fundamental aspect to be taken into account is the durability of the prosthesis, as well as of the implantation zone: operating on increasingly younger patients has seen a progressive and substantial increase in the need for subsequent operations for the installation of revision prostheses, which naturally affect a larger joint section than that of the preliminary prosthesis, so the use of monocompartmental prostheses delays, and in some cases avoids, more invasive prostheses. This treatment can affect any of the articular sectors of the knee, medial compartment, lateral compartment, or patella, but also in light of what has been said previously about the greater incidence of arthrosis on the medial compartment and the link it has with a disturbance in joint kinematics due to misalignment, its replacement is the most frequent [21].



Figure 2-6: Unicompartmental knee arthroplasty (UKA) [23]

2.3.3 HTO

Let us now look at what is by nature the most conservative surgical technique, as it totally preserves the patient's articular surfaces, the high tibial osteotomy (HTO). This is the technique of choice for the correction of the mechanical axis, which allows a restoration of the correct relative position of the articular surfaces and thus an appropriate redistribution of loads, thus making it possible to halt or at least delay the course of knee arthritis. This procedure, in addition to its effect in the short term, thus has the objective of delaying and/or avoiding the need for an actual prosthetic joint operation, acting in a preliminary phase of the pathology and blocking its course. As this thesis work is based on the mechanic-functional evaluation of a series of subjects undergoing such surgical treatment, it is deemed appropriate to devote the entire next section to it, in order to better assess its characteristics.

2.4 Standard HTO

Osteoarthritis of the knee, as of other joints, is almost certainly attributable to mechanical events. For example, a rise in the contact pressures applied to articular cartilage produced by meniscectomy or the malunion of tibial to femoral surface may give rise to osteoarthritis in the presumably overloaded compartment, but not initially elsewhere in the knee. The initial change affect the cartilage, and it is at least probable that fragmentation of the collagen fibre network, cause by fatigue failure in the face of raised contact stresses, is the fundamental event [24]. The aim of the high tibial osteotomy is precisely to intervene on the mechanics of the knee, producing a realignment of the load axis so as to restore the joint to an adequate stress condition. For this reason, it is the technique of choice in the treatment of pathology in its preliminary stage, especially in young subjects with an active lifestyle and therefore unsuitable for prosthesis. The basis of realignment osteotomy about the knee is to transfer weightbearing forces from the arthritic area of the knee to a healthier location. The goal of osteotomy include pain relief, functional improvement, and ability to meet heavy functional demands otherwise precluded by prosthetic replacement.

2.4.1 Open or closed wedge

There are two main approaches to osteotomy: the closed wedge osteotomy and the open wedge osteotomy, let us now look at the main features of both surgical methods.

- Lateral closing wedge osteotomy is the historic approach and is more familiar to some surgeons. The advantages are greater potential of correction, no need for bone grafting, and faster healing. Disadvantages are concomitant fibular osteotomy or release of the proximal

tibiofibular joint, risk of peroneal nerve injury (occurs in 3.3-11.9%), the need for two bone cuts, ability of malalignment correction in only one plane (frontal), shortening of the leg, loss of bone stock, and more difficult conversion to arthroplasty with muscle detachment [25].

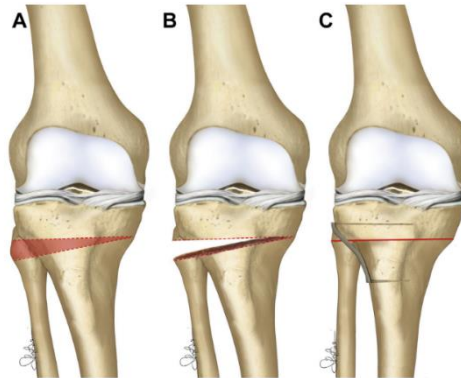


Figure 2-7: LCWO. (A) Varus knee with bony cuts highlighted. (B) Removal of bony wedge from tibia and fibula. (C) Closing the gap and fixation [26]

- Medial open wedge osteotomy has been more popular recently. The advantages are the ability to correct the alignment in two planes (coronal and sagittal), no need for fibular osteotomy, little risk of peroneal nerve injury, no limb shortening, use of a single cut with no need to detach the muscles, no bone loss, easier conversion to arthroplasty, and ability to adjust the amount of correction during surgery. Disadvantages are the need for bone graft, and the risk of delayed union or non-union [25].

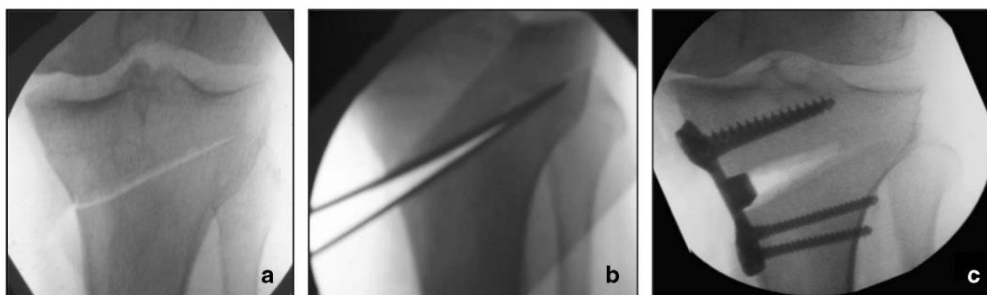


Figure 2-8: (a) osteotomy saw cut. (b) progressive wedge opening to the final plate size. (c) final intra-operative fluoroscopic imaging of the definitive plate [27]

In this master thesis work, we are going to make analytical evaluations of pre- and post-surgery data for a medial open wedge HTO operation, in which a custom-made fixation plate was used for the first time, which we will discuss in a separate section in the chapter on materials and methods. In the following paragraph, however, we want to highlight the importance and contribution of the custom approach and the use of 3D technologies from preoperative assessments to planning to surgical instrumentation.

2.4.2 Accuracy of 3D-planned patient specific instrumentation

One of the leading principles in HTO is to perform axis correction as precisely as possible because under- or over-correction is known to be the main reason for clinical failure [28]. Another challenge in HTO is the maintenance of the posterior tibial slope (PTS), wherefore a meta-analysis by Nha et al. [29] showed an increase of PTS in medial open wedge HTO of 2.0°, possibly caused by incomplete posterior corticotomy or due to a too anterior position of the fixation plate. However, unintended slope changes can result in anteroposterior knee instability and increased stress on the cruciate ligaments. Planning of HTO in the conventional way is based on standing radiographs. However, the surgical execution can be challenging without surgical navigation. It has already been shown that the use of patient specific instruments (PSI) improves precision of the reduction task in osteotomies in different orthopedic regions. In a 2020 study by Sandro F. Fucentese et al. 23 patients were considered to assess the accuracy of the correction angle as well as the change in postoperative PTS, concluding that the use of PSI (such as cutting guides and guides for predefined screw holes), combined with an accurate preoperative assessment and planning using 3D models results in accurate correction of mechanical leg axis. In contrast to the known problem of unintended PTS changes in conventional HTO, just slight changes of PTS could be observed using PSI. The use of PSI in HTO might be preferable to obtain desired correction of angle and to maintain PTS [30]

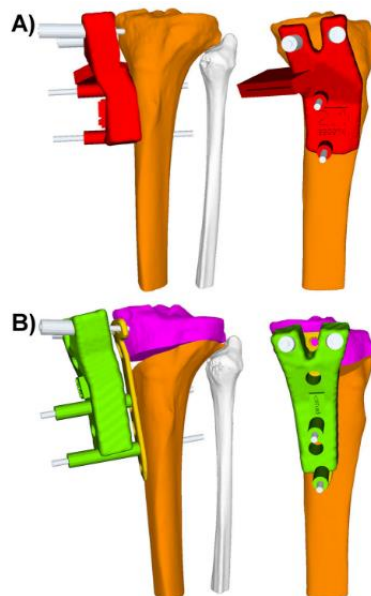


Figure 2-9: (A) cutting-guide with the slot for the saw. (B) post-reduction guide with pre-defined drill holes [30]

3 GAIT ANALYSIS

Instrumented 3D-gait analysis (3D-GA) is an important method used to obtain information that is crucial for establishing the level of functional limitation due to pathology, observing its evolution over time and evaluating rehabilitative intervention effects [31]. This technique exploits the movement tracking a set of markers that are placed on the patient's skin at specific anatomical points (defined through a specific procedure) to reconstruct the patient's movement and extrapolate a large amount of data, the interpretation of which allows the functional mechanics and the main stresses at the joint level to be assessed. It is a technique that allows the assessment of osteo-articular kinematics and dynamics in a non-invasive manner. This analysis is based on the correspondence on particular anatomical point identifiable on the skin with specific point on the skeleton, tracking the movement of the marker with a stereophotogrammetric system, the software reconstructs the motion of the bone segment and calculate the reciprocal movement and other parameters of interest in the cartilage.

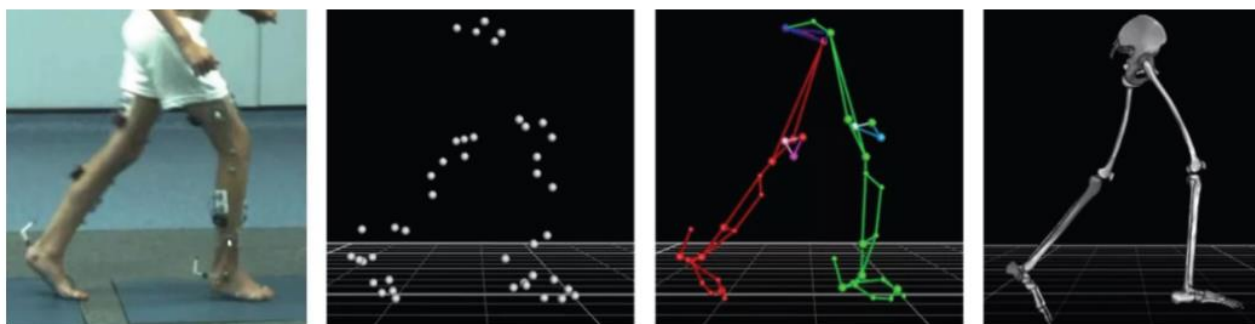


Figure 3-1: Basic scheme of the gait analysis technology, from the marker to the skeleton [32]

In addition to the stereophotogrammetric system, gait analysis takes advantage of the use of dynamometric platforms placed under the floor so as to detect the ground constraining reaction force, from which, by cross-referencing the data with instantaneous positions, information is obtained on the applied forces and the respective moments that are created for each of the three main joints involved in gait, namely hip, knee and ankle. To complement the dynamic and kinematic data with what is the muscle work and to have a functional and clinical assessment of the activity of each muscle during a specific motor task, the patient can be further instrumented with surface electromyographic sensors that go to sampling the biopotential corresponding to the activity of each of the main muscles of the lower limb. We will postpone to a specific section the description

of the acquisition systems and a more accurate description of what are the output data of the walk analysis.

3.1 Gait cycle

The study of walking is based on defining and then surveying specific events of the walking cycle, so as to standardize this activity and be able to analyse event after event what is the dynamic and kinematic evolution. For this purpose we report what are the events that mark the various phases of walking.

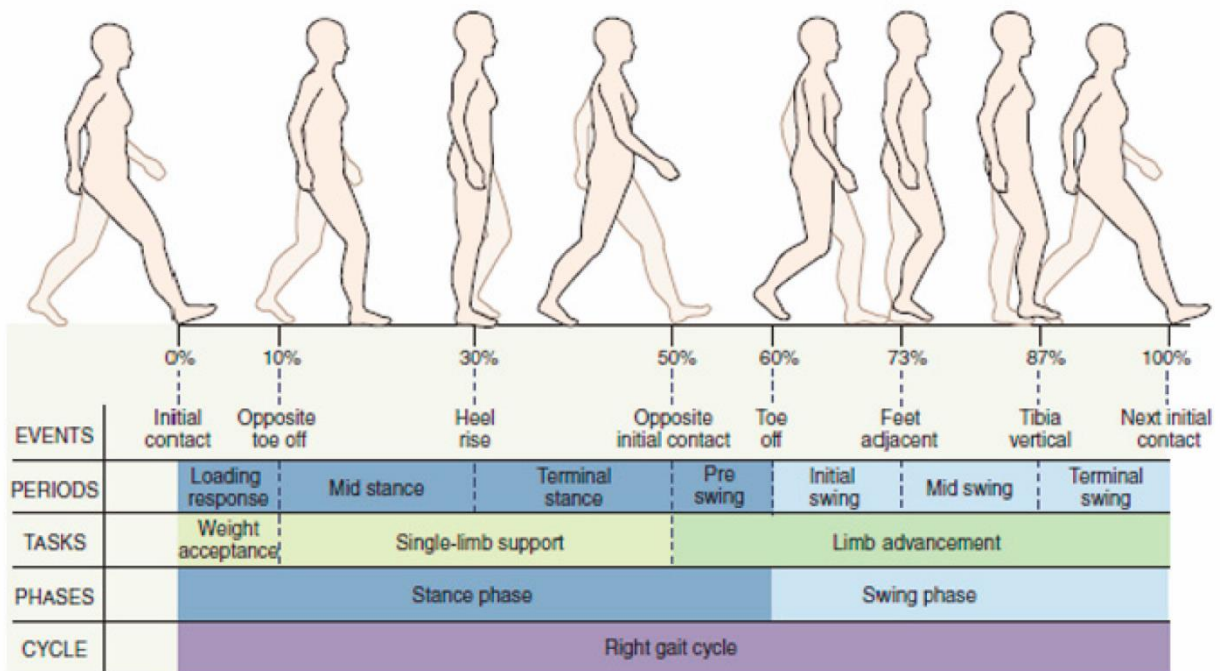


Figure 3-2: main events and periods of gait cycle [33]

For each foot we can identify two main phases during the cycle: a stance phase, 60% of the cycle, which usually begins with the heel contact with the ground and ends with the toes coming off it, and the swing phase, 40% of the cycle, during which there is no foot-ground contact. As can be seen from the diagram these two phases follow one another on the same foot but there is partial overlap of the stance phase during normal walking, there is in fact a bipodal stance phase. Looking at the position of the contralateral limb, we can identify three tasks:

- **Weight acceptance:** covers approximately 10% of the cycle and goes from the initial contact to the toe off the opposite foot; in this phase, both feet are in contact with the ground and the load progressively shifts from one foot to the other.

- **Single-limb support:** covers approximately 40% of the cycle and goes from the opposite toe off to the opposite initial contact; during this phase all the load is concentrated on one foot, we speak of monopodal support.
- **Limb advancement:** covers approximately 50% of the cycle and goes from the opposite initial contact to the next initial contact.

This percentage are referred to a normal gait, if we increment the speed, we have a reduction of the double contact time, and increase the speed again we have a fly period without any contact, but for the purpose of this analysis we can refer to a normal gait cycle.

Finally, it is possible to define even more specific periods of the cycle marked by the events that are identified:

- Initial contact (0%) – Opposite toe off (10%) → **Loading response:** during this phase, we have the task of weight acceptance, the body weight is transferred onto the forward limb. The knee is flexed for shock absorption and the sole is completely in contact with the ground.
- Opposite toe off (10%) – Heel rise (30%) → **Mid Stance:** this is the first part of the single-limb support period. The contralateral foot is in the swing period and overcomes the support foot. The centre of gravity reaches his highest point through leg extension. In the ground reaction force diagram, the end of this phase is represented by the minimum of its vertical component.
- Heel rise (30%) – Opposite initial contact (50%) → **Terminal Stance:** this is the second part of the single-limb support period. The heel loses contact with the ground and starts the propulsion phase. The knee increases in extension and begins to flex slightly. This phase ends with the heel strike of the contralateral foot.
- Opposite initial contact (50%) – Toe off (60%) → **Pre Swing:** It is the terminal double-limb support period and the second loading period. In the vertical component of the ground reaction force, the second loading peak occurs as we prepare to propel our foot off the ground.
- Toe off (60%) – Feet adjacent (73%) → **Initial Swing:** this is the first part of the swing period. The flexors muscles are activated thus there is a decrease of the leg's moment of inertia and an increase in the angular velocity.

- Feet adjacent (73%) – Tibia vertical (87%) → **Mid Swing**: it is the second part of the swing phase. Advancement of the limb anterior to the body line is gained by further hip flexion. The subject is getting ready for the upcoming foot contact.
- Tibia vertical (87%) – Next initial contact (100%) → **Terminal Swing**: this is the last part of the swing period and the main concern is the upcoming foot contact [34].

In the walk cycle, we can also define a series of geometric and morphological parameters useful for its evaluation:

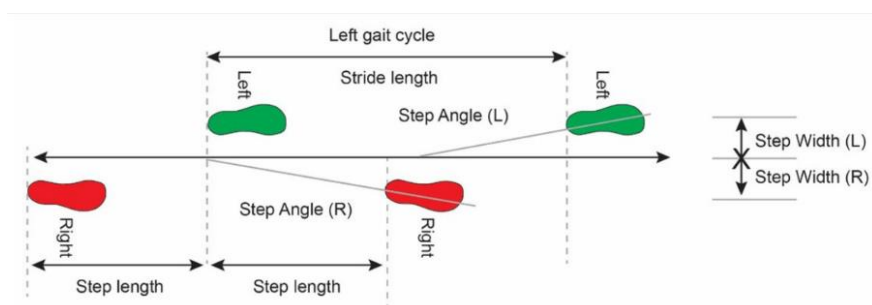


Figure 3-3: geometrical parameters of the gait cycle [35]

- The **stride length**, which is the distance between two successive impressions of the same foot (naturally, the measurement should be taken at the same point of the impression, such as at the heel).
- **Step length**, is the measure of the space from the beginning of the impression of one foot to the beginning of that of the next foot. Therefore, the sum of right and left step length gives the stride length.
- **Step angle**, is the angle in degrees between the direction of progression and a reference line on the sole of the foot. [35]

3.2 Variables of interest

The output of gait analysis is a large amount of data, which makes the technique a source of a great deal of information on the functional status of the locomotor system and in particular on joint mobility and muscle activity. Naturally, these parameters, which will also be evaluated for the purposes of the current thesis work, although they refer to the three main joints of the lower limb, come from data that can be acquired in stereophotogrammetry and with other external instrumentation, and processed by means of the anatomical-functional conventions seen in the first chapter, such as the Grood and Suntay convention, as well as from anatomical models of the osteoarticular apparatus. It would be unthinkable to acquire dynamic and kinematic data directly at

the joint level in vivo as it would require instrumentation of the joint as well as the bone segments involved with markers and strain gauge sensors, which would be totally unjustifiable for the purposes for their invasiveness. Therefore, in evaluating the data that we will see in the chapter on results, we must take into account the limitations of the accuracy of these data due to the acquisition method, although this does not detract from their validity and reliability in anatomical and functional evaluations, as well as their application for clinical purposes, which has been amply demonstrated by countless works and which have made them one of the techniques of choice to date, with a vast field of application ranging from research in the orthotic/prosthetic field, to the clinic, to orthopaedic surgery.

3.2.1 Rotation angles

The first variable of interest provided by gait analysis is joint rotation, or rather, the reciprocal rotation of the main bony segments of the lower limb at the joints, which from a mechanical point of view are similar to moveable joints. In accordance with the conventions seen on anatomical planes and joint movements, for each of the three joints under examination (hip, knee and ankle) we will have a measure of rotation for each of the three anatomical planes (antero-posterior, medio-lateral and proximal-distal) during the entire gait cycle. Of course, this will not be point data, but we will have graphs describing the trend over the period-cycle. Since we are dealing with rotations rather than planes, it is useful to refer to the rotational movement that occurs in the respective anatomical plane, we will therefore have:

- **Flex-Extension:** the rotation that occurs in the sagittal plane, around the mid-lateral axis; with reference to gait analysis, but also extending to the other motor tasks we will discuss, it is limb rotation with the largest dynamics and its variation produce a great alteration of the normal deambulation;
- **Abd-Adduction:** rotation that occurs in the frontal plane, around the antero-posterior;
- **Int-External:** is the rotation which is in the trasversal plane, around the prox-distal axis;

The evaluation of rotation angles and their dynamics during the gait cycle provides an overview of the correctness of the movement of the various segments during gait and joint mobility, thus allowing an assessment of the state of the joint surfaces, as well as the mechanics. An alteration in range of motion, or any alteration at all, as well as incorrect gait, may indicate the presence of joint mechanics disorders such as varus or valgus, or arthrotic pathology.

For an evaluation of the loads and stresses to which the joint is subjected, one goes instead to assess the ground reaction force (GRF) and the mechanical moments it causes in the hip, knee and ankle.

3.2.2 GRF

The ground reaction force (GRF) is technically the only force that acts on the lower limbs and therefore stresses the joints during walking. It is the force due to the floor in opposition to the weight force. It is also the only measure of force that can be acquired non-invasively, thanks to the use of force platforms placed in the floor. It is a vector with origin in the centre of pressure (COP) that varies its direction in an antero-posterior and medio-lateral direction, as well as its intensity, during the stance phase.

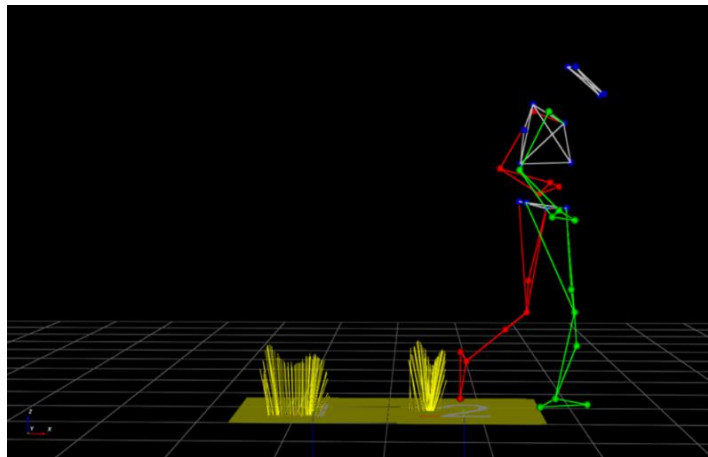


Figure 3-4: plot of the GRF during gait analysis [36]

The study of GRF is fundamental for assessing joint stress, in fact there is evidence that each degree of tibiofemoral malalignment results in a 51 N increase in medial compartment contact force during walking [37] and for this reason in the case of subjects with malformations in varus the GRF plays a fundamental role in a stress analysis. As already mentioned, the main objective of HTO is precisely to correct the mechanical axis of the lower limb so as to lateralise the GRF and relieve the load on the medial compartment of the tibial plateau and make the load distribution closer to the physiological one.

3.2.3 Torque

Starting from the GRF measurement and exploiting the spatial relationships between the markers and the bone segments, the mechanical moment acting on the joints is calculated. It is calculated as the vector product of the magnitude of the GRF and the perpendicular distance of the line of action of the force from the axis of rotation, i.e. from the articular centre [38]. Given the

impossibility of calculating joint forces directly, joint moments defined in this way are the best representation of contact forces. As with rotations, the data we will analyse for the moments are always given as a function of the three axes of rotation and the three joints of the leg, respectively.

3.2.4 EMG signals

In gait analysis to correlate osteoarticular kinematics and dynamics with muscular activity, surface electromyography sensors are used to pick up the EMG signal during the cycle. By exploiting several sensors and accurate positioning on the patient, it is possible to distinguish the signals of the main locomotor muscles of the lower limb. A comparative analysis of these signals with kinematic and dynamic data is useful to understand the compensatory behaviours that are triggered in pathological cases and can be used in clinical diagnostics, but also to assess the post-surgery progress.

4 STUDY PROTOCOL

This thesis work is part of a broader study already underway at the Rizzoli orthopaedic institute, in collaboration with the polytechnic institute of Turin, as well as the university of Bath and 3D Metal Printing Ltd, involving numerous professional figures such as doctors, surgeons, technicians and engineers. For this reason, the following chapter is dedicated to summarising the procedure by which this work was carried out.

4.1 TomoFix® HTO

Tailored Osteotomy Knee Alignment (TOKA®) is a patient specific surgical treatment for knee osteoarthritis specifically designed for young and active patients. As mentioned in the specific paragraph, the surgical treatment of choice for young patients with an active lifestyle for the correction of knee varus is HTO, and although the surgical technique has become increasingly popular over the years, it has achieved remarkable results thanks mainly to the implementation of surgical programming, modelling and 3D printing techniques. Along these lines is the TOKA project, which for the first time exploits a synergy between medical and engineering personnel from the pre-operative phase to surgical treatment, exclusively proposing the use of a special custom-made plate designed for the specific patient and the specific surgical treatment.

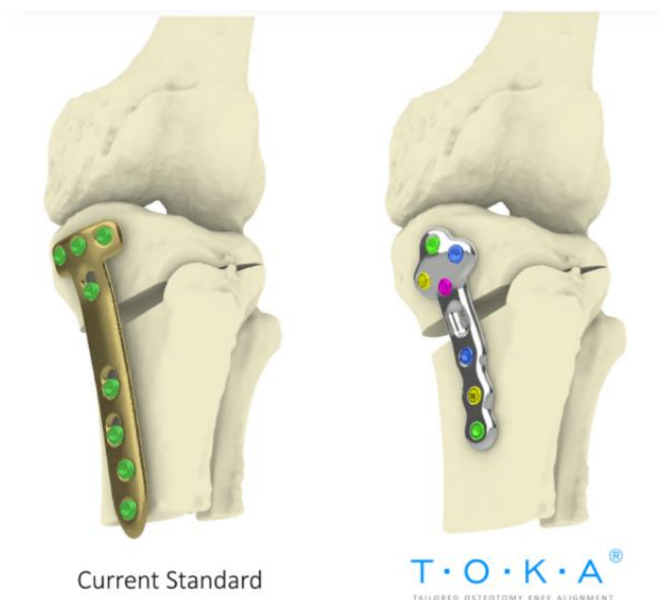


Figure 4-1: difference between the current standard plate (on the left) and the TOKA plate (on the right) [39]

Previous work has exploited 3D technology to aid the surgeon in planning, and some studies have experimented with the use of cutting guides designed for the specific case, but still using a standard fixator plate available in limited sizes that the surgeon then had to adapt to the specific case.

Although this approach has already had considerable success, it is plagued by the following problems from a biomedical point of view:

- from a surgical point of view, the limited availability of sizes, coupled with the standard shape of the plates used, made the surgical procedure more difficult, as it required the surgeon to adapt the instrument to the patient's particular anatomy, which can result in having to make a compromise between the desired morphology for optimal correction of the mechanical axis and the possibility of adapting the plate.
- From the patient's point of view, this need for compromise and the reduced availability of sizes translates into the need for a significantly larger plate in order to provide the necessary stability and thus a non-negligible surgical opening and discomfort, or often pain, due to the plate itself not following the personal bone surface anatomy, which can cause different compression zones and thus uneven stress.
- From an engineering point of view, there is a not insignificant issue concerning the CE marking, which is mandatory for all mass-produced medical devices. This marking acts as a guarantee of the minimum safety and quality standards of the device, but obviously refers to the product in its original form; all the checks and tests are carried out on the product in the state in which it is supplied, but the marking loses its validity in the event of incorrect use or manipulation of the same, in the specific case of the fixation plate, in order to make it adapt as much as possible to the specific bone surface of the patient, the surgeon often resorts to manipulating it, but this modification could affect the initial mechanical properties, thus making the marking lose its validity.

The use of a custom-made plate, as proposed in this project, overcomes all these problems: the use of a device designed for the specific clinical case and the consequent realisation of a custom-made plate in fact allows a perfect match between the plate and the bone surface, and therefore an optimised design, with reduced dimensions and allowing the use of less invasive fixation screws. All mechanical tests to guarantee the highest standards are referred to the final device as it will be implanted, thus overcoming the problem of branding, and furthermore, as it is a custom device, current regulations allow it to be used without specific branding of the individual component.

4.2 Ethical considerations

Regulatory approvals from the Research Ethics Committee and the Rizzoli Research Authority will be obtained prior to starting the study. Furthermore, the protocol and study follow Good Clinical Practice principles and abide by the ethical principles discussed in the declaration of Helsinki, the Council of Europe Convention for the Protection of Human Rights and Dignity of the Human Being in the Application of Biology and Medicine 38 (Convention of Oviedo 04/04/1997) and Italian Codes of medical ethics of health care professions, current Regulations and current anti-corruption laws. [40]

This study opens a whole new chapter in the story of custom-made devices. So far, personalized implants have only been used in compassionate surgery. For this study, the Ethics Committee gave the approval to use this investigational medical product in patients without a life-threatening condition or with a serious disease.

4.3 Obtaining participant consent

If the potential participants have given verbal agreement to enrol in this study, was obtained consent of participant with a specific module reported as appendix in the clinical investigation protocol. They have given also their availability for the recording of the pre and post-surgery data needed for the study: planned medical imaging and functional assessment (gait analysis), Knee Osteoarthritis Outcome Score (KOOS), the ED-5D score, the Tegner score, the knee society system score (KSS), pain measurement by Visual Analogue Scale (VAS) during rest and activity. Participants were also asked to give their consent to use the anonymous medical images for further research on personalized devices. Routine care for these patients from their clinic appointment have included several radiographs of the affected knee and an assessment of their active and passive range of motion of the knee. All information collected pre-operatively have been used to compare post-surgery progression.

4.4 Pre-clinical trials

Being an innovative and unique device, it has not been subjected to any previous clinical experience, so a pre-IDEAL framework was conducted prior to the use of the device in human.

- Firstly, Laboratory/Experimental testing was performed using composite tibiae and finite element simulation to evaluate the influence of plate design variables on clinical factors.

- To test the safety of the device, in silico virtual trials have been done which simulate the presence of the fixation plate within patients and give an understanding of the device performance.
- A surgeon training was conducted prior to cadaver tests using models, videos and planning software.
- Finally, a number of cadaver tests have been performed to optimise the design and analyse the finer details of the surgical procedure. Following these tests, a validation process was undertaken to examine the agreement between pre and post-surgery correction.

4.4.1 In silico virtual trials

In-silico testing is a very versatile tool for testing the safety of a device, thanks to computational model offers the unique possibility to virtually perform multiple surgeries on the same patient to compare the outcomes of the interventions. The CT scans were used to generate the intact (un-operated) models of each patient's proximal tibia. The interventions were all made on computer models. The correction angle was calculated such that the post-surgery mechanical axis will pass through Fujisawa's point (62.5% of the tibial width from medial to lateral). Virtual HTO surgery was performed on each patient to realign the mechanical axis creating a medial opening-wedge osteotomy. Then, each virtual patient was duplicated so that the osteotomy could be stabilised using a generic and a personalized fixation plate.

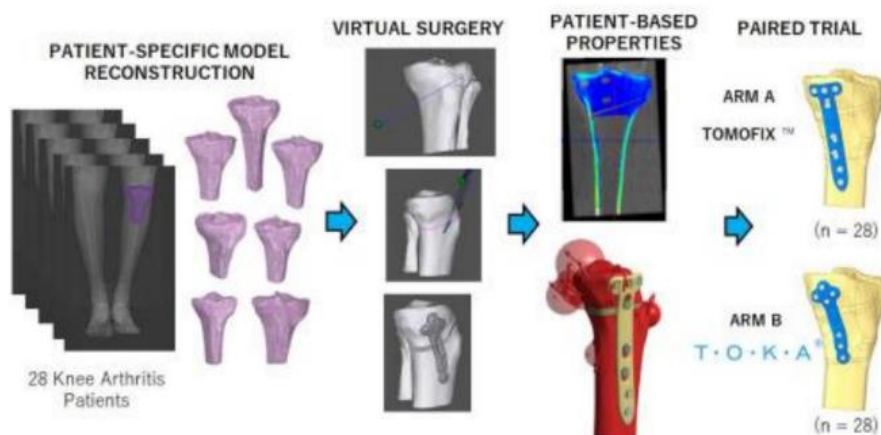


Figure 4-2: In silico trial workflow [41]

A finite-element model was then created for each patient from the CT images on which operating simulations were performed with both types of plate (tomofix and TOKA). To study the behaviour

of the implant during the bone healing phase, tests were conducted simulating a progressive increase in Young's modulus of the osteotomised region, specifically, four moments were analysed:

- HS1: immediately post-surgery;
- HS2: after 2 weeks;
- HS3: after 6 weeks;
- HS4: 12 weeks after the surgery;

The patient-specific model was also exploited for an evaluation of the osteo-articular forces for three physiological activities:

- ACT1: fast walking;
- ACT2: chair rise and seat;
- ACT3: squatting;

as an additional parameter in the evaluation of the model, three different screw configurations were considered in order to study their influence as a function of the dimension of the femoral stem:

- SC1: all screws present;
- SC2: the screws closest to the osteotomy site removed to simulate a longer stem;
- SC3: the most distal screws removed to simulate a shorter stem;

The key output variables were the maximum equivalent stress within the plate (Von Mises σ_{VM}), the proportion of solutions for which σ_{VM} exceeded the fatigue limit of 180MPa, the maximum equivalent strain at each bone-screw interface and the 3D inter-fragmentary movement at the osteotomy site. Screw configuration has relatively little effect upon plate stress or bone strain. The healing stage has a dramatic effect on reducing plate stress as healing progresses. TOKA® plates have generally slightly higher maximum Von Mises stresses because they are tailored to each patient while the generic plate is over-engineered by inclusion of a generic safety factor.

4.5 Clinical investigation information

This thesis work is therefore part of a 32-month pilot project aimed at evaluating the performance of customised HTO using an innovative and fully customised prosthetic device using the latest 3D technologies. The primary objective is the evaluation of the morphological change of the knee joint with particular regard to the progression of OA following TOKA treatment. Secondary objective is the evaluation of the functional outcome in the knee joint after this treatment.

4.5.1 Outcome

The morphology of the knee joint is assessed verifying the matching between the planned correction and the post-surgery imaging, measured through the correction angle, hip-knee-ankle angle (HKA – mechanical axis) and posterior slope, using the imaging techniques.

The functional outcome of the knee joint is assessed by performing a gait analysis of the patient pre and post-surgery.

Specifically this elaborate have the purpose of analysing the functional outcome of the entire data set, but also to report and use an innovative approach that combines functional and morphological data to obtain a new method for the assessment of knee joint mechanics: the GRF superimposition in the tibial plateau plane proposed in a previous work by the same research group at which this work was carried out [42].

4.5.2 Inclusion and exclusion criteria

Inclusion criteria:

- Patients undergoing opening wedge HTO at the Rizzoli Orthopaedic Institute
- Patients must have completed a consent form for the study
- Patients must be prepared to comply with the pre and post-surgery investigations, rehabilitation, attendance schedule and questionnaire schedule of the study
- Patients in whom any varus deformity present is $< 20^\circ$
- The diagnosis is of unicompartmental medial osteoarthritis of the knee
- The patient has a primary diagnosis of Non-Inflammatory Degenerative Joint Disease (NIDJD)
- BMI < 40
- Age range 40 to 65 years

Exclusion criteria:

- Refusal to consent to the study
- Pregnancy
- Prisoners
- A patient known to have substance abuse or psychological disorders that could interfere with their ability to comply with the post-surgery rehabilitation and assessment schedules
- Patients unable to read or understand the patient information leaflet and consent form
- Patient has a known sensitivity to device materials

- BMI \geq 40
- Patient has an active or suspected latent infection in or about the affected knee joint at the time of study device implantation
- Patient has received any orthopaedic surgical intervention to the lower extremities within the past year or is expected to require any orthopaedic surgical intervention to the lower extremities, other than the HTO to be enrolled in this study, within the next year
- Patient requires bilateral HTO or has a history of unsuccessful contralateral partial replacement or HTO
- Patient has chronic heart failure (NYHA Stage \geq 2)
- Patient has a neuromuscular or neurosensory deficiency, which limits the ability to evaluate the safety and efficacy of the device
- Patient is diagnosed with a systemic disease or a metabolic disorder leading to progressive bone deterioration
- Patient is immunologically suppressed or receiving steroids in excess of normal physiological requirements
- Patient has very poor bone quality, with extensive bone deterioration that could compromise the use of the implanted device.

4.5.3 Study population

The study comprises 25 adult patients aged between 40 and 65 years, enrolled consecutively under the care of the Rizzoli Orthopaedic Institute. There is only one pre-operative visit required and 5 visits required for post-surgery follow-up at 1, 3, 6, 12, and 24 months. The study will be conducted in the 2nd Orthopaedic and Traumatology Clinic at the Rizzoli Orthopaedic Institute.

5 MATERIAL AND METHOD

5.1 Acquisition system

5.1.1 Weight bearing CBCT

The possibility offered by imaging techniques such as CT (Computed Tomography) or MR (Magnetic Resonance Imaging) of acquiring a three-dimensional model of the osteoarticular system represented a considerable advantage in clinical and morphological investigation, but as far as the lower limb was concerned, a fundamental problem remained open: these acquisition techniques require the subject to be in a supine position and therefore in a condition of no load on the lower limb joint. The need to perform an accurate study of the joint correspondences and the reciprocal position of the various bone segments sublimated the need not to be able to ignore the load to which the joint is subjected and therefore the need to be able to acquire images in a physiological load situation.



Figure 5-1: Non-weight-bearing (a) and weight-bearing (b) posteroanterior knee radiographs [43]

Many orthopaedics conditions are best evaluated by imaging studies acquired to simulate functional positions and weight bearing activity. This is especially true of diseases that involve the articular surfaces of the joints, such as fractures, malalignment syndromes, and degenerative diseases, in response to this need the weight bearing CT was devised. This aspect has been highlighted by several recent studies that have shown that in follow-ups of knee osteoarthritis cases there is a significant difference between CT images acquired with and without loading [43]. WBCT is a relatively new imaging technology that allows excellent evaluation of dynamic bony deformities. It enables

improved visualization of the joint under natural load to help diagnose surgical and non-surgical candidates.

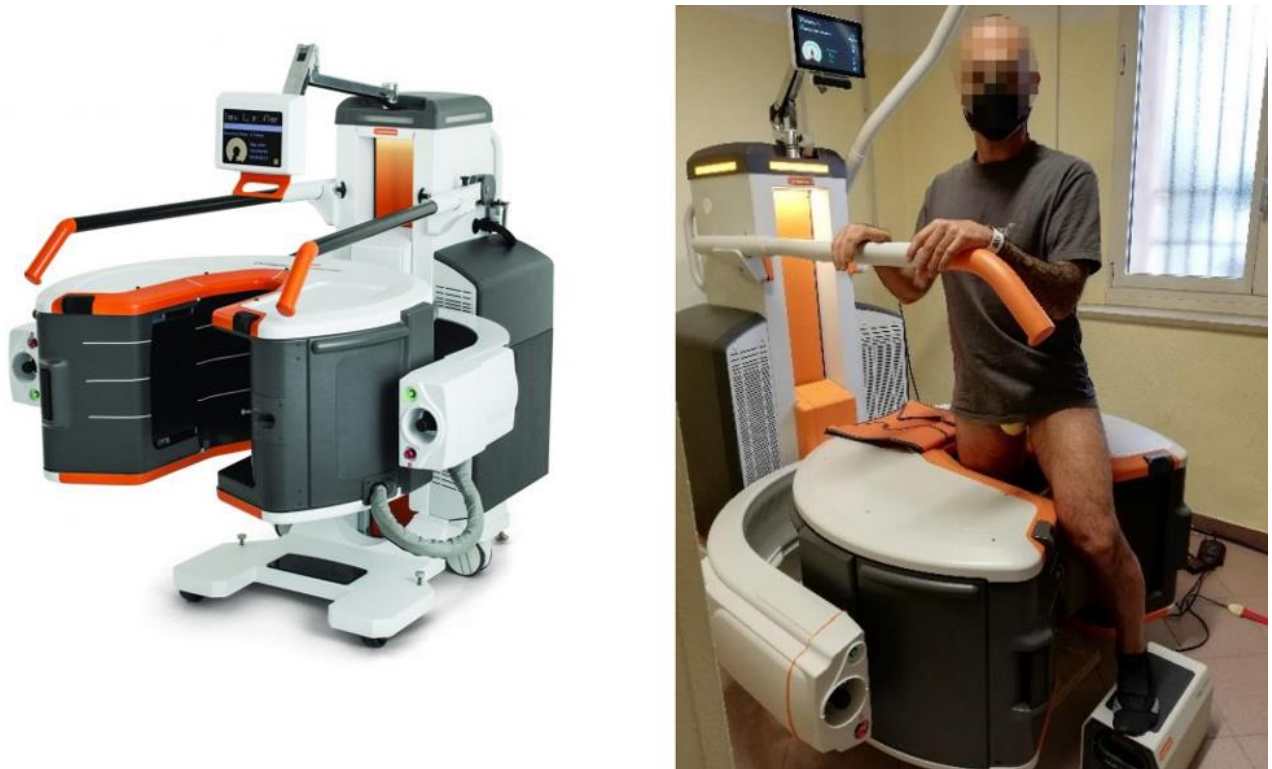


Figure 5-2: Carestream OnSight 3D Extremity System [44] and its use for acquisition in the IOR laboratory

In this study, weight-bearing cone-beam computed tomography (CBCT) was used, thanks to which it was possible to reconstruct an accurate osteoarticular model showing the interactions and relative positions of the articular surfaces during the normal stance phase and thus when the three main joints of the lower limb support the anatomical load. Weight-bearing CBCT allows to obtain weight-bearing images that can be viewed in all three planes and to construct three-dimensional models, similar to those constructed from traditional CT scans, as well as exposing patients to less radiation than do traditional CT scans. Other advantages of using this acquisition system are related to cone beam technology and are: very low radiation dose absorbed by the test subject, limited acquisition time and the large field of view (FOV). A cone beam is a rotating XR, where the centre of rotation is the investigated object, the photon source is at one end of the diameter axis, and the target (a digital silicon detector panel) at the other. The target is continuously projected with the photons which have traversed the object, and the result is an intermingled array of lines and shades called a sinogram (Fig. 5-3), which has to be interpreted using mathematical transforms (the Fournier, which reconstructs multiple simple sinus functions from a single complex one, and the Radon, which reconstructs a set of 3D coordinates). The result is a 3D cylindrical volume or field of

view (FOV), which varies in diameter between 10 cm and 40 cm. This is divided into smaller cubes or voxels: the 3D equivalent of 2D pixels. Acquisition time is typically under a minute. In terms of radiation exposure, a CBCT scan with single foot FOV is around 2 Micro Sieverts (μSV), a large FOV bilateral foot scan around 6 μSV . As a comparison, United States daily background exposure is around 8 SV, 1 μSV for an extremity conventional XR, 2 μSV for a chest XR and 25 μSV to 100 μSV (or typically 70 μSV for an ankle scan) for an extremity CT. [45]

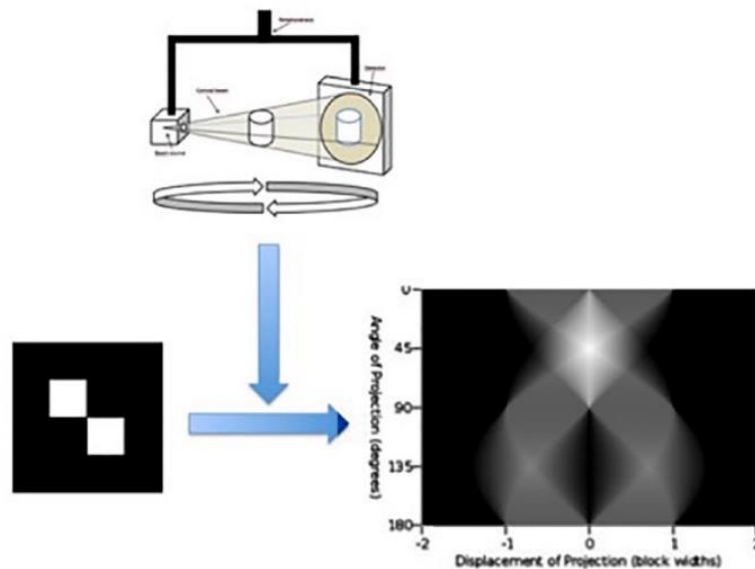


Figure 5-3: Technical principles of cone beam technology [45]

5.1.2 Gait laboratory and protocol

This section provides a brief description of the GAIT data acquisition system in use at the *Movement Analysis Laboratory and Functional-Clinical Evaluation of Prostheses within the IRCCS Istituto Ortopedico Rizzoli*, where this work was conducted. The operating principles of this analysis technique have been reported in a previous paragraph, together with the basics of the gait cycle essential to conduct such analysis and understand its results, now we will focus on the instrumentation used and in particular on the proposed set of markers thanks to which it was possible to perform a match between morphological data (from CBCT images) and functional data (obtained from gait analysis).

5.1.2.1 VICON system

For the stereophotogrammetry it was used The VICON system, a video acquisition system for motion capture technology that records the movements of the patient walking through a walkway Force Platform. This system is composed by eight high-resolution cameras (sample rate 100 Hz) positioned on the perimeter of the laboratory, the acquisition system uses infrared, which is why each camera

has a ring of LEDs around the lens. As anticipated, the subject is instrumented with photo-reflective markers, which then, when illuminated by the LEDs, reflect the signal that is detected by the cameras. In order to reconstruct the exact position of a marker, it is sufficient for it to be detected by two cameras at the same instant; the use of a greater number of cameras is justified by the need to be able to trace the exact position of all markers during the entire motor task. The 2D data from the individual cameras are acquired by the workstation which, thanks to special stereophotogrammetry software, reconstructs the position in three dimensions of the individual markers and notes these, that of the osteoarticular segments.

5.1.2.2 Force platform

For a functional analysis during movement, a key role is played by force platforms. The laboratory at the IOR is equipped with Force platforms Kistler, Einterthur, CH, which are positioned under the floor in the centre of the laboratory so that the subject can walk on them during normal walking. Each force plate has a set of three orthogonal force sensors in each of the four supporting corners. These sensors may be strain-gage or piezoelectric transducers and produce an electrical output proportional to the force applied and the location of the contact point. Force platforms give in output several information (sample rate 2000 Hz). They give a three-dimensional description of the ground reaction force (GRF) which has equal intensity and opposite direction to the force experienced on the foot of the weight-bearing limb. It is important that the specific position of the platforms is not easily identifiable by the subject so that he or she is not led to alter the gait. For this functional analysis, there is no real standard for the length of the path, but it is important that it is sufficient to have a normal walk, without being affected by the effects of the beginning and end of the motor task. This laboratory is equipped with a 5-metre path and two areas of interest, one for each foot, for the 60cm x 120cm force platforms.

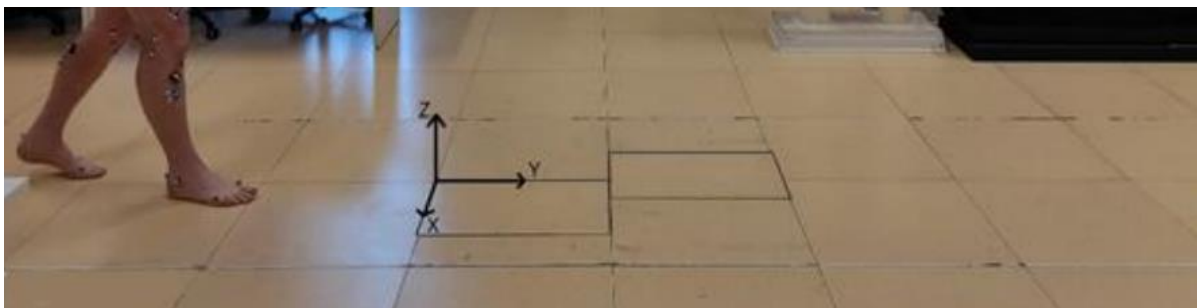


Figure 5-4: force platform in the GAIT laboratory of the IOR center and global reference frame of the analysis

Force plates define the laboratory reference frame that is also the global reference frame used in this work. This frame is so defined:

- its origin is located on the lower left corner of the first plate
- the y-axis lies on the force plate and its positive direction is the direction of motion
- the x-axis lies on the force plate and its positive direction is from left to right
- the z-axis is perpendicular to the x-y plane and its positive direction is proximal.

Force platforms also give in output the three coordinates of the centre of pressure (note that the z coordinate is zero when walking on the ground) which can be useful for the identification of abnormal patterns of foot contact. Moreover, force plates give in output the moments about the x, y, and z axes. Joint moments are calculated as the vector product of the position vector of the joint centre and the ground reaction force.

5.1.2.3 IOR gait protocol

For a correct evaluation of functional data by means of gait analysis, it is necessary to follow a protocol that makes the operation fast and repeatable to eliminate intra- and inter-subject variability. To this end, the operational protocol developed previously at the IOR motion analysis laboratory was adopted in this work, which for the sake of completeness is reported below. The setting of the instrumentation is pre-set and uses the software provided by the VICON system described above, now we will turn instead to the preparation of the subject to be analysed, who for this purpose must be instrumented with markers and a set of EMG sensors. [46] [47]

Marker placement: four rigid segments are identified for the lower limb, pelvis, thigh, shank, and foot; for this purpose the following anatomical landmarks are tracked in space applying a 10 mm diameter marker to:

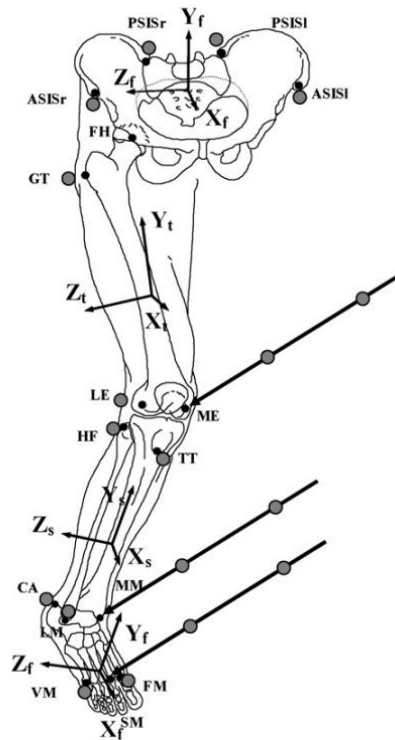


Figure 5-5: locations of the anatomical landmarks (small black circles), and the reflective markers (grey circles) [46]

- RASIS, LASIS: the two most anterior margins of the iliac spines (right and left)
- RPSIS, LPSIS: the two most posterior margins of the iliac spines
- GT: the most lateral prominence of the great trochanter
- LE: the most lateral prominence of the lateral epicondyle
- HF: the proximal tip of the head of the fibula
- TT: the most anterior border of the tibial tuberosity
- LM: the latera prominence of the lateral malleolus
- CA: the aspect of the Achilles tendon insertion on the calcaneus
- FM: the dorsal margin of the first metatarsal head
- VM: the dorsal margin of the fifth metatarsal head
- FH: the centre of the femoral head which is assumed to coincide with the centre of the acetabulum (there isn't a real marker in this point, it is reconstructed by a geometrical prediction method based on the location of the four anatomical landmarks of the pelvis. FH, GT and LE enable the reconstruction of a technical frame on the femur)
- ME: the most medial prominence of the medial epicondyle
- MM: the most medial prominence of the medial malleolus
- SM: the dorsal aspect of the second metatarsal head

The centre of the hip, knee and ankle joints are taken respectively as FH, the midpoint between LE and ME, and the midpoint between LM and MM.

The main purpose of gait analysis is to derive functional data from the lower limbs, but for a correct evaluation it is important to also consider the upper body, which, however, for simplicity is considered as a rigid body in this analysis and identified through the use of a set of 14mm markers arranged as follows:

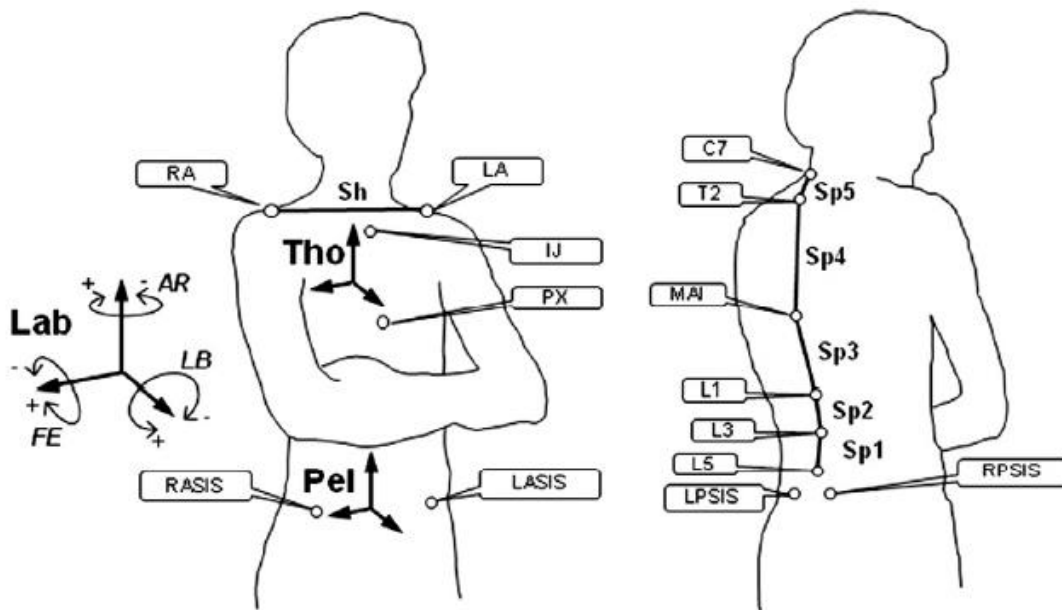


Figure 5-6: Marker placement diagram with marker labels from (Leardini et al., 2011) [48]

- C7: the seventh cervical vertebra
- T2, T8, T10: the second, eight, tenth thoracic vertebrae
- L5: the fifth lumbar vertebra
- IJ: the deepest point of incisura jugulars, i.e. suprasternal notch
- PX: the xiphoid process, i.e. the most caudal point of the sternum
- RA, LA: the right and left acromions
- RASIS, LASIS: the right and left anterior superior iliac spines
- RPSIS, LPSIS: the right and left posterior superior iliac spines
- SACRUM: the spinal process of the second sacral vertebra

5.1.2.4 Electromyography

For a complete functional musculoskeletal assessment in this analysis, surface EMG sensors are used to acquire signals from the main leg muscles and assess their activity during the various phases of

walking and other motor tasks. These sensors are placed on the subject's skin by means of double-sided tape and are able to pick up the electrical signal resulting from the activation of muscle fibres, which during contraction vary their potential according to the degree of fibre recruitment.



Figure 5-7: EMG electrodes placements

In a standard sEMG-GA session (gait analysis that includes the recording of EMG signals), sensors are placed, at least, over tibialis anterior (TA), lateral gastrocnemius (LGS), rectus femoris (RF), and lateral hamstrings (LH), bilaterally. This way, it is possible to analyse at least a pair of agonist-antagonist muscles acting at each joint of the lower limbs (ankle: TA/LGS, knee: LH-LGS/RF, hip: RF/LH). [49]

5.1.2.5 Motor task

Gait analysis is the technique of excellence for a functional assessment of lower limb joint mobility, thanks to this technique we are able to follow the course of joint movements (as measures of relative rotations) during a normal walking cycle and through mechanical extrapolations, we are able to provide information on the loads (as joint moments) to which each joint is subjected. In this examination case, since this is an operative technique aimed at correcting a mechanical deformity in a non-serious form and in patients who do not have a major joint pathology, it was decided to use four additional motor tasks that are more demanding for the joint in order to have a more complete functional picture. In order to ensure repeatability of the result and/or analysis, we briefly report the motor tasks used and how they were performed:

- **Gait:** the subject is asked to walk through the functional analysis laboratory as naturally as possible and the entire cycle is recorded. As the data from the markers will need to be

correlated with the data from the force platforms, the crucial point is the middle part of the walk, and the operator will ensure that the subject steps on each platform with a single foot during the walk in order to capture the GRF data of each, but without requiring the subject to centre the platforms to avoid altering the normal walk;



Figure 5-8: gait

- **Chair:** the operator has the subject position himself with his feet as centred as possible on the footplates while sitting on a chair. The task required is to get up from it without the help of the arms so as to maximise the use of the legs during the task;



Figure 5-9: chair motor task

- **Squat:** starting from a similar position, again with each foot centred on one of the platforms, but in a standing position, the subject is asked to perform a squat as deep as possible and then return to a standing position;



Figure 5-10: squat

- **Climbing and descending steps:** these motor tasks require a special experimental set-up consisting of a series of four modular wooden steps, made in such a way as to have the second and third steps perfectly corresponding to the footplates below (so that when trodden on, the entire load is transferred to the footplate below), at 20.7cm and 36.7cm above the ground respectively. The first and fourth steps, on the other hand, are outside the dynamometric footplates and only serve to complete the entire motor cycle and are 4.7cm and 52.7cm above the ground. This set-up is used for both motor tasks (ascent and descent) and subjects are only required to start with the right foot and place one foot on each step;



Figure 5-11: climbing steps



Figure 5-12: descending steps

In order to be able to carry out a repeatability analysis of the results for each motor task, more repetitions are acquired. Specifically, the protocol adopted provides for 3 repetitions for the four additional exercises and 5 repetitions for walking, which, despite being less demanding, remains the motor task most frequently used and thus a reference with respect to other jobs. Furthermore, it is of fundamental importance to emphasise that gait is the only task for which there is a reference band that can be considered as normal, making it possible to make a complete comparison with pre- and post-surgery situations.

5.2 Data processing

Once we have described the materials used to collect the data and defined the operational protocol adopted, we go on to define the methods used to analyse the data and how the results were obtained, which we will see in the appropriate chapter. Starting with the images acquired with CBCT, the purpose of the processing is to obtain a 3D model of the knee joint, which will then be used for pre-operative definition and planning, for the design of implantable surgical devices, and for conducting all pre- and post-surgery morphological analyses, in order to qualitatively assess the results obtained through surgery and to be able to correlate them with functional data. In the specificity of this thesis work, the creation of a three-dimensional osteoarticular model, combined with the position of the individual markers, plays a fundamental role. It is in fact thanks to the simultaneous acquisition of the markers and the knee anatomy in CBCT that it was possible to combine these two data sets in order to elaborate a morpho-functional analysis of the knee joint.

5.2.1 Morphologic data

5.2.1.1 Mimics Innovation Suite®

Starting from the CT images, the first step is their processing using segmentation software to create a three-dimensional model. For this purpose, in order to guarantee good accuracy, it was decided to use Mimics Innovation Suite®, a semi-automatic segmentation software that takes the DICOM file containing the images of each individual slice acquired as input and by appropriately modulating the threshold levels in Hounsfield units (dependent on the material density) recreates a volume corresponding to the bone segments.

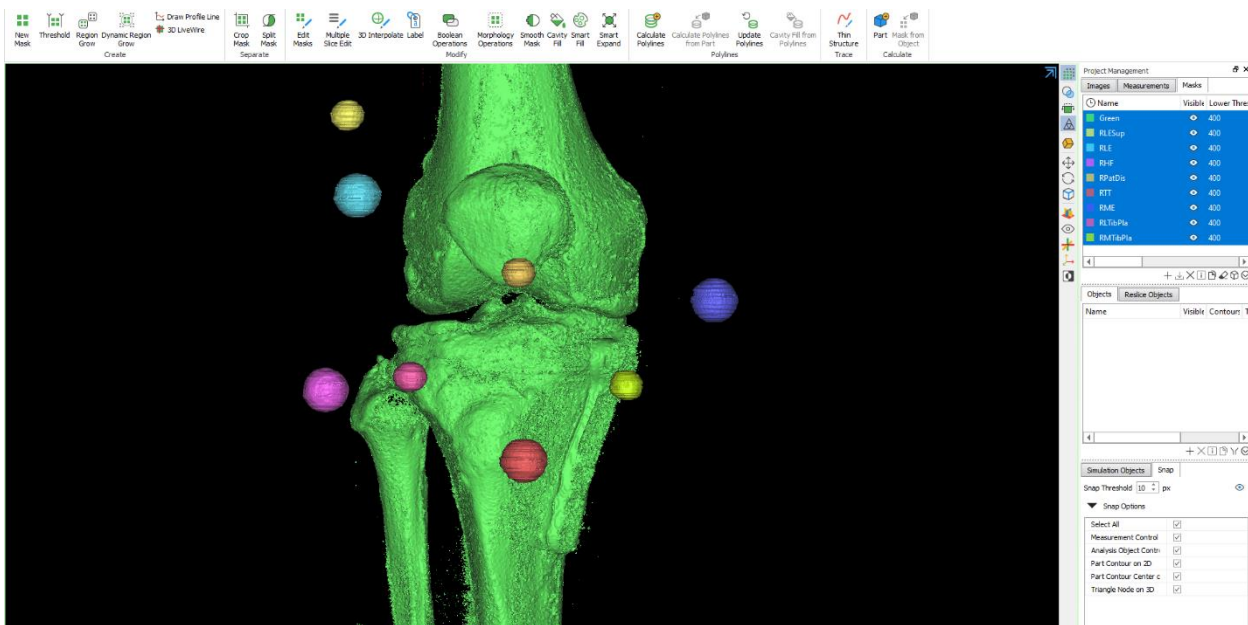


Figure 5-13: 3D image obtained in Mimics®

Once this initial operation has been performed, the model must be re-processed to recreate the correct volumes and correctly segment each element in an appropriate “mask”, each one will correspond to a solid object in the model. This operation requires good preparation on the part of the operator and an excellent knowledge of the anatomy in order to avoid possible artefacts that may be derived from problems in the acquisition phase, and metal artefacts that are always present in post-surgery images due to the presence of the fixation plate as well as screws. It is precisely the presence of these objects, as well as their greater elasticity, that led to the decision to use semi-automatic segmentation software, which, although requiring a considerable amount of operator time and greater preparation and knowledge, if used correctly allows us to obtain considerably more accurate three-dimensional models [50]. As anticipated for this work, it was essential to correctly segment the markers as well as a tibia segment so that the relative position of the joint markers

could then be correlated with that derived from the functional analysis, from which the position of the markers in relation to the GRF is derived [42].

5.2.2 Functional data

5.2.2.1 Matlab®

With regard to the functional data, the output from the gait analysis is a file.csv containing a series of data and parameters, including those of interest to us that were analysed and processed for the purposes of this work: rotations and joint moments (all for the three joints and in the three anatomical planes), GRF value, centre of pressure and EMG signals for the six muscles considered, during the entire acquisition period. This is therefore a considerable amount of data which, if properly interpreted, allows a functional analysis of the three joints of the lower limb, hip, knee and ankle. The project in which this work is inserted is centred on the knee joint, but it must be taken into account that the mechanical behaviour of one invariably influences the others, cooperating for the same task, that is to support the body load and to control and stabilise the movement. Before the data can be processed, it must be exported to the calculation environment Matlab® and, where necessary, corrections such as rototranslations must be made and referred to the main gait events as seen in the specific section on the gait cycle (3.1) to ensure that all data are consistent and referred to the same reference system (for details see Ruggeri Miriana's master's thesis work [42]). This was done by using the Matlab® calculation environment for the subsequent analysis of the entire data, arriving at a point-by-point functional evaluation for each patient participating in the study, but also at an aggregate data analysis, which gave statistical significance to the study conducted with a large data set of no less than 25 patients for this study, i.e. the entire data set of the TOKA project.

5.2.3 Matching

A study by this same research department carried out earlier and which led to the publication in 2022 of a research paper by Ruggeri et al. entitled *“Superimposition of ground reaction force on tibial-plateau supporting diagnostics and post-surgery evaluations in high-tibial osteotomy. A novel methodology”* proposed an innovative approach for studying the knee joint that combines the two approaches used to date, the anatomical and the functional, by visualising the point of application of the GRF in the plane of the tibial plateau. This method uses the localisation of a special set of additional markers (reported in the Figure) that can be detected in both CBCT and gate analysis and then calculates a rotation matrix that allows the projection of the GRF in the tibial plateau reference

system to be reported instant by instant. In this work, this approach is then applied to all patients in the study and new measurements and parameters are also proposed that exploit this method to provide an anatomical-functional assessment.



Figure 5-14: new marker set for the matching of the data

5.3 TomoFix® HTO

For the sake of completeness, in this last paragraph we report the technical specifications of the surgical instrumentation used in this work, with particular regard to the two innovative elements, namely the cutting guides and the custom plate based on the 3D model of the specific patient.

5.3.1 Fixation plate

The product is a customised medical device (implantable plate and accessories) for use in HTO, designed and manufactured in compliance with the relevant medical standard. It can be inserted in the IIb risk class, given the rules of the Medical Device Directive 93/42/EEC (Rule 8). The device is designated using CAD file created from the medical images of each patient. The CAD file are imported and manipulated using an internal software, to positioning the bone geometries in accordance with the surgeon's plan and assists with the creation of plate and surgical guide/accessories like screw cut guide and blade. The TOKA medical device consists in implantable and non-implantable components, the core implantable product comprises:

- Custom fixation plate
 - Made of TI-6Al-4V ELI Grade 23 titanium powder
 - Typically includes 7 holes for locking screws
 - Will be patient specific
 - Will be flush against bone
 - Will have no sharp edges or protrusions that could causa irritation
 - The head of the screws will not protrude substantially from the plate

6 RESULTS

In this chapter, we report the results obtained from the processing and analysis of functional data, as well as those obtained by combining morphological and functional data. As this is a study which includes the entire data set and thus the data of 25 pre- and post-surgery patients, for reasons of space and in order to avoid the discussion from being cumbersome, it was decided to present each result for a limited number of representative patients and as an aggregate analysis of the statistical sample. Naturally, the accumulated data will be reported in a separate appendix so that they can be consulted by anyone who is interested.

6.1 Functional data: rotations and moments

Functional data, or in other words those deriving from gait analysis, are aimed at assessing the state of the articulation by evaluating its kinematics and dynamics. Specifically for this work we have focused on two quantities that, also from previous studies, have been elected as reference for the functional evaluation of the osteo-articular system: rotations and moments. The gait analysis allows us to evaluate the data of the three joints of the leg (hip, knee and ankle) and since we are dealing with displacements and stresses that occur in a three-dimensional space, in order to better evaluate their incidence depending on the movement and in accordance with what has been seen in the specific paragraph, these variables will be represented and evaluated following the conventions defined on the anatomical planes. For this reason, the data we will present in this work will often be reported as 3x3 matrices in which we will have the variable of interest evaluated for the three joints, hip, knee and ankle, and for the three rotations, flexion-extension (flex/ext), abduction-adduction (abd/add) and internal-external (int/ext). Furthermore, it should be noted that each processing was repeated for all 5 motor tasks described in the chapter on materials and methods used.

6.1.1 Repeatability

As a first step to verify the consistency of the acquired data, their repeatability was checked for each patient between the various repetitions (intra-patient) and that between all subjects involved in the study at the two moments under investigation, i.e. pre- and post-surgery.

6.1.1.1 Intra-patient repeatability

The operative protocol adopted requires the acquisition of a certain number of repetitions for each motor task in order to avoid random errors, the data of each patient were then evaluated by plotting

the individual repetitions and then calculating the mean and standard deviation. Below we report the data obtained for the two functional variables, for each motor task, of three patients who can be taken as a model (aggregate data can be found in Appendix A):

- GAIT
 - Joint Rotation

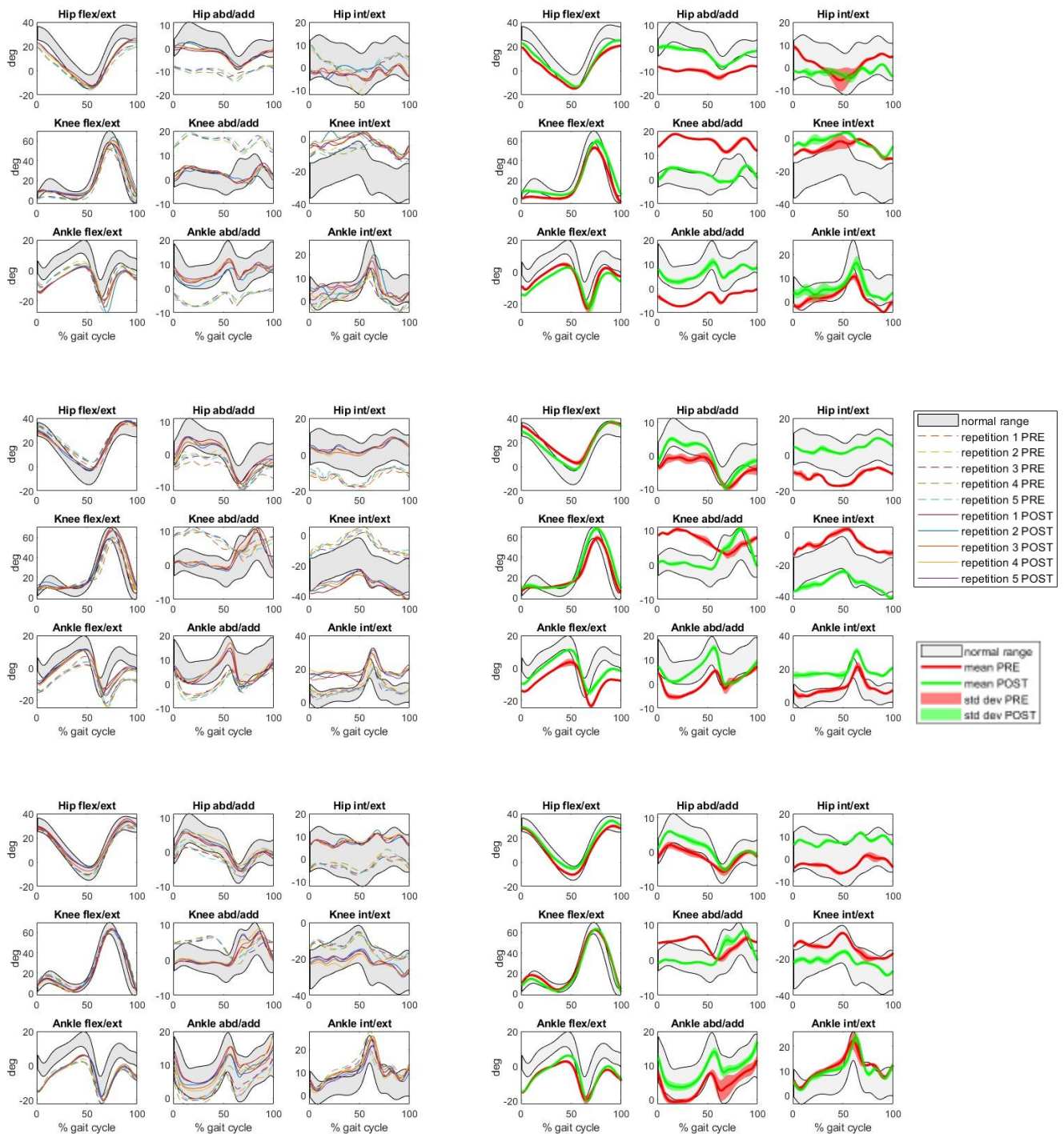


Figure 6-1: joint rotations in the five repetition (on the left) and their mean and standard deviation (on the right) pre- and post-surgery during the gait for three patients

○ Joint Moments

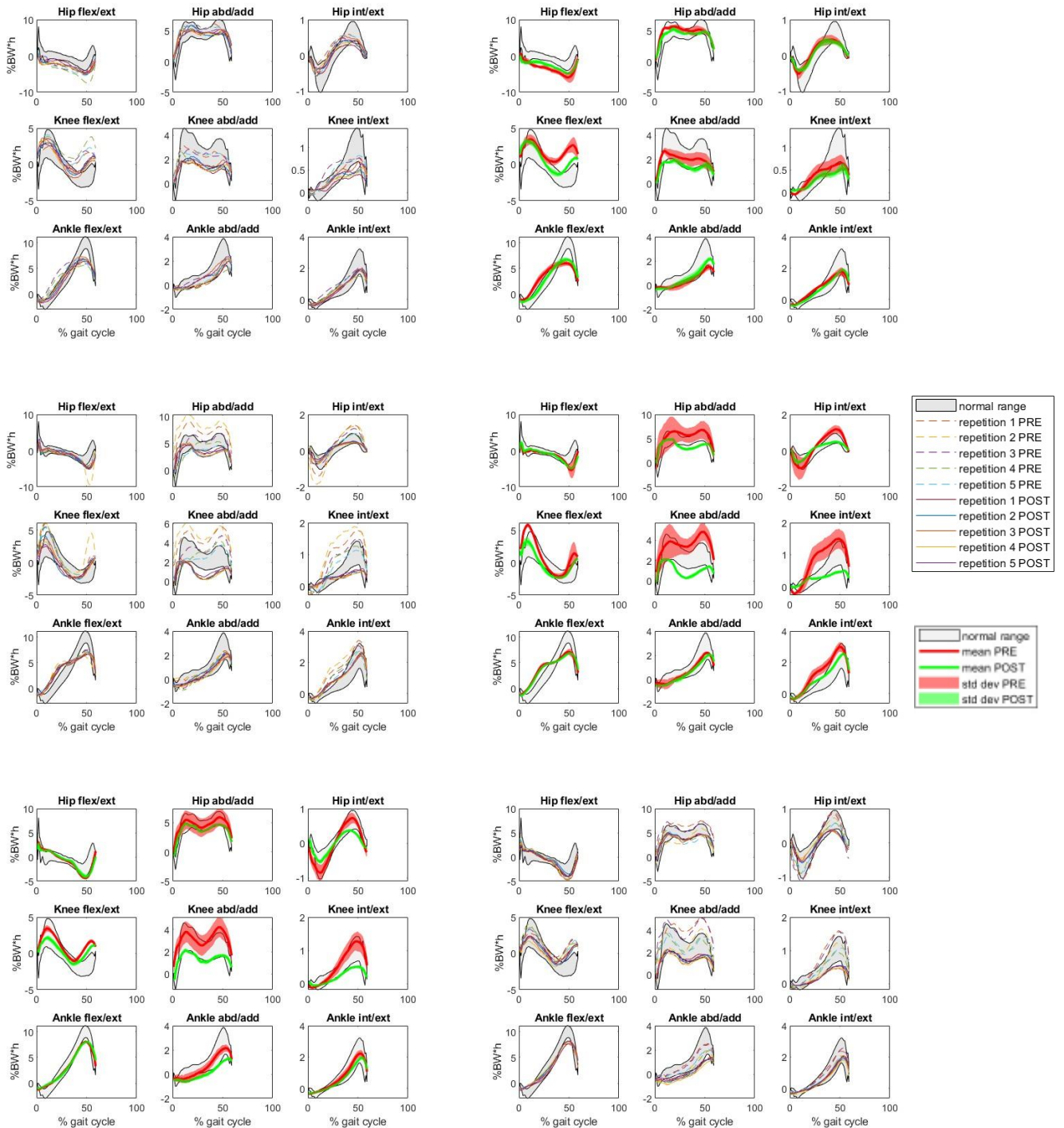
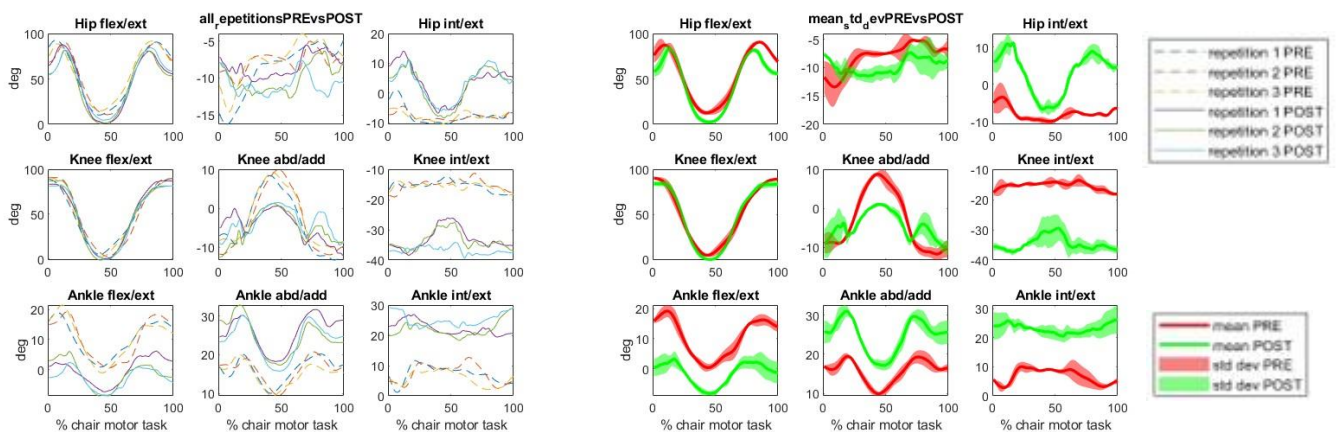


Figure 6-2: joint moments in the five repetition (on the left) and their mean and standard deviation (on the right) pre- and post-surgery during the gait for three patients

Analysing the graphs shown, we can see that the data has good repeatability and therefore there do not seem to have been any random errors during the acquisitions. In all patients it was seen that beyond the numerical differences that are normal during such acquisitions, there is a repetition of

the same patterns and therefore the same trends during the gait cycle considered. From the same graphs, one can also see a first encouraging result regarding the success of the operating technique and consequently an improvement in joint mechanics. It should be noted how the standard deviation values calculated at each instant of the cycle considered had a considerable reduction from pre- to post-surgery, which can be interpreted as a greater stability and control of the movement in the stance phase. In this elaboration it was also possible to exploit the knowledge of patterns acquired on a data set of non-pathological patients, which allowed the creation of normality bands for this motor task. The knowledge of these ranges makes it possible to carry out a real analysis of joint function as it represents a term of comparison. By comparing the bands obtained from the processing of the data at the two different times with these bands, it is possible to see how the data acquired on the patients at 6 months after the operation has recorded an evident approximation to what is the normal trend, further confirmation of the quality of the technique under examination. Let us now turn to the next motor task and postpone further concluding remarks on these initial elaborations to the end of the paragraph.

- CHAIR
 - Joint Rotations



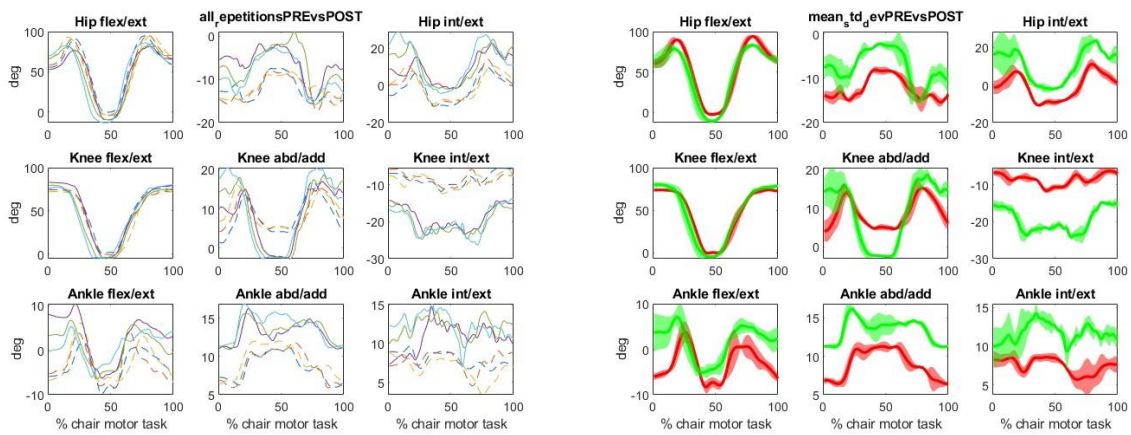
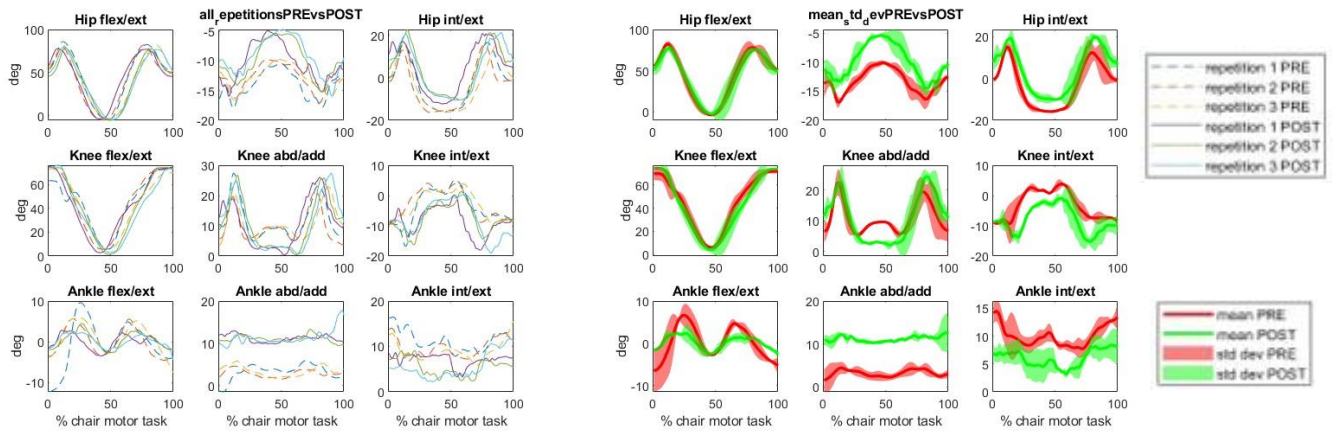
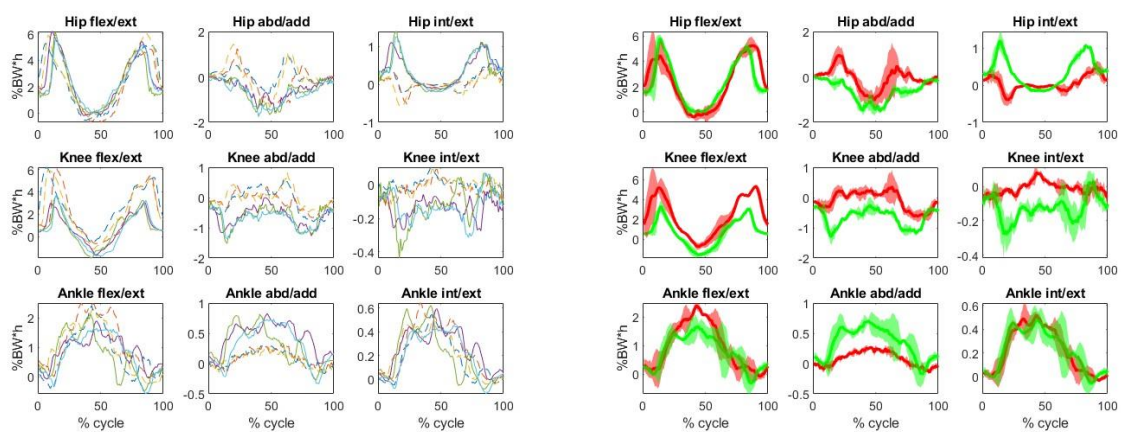


Figure 6-3: joint rotations in the three repetition (on the left) and their mean and standard deviation (on the right) pre- and post-surgery during the chair motor task for three patients

○ Joint Moments



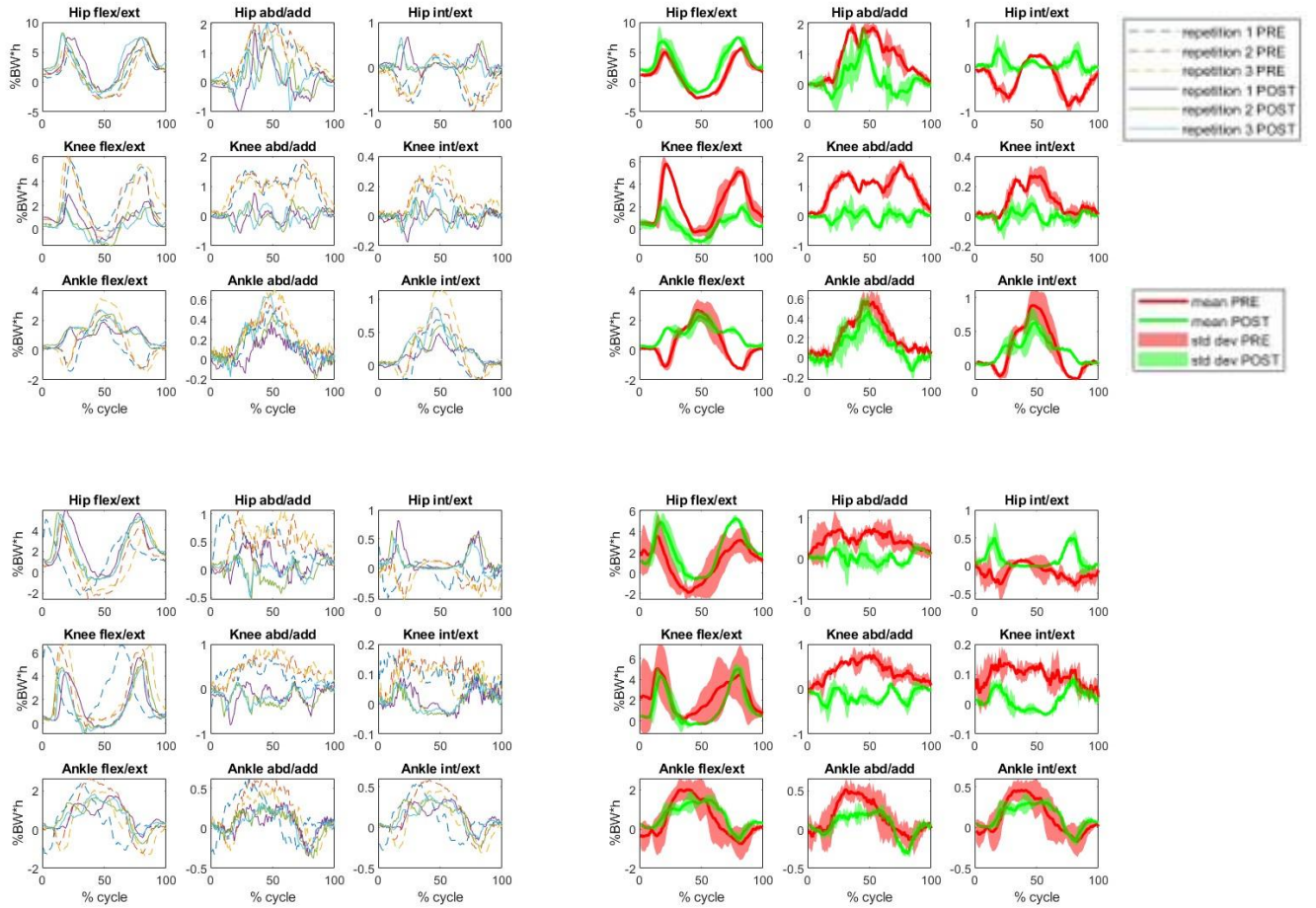
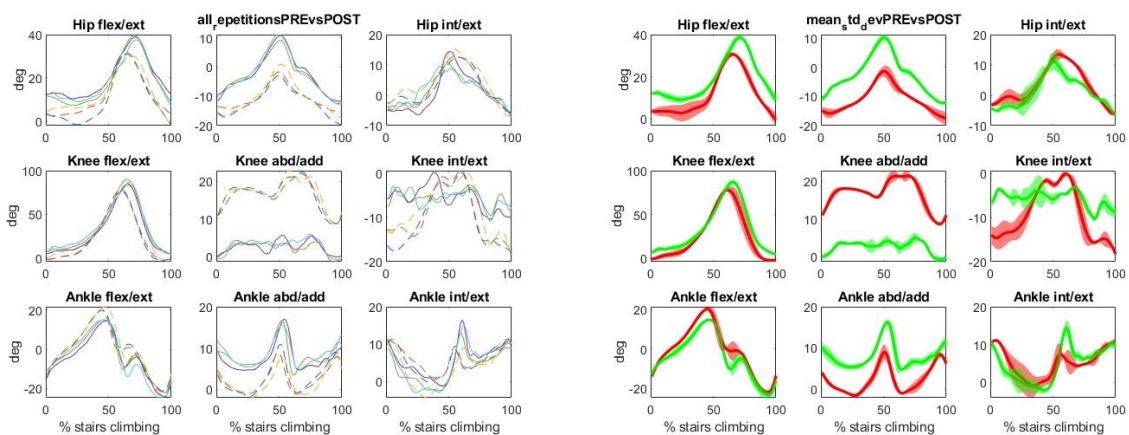


Figure 6-4: joint moments in the three repetition (on the left) and their mean and standard deviation (on the right) pre- and post-surgery during the chair motor task for three patients

- STAIRS CLIMBING

- Joint Rotations



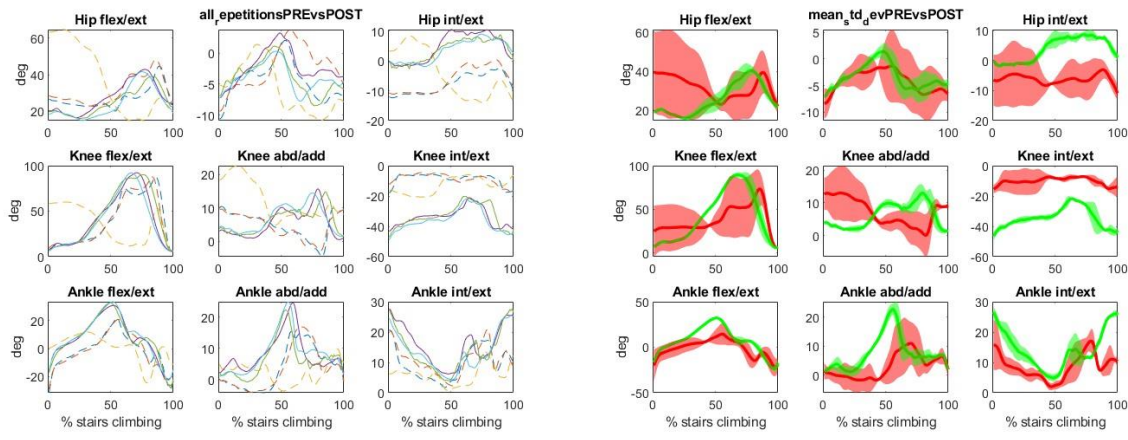
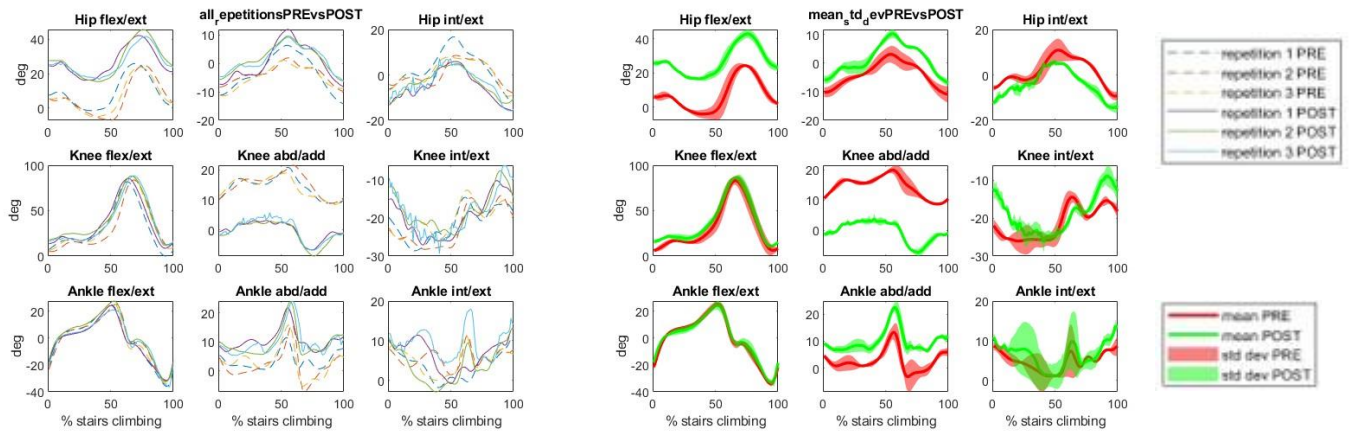
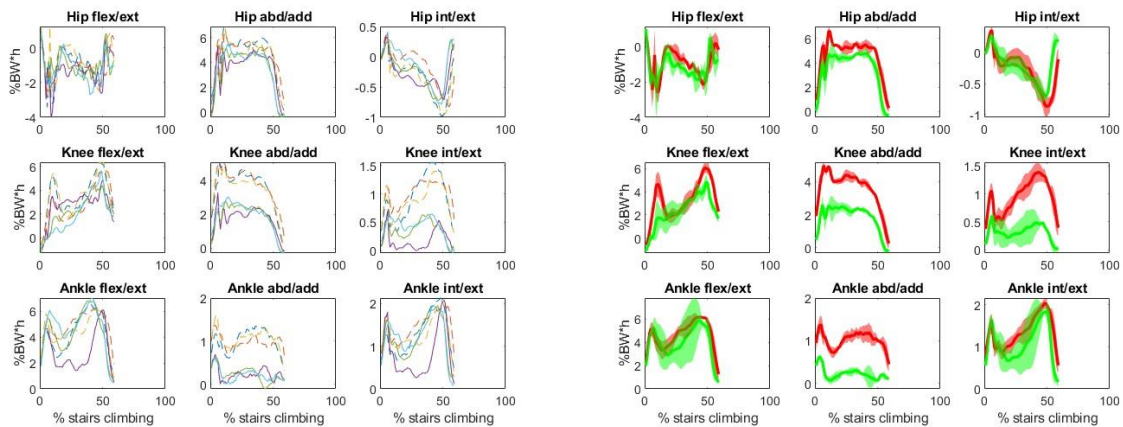


Figure 6-5: joint rotations in the three repetition (on the left) and their mean and standard deviation (on the right) pre- and post-surgery during the stairs climbing for three patients

○ Joint Moments



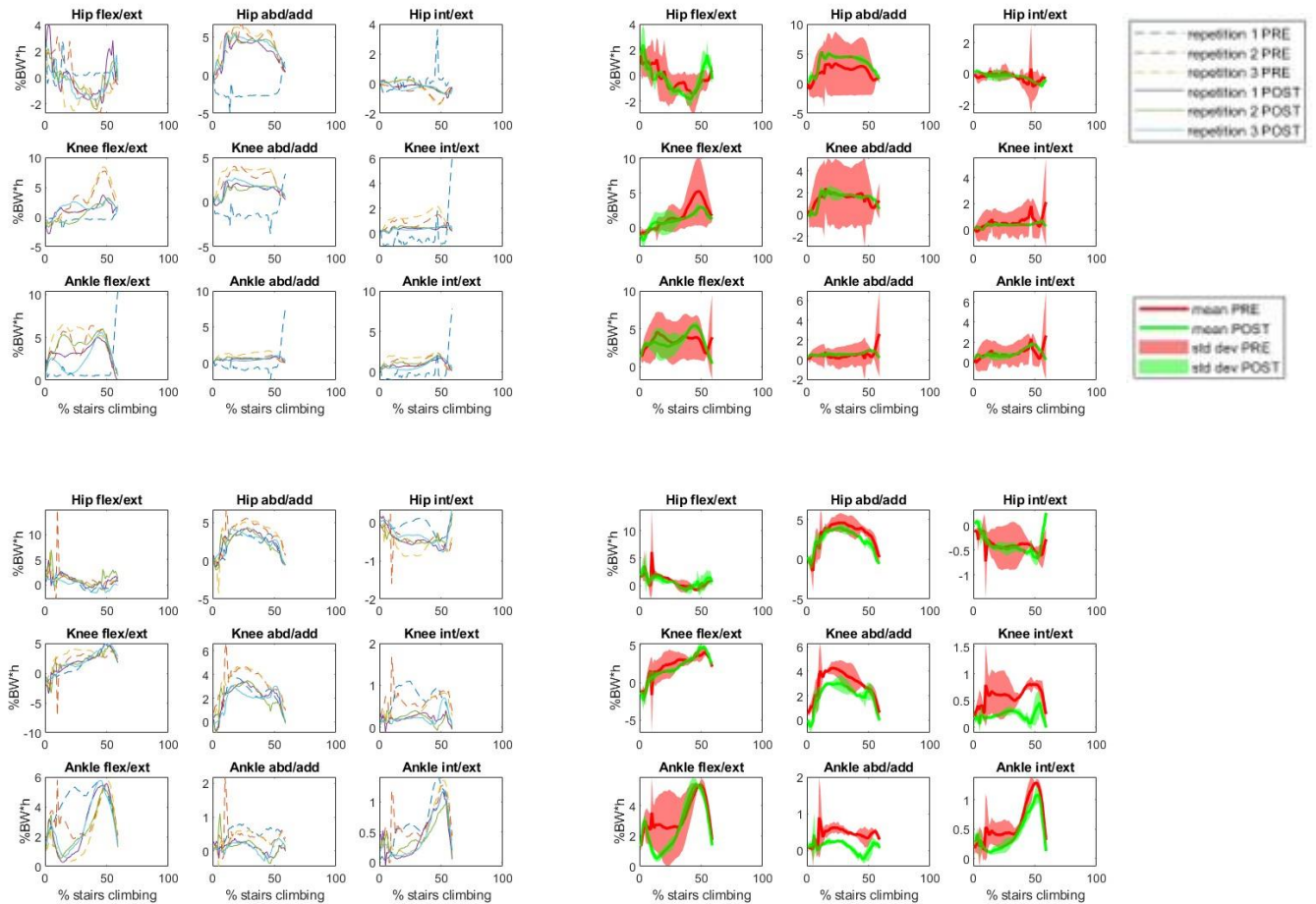


Figure 6-6: joint moments in the three repetition (on the left) and their mean and standard deviation (on the right) pre- and post-surgery during the stairs climbing for three patients

Analysing the graphs shown, it is possible to grasp another important aspect that highlights the need for a precise analysis of the individual tracings and a good knowledge of the articular mechanics under investigation: in fact, we can note that some repetitions present anomalous peaks, probably due to accidental errors during acquisition, which must be taken into account in the subsequent elaborations (see, for example, the trends of the articular moments in the exercise that required climbing steps, Figure 6-6). By directly plotting the average trend between repetitions and the standard deviation, it becomes impossible to recognise whether these anomalies are a symptom of a functional disorder, or caused by acquisition errors, and this is all the more detrimental if a single repetition has to be evaluated for subsequent processing, such as when studying the entire data set of subjects involved.

- STAIRS DESCENDING
 - Joint Rotations

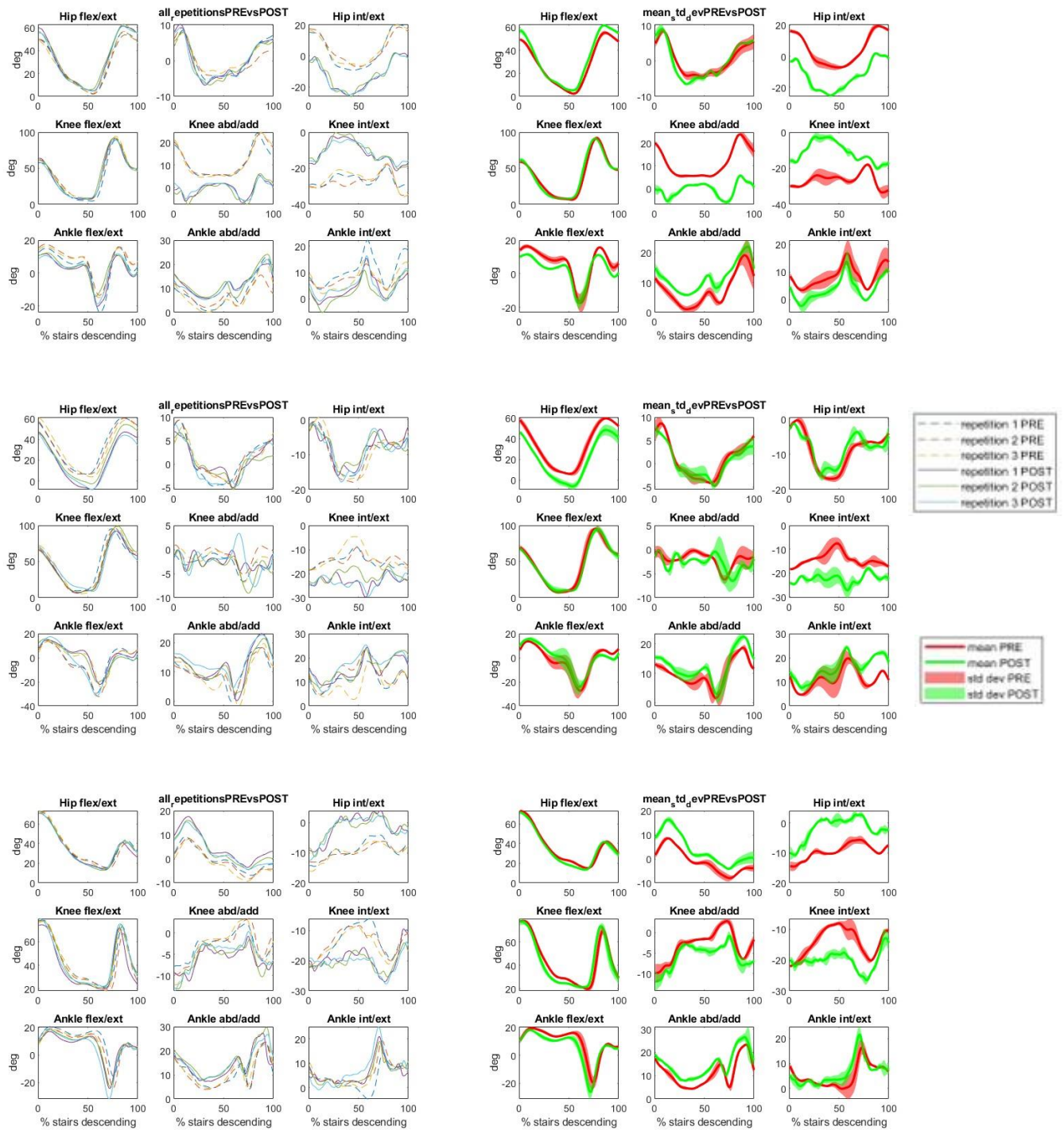


Figure 6-7: joint rotations in the three repetition (on the left) and their mean and standard deviation (on the right) pre- and post-surgery during the stairs descending for three patients

○ Joint Moments

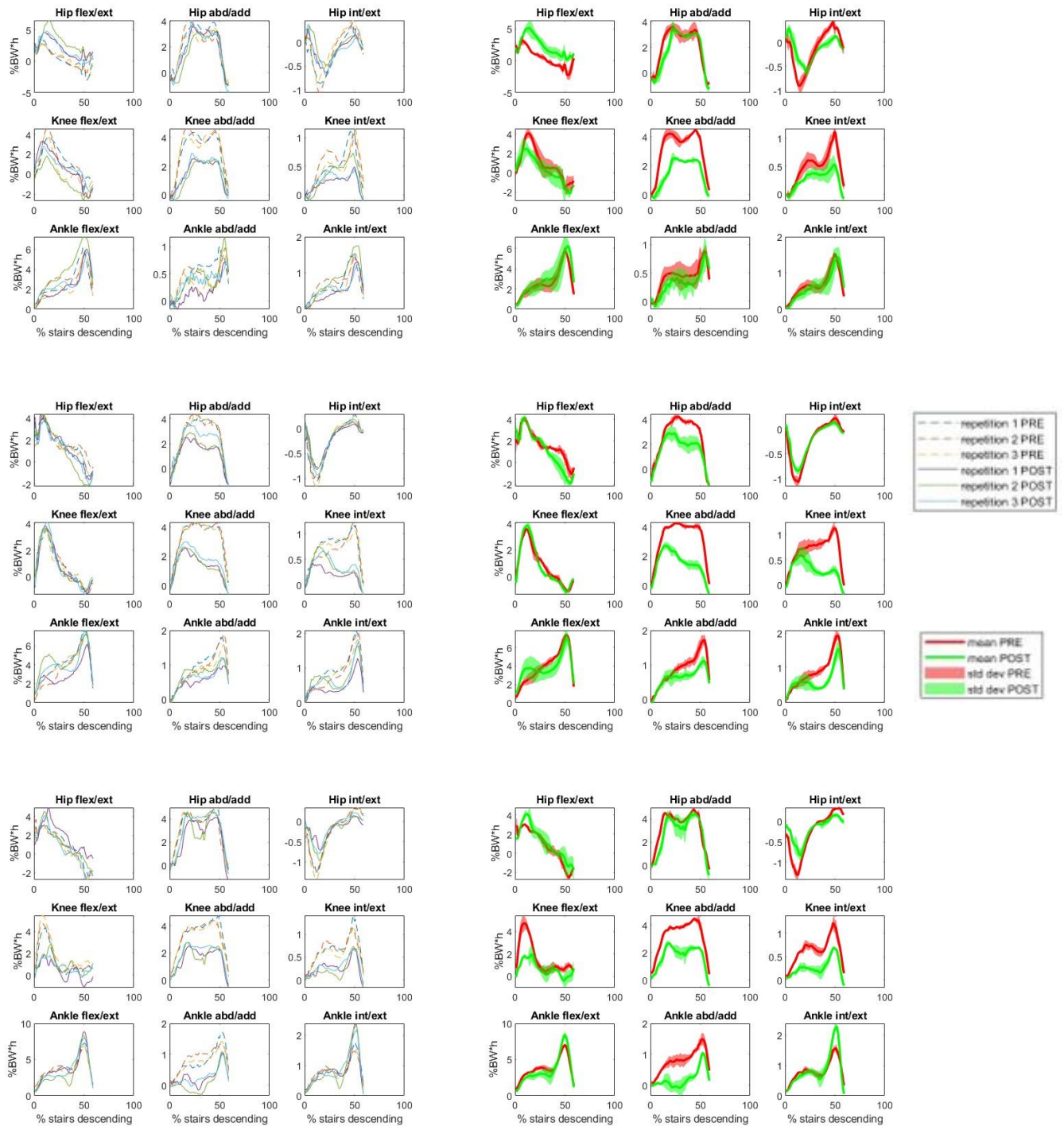


Figure 6-8: joint moments in the three repetition (on the left) and their mean and standard deviation (on the right) pre- and post-surgery during the stairs descending for three patients

- SQUAT
 - Joint Rotations

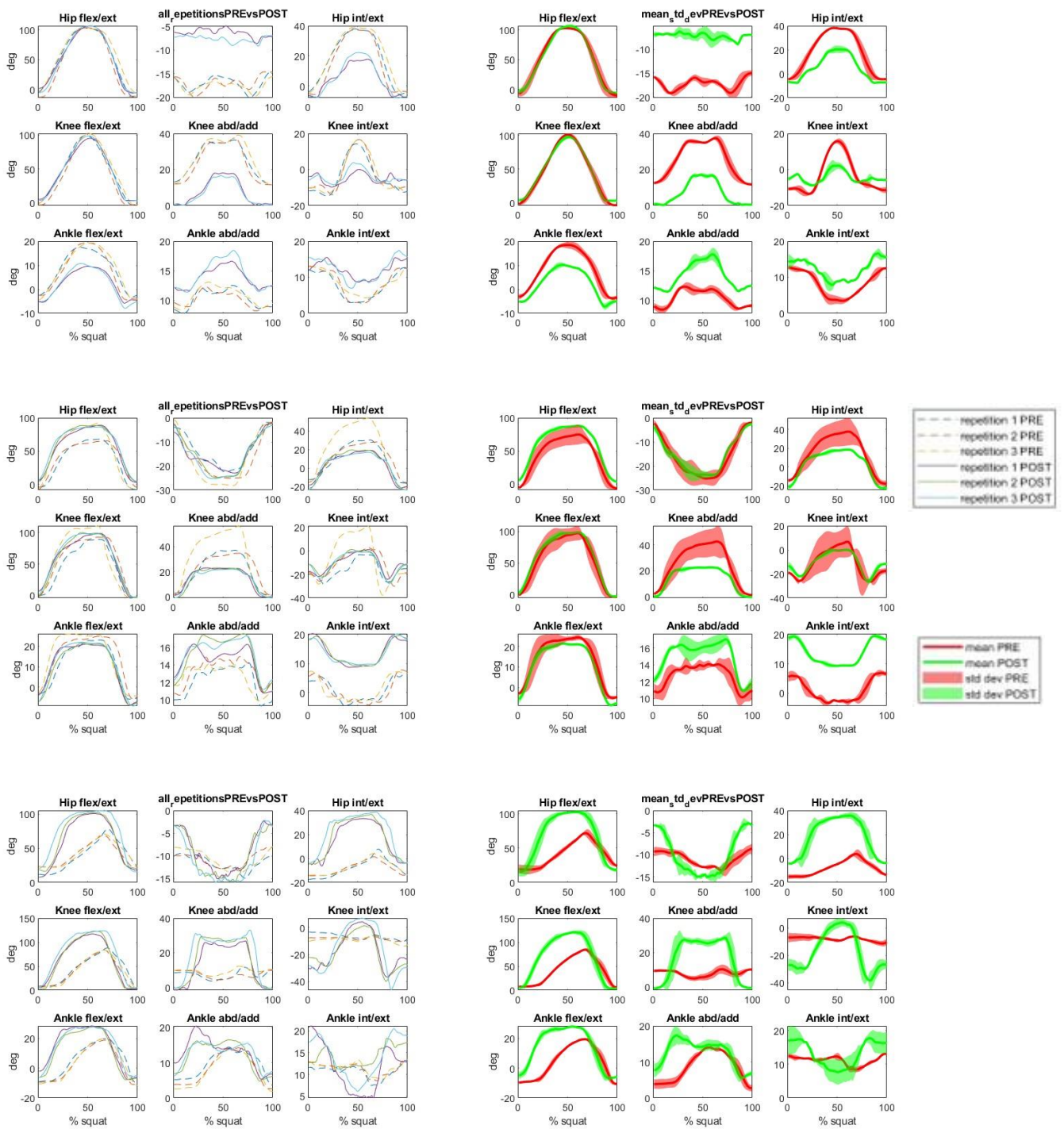


Figure 6-9: joint rotations in the three repetition (on the left) and their mean and standard deviation (on the right) pre- and post-surgery during the squat for three patients

○ Joint Moments

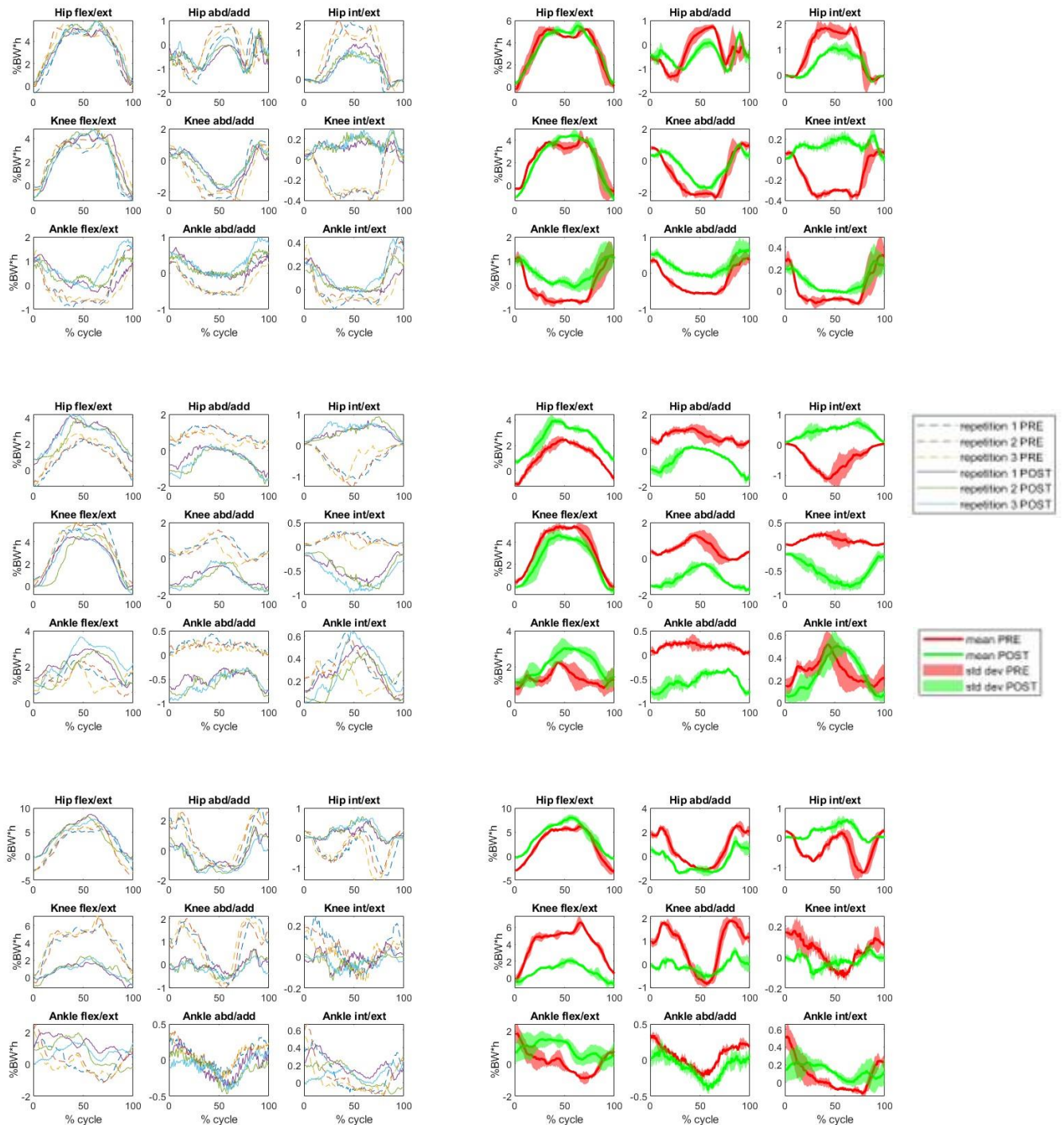


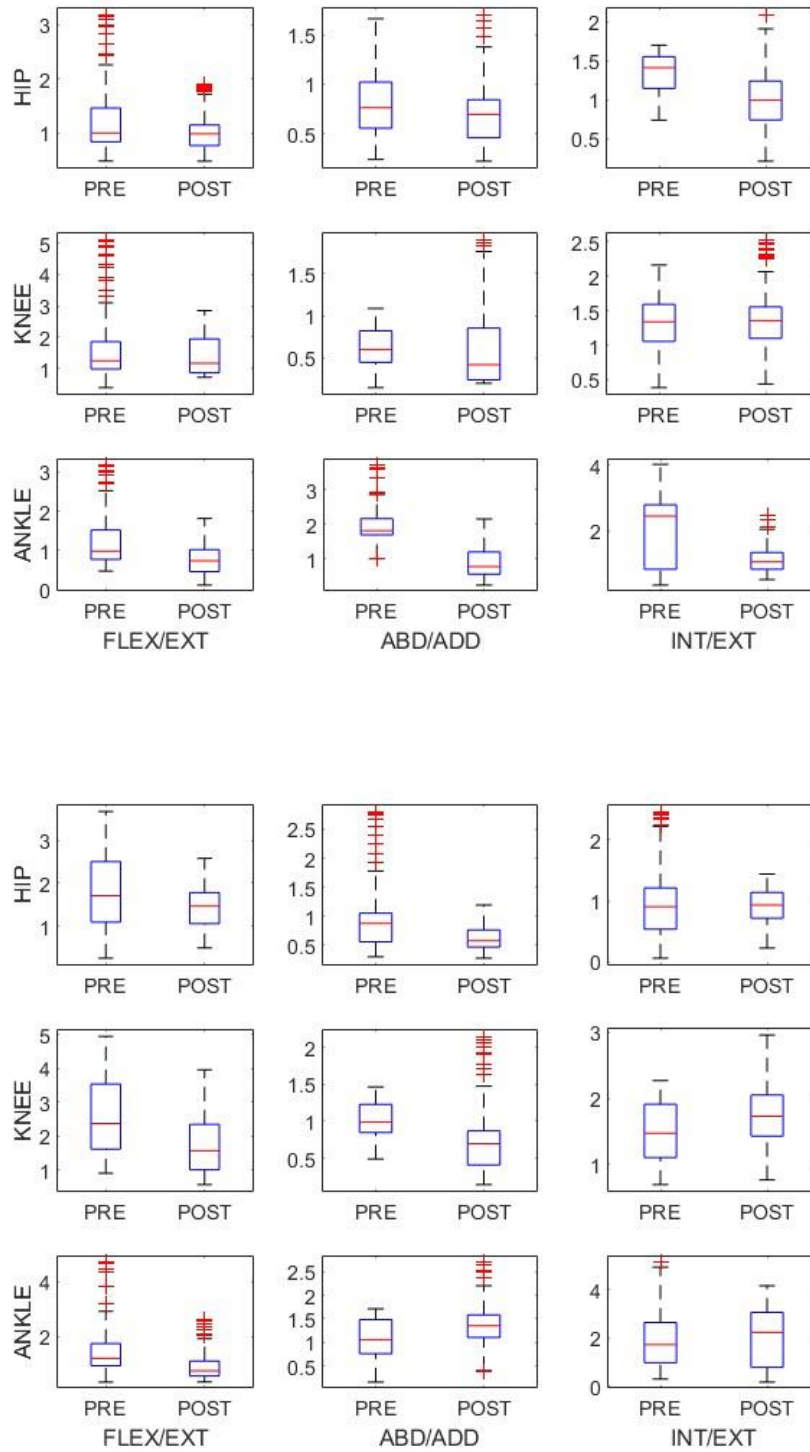
Figure 6-10: joint moments in the three repetition (on the left) and their mean and standard deviation (on the right) pre- and post-surgery during the squat for three patients

The analysis of the results shows a good repeatability of the data obtained, which even if with some punctual variations that are due to the impossibility for the subject to perform exactly the same movement. The data show a characteristic trend that supports their use to demonstrate a change between pre- and post-surgery. We speak generally of a change and not of an improvement because

the lack of a reference data set for the four motor tasks added to the gait does not allow a similar evaluation. The only motor task for which an assessment of correction is possible and therefore for which an improvement can be seen is gait. An aspect, however, that leads to a plausible assumption of a general improvement in joint function is the decrease in the standard deviation: a high variability of the data between the tests acquired on the same subject and under the same operating conditions can be considered a symptom of a mechanical instability that causes a variation in the manner in which the motor tasks are performed, and therefore an average decrease in the standard deviation between pre- and post-surgery can be interpreted as an improvement.

To better investigate this aspect and assess whether there is indeed a variation in the standard deviation, the data were analysed with box plots that allow us to show the mean variation, the dispersion of the data and, unlike other statistical methods, allow us to take into account those anomalous data due to random acquisition errors by labelling them as outliers. We give as example the graphs obtained for some significant subjects:

- Joint Rotations



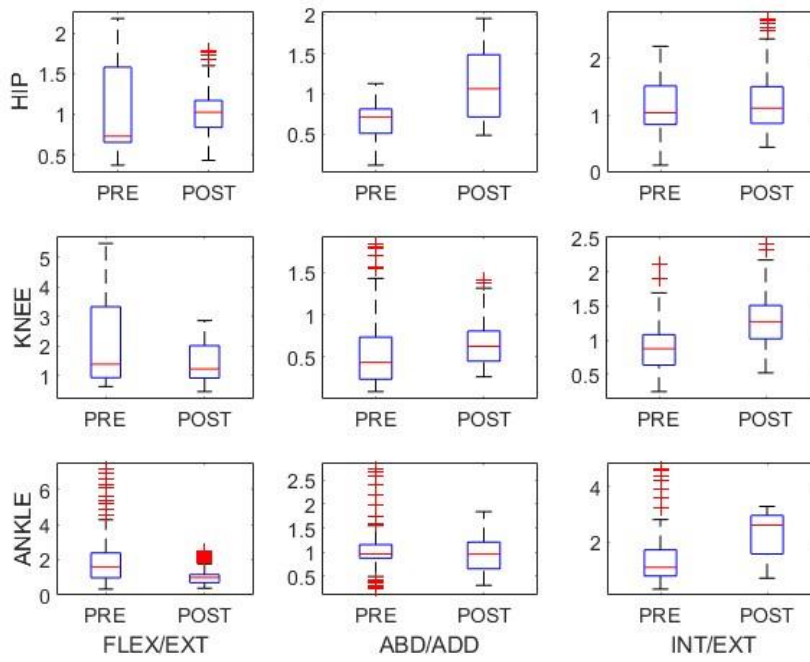
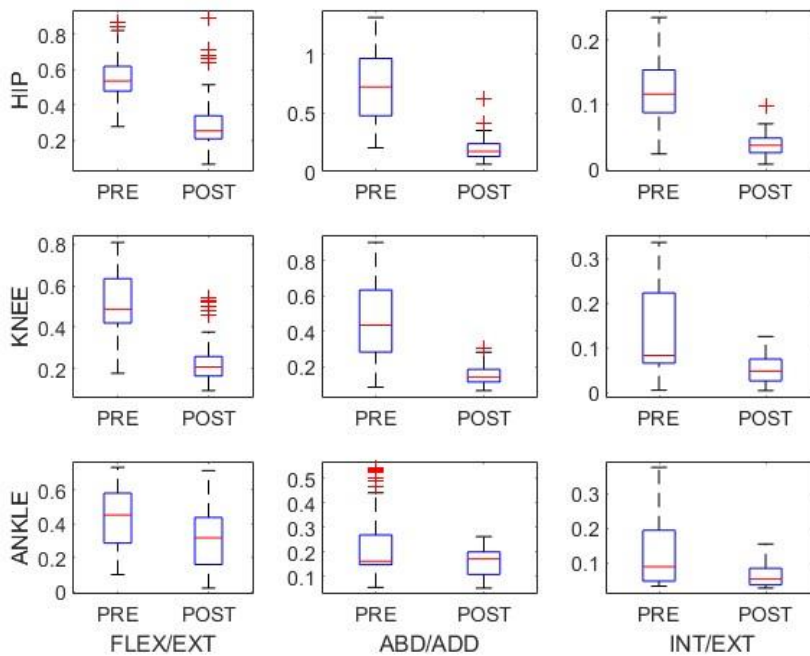


Figure 6-11: comparison of the rotation standard deviation values of three patients to assess their variation

- Joint Moments



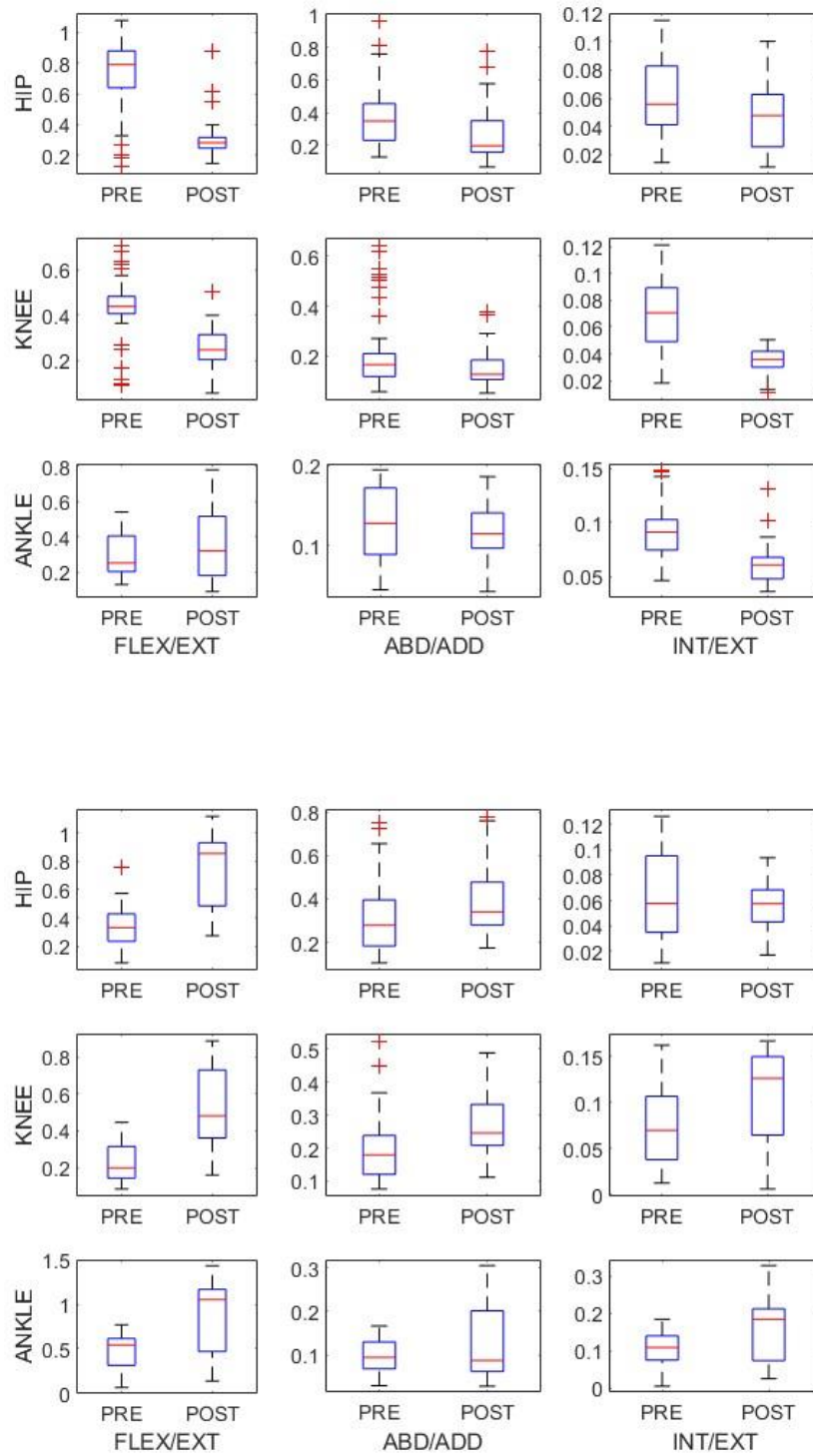


Figure 6-12: comparison of the moment standard deviation values of three patients to assess their variation

6.1.1.2 Inter-patient repeatability

In this section we will instead analyse the repeatability of the intra-patient data in order to verify the existence of specific patterns in the data or at least a band within which they fall. It should be noted that this comparison is made possible by normalising the data on joint moments. In the case of the rotations, although there is a certain dependence on the specific anatomy of the subject, but this can be neglected and therefore the data used for this work are the rotations obtained as output of the acquisition system, while to evaluate the articular moment, since there is a strong dependence on the body mass index as well as on the height, in order to be able to compare the data of the different subjects, a normalisation of the data was carried out.

- GAIT

- Joint Rotation

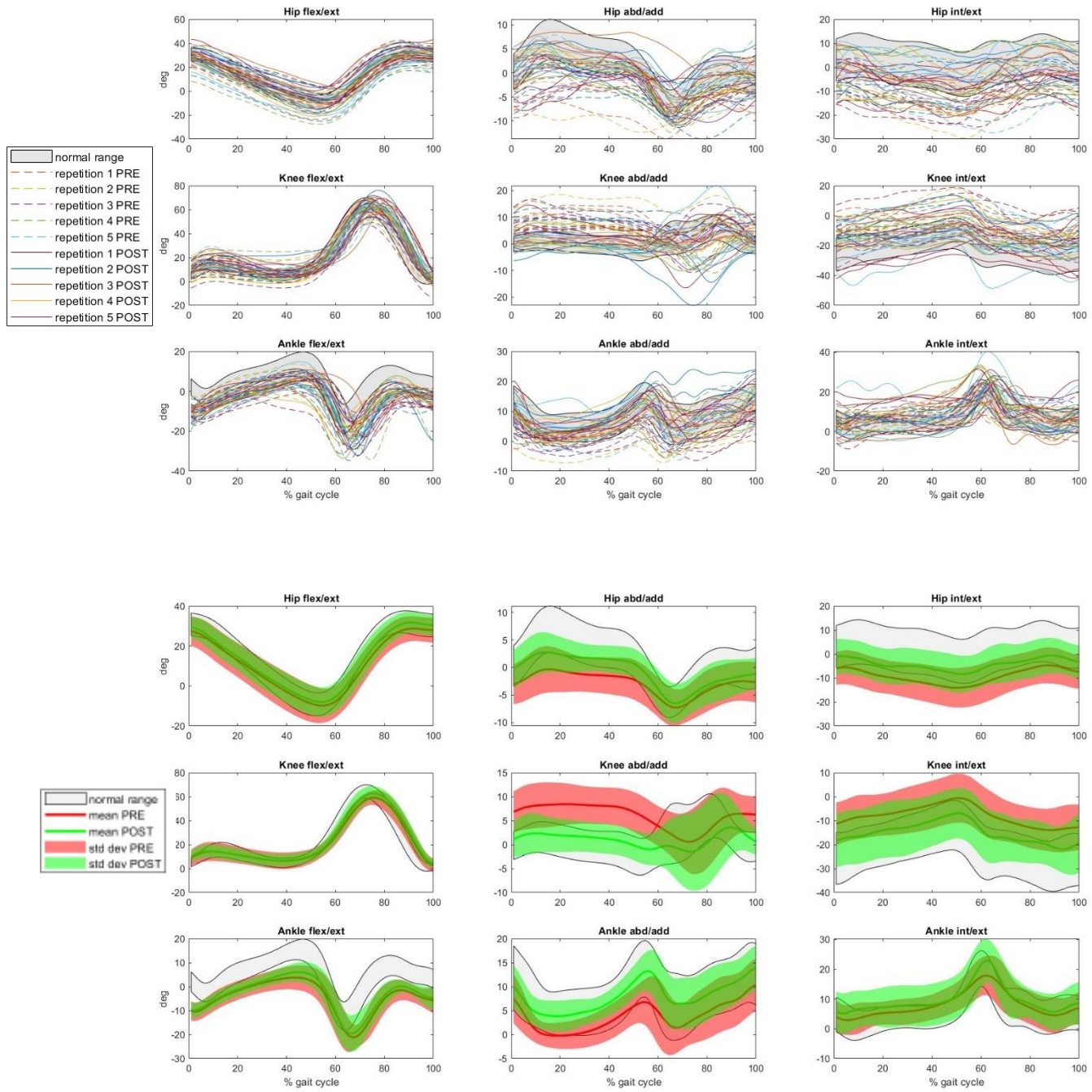


Figure 6-13: plot of the rotations data for a single repetition (in the upper figure) and with mean and standard deviation (in the bottom figure) of all patients during the gait analysis

○ Joint Moment

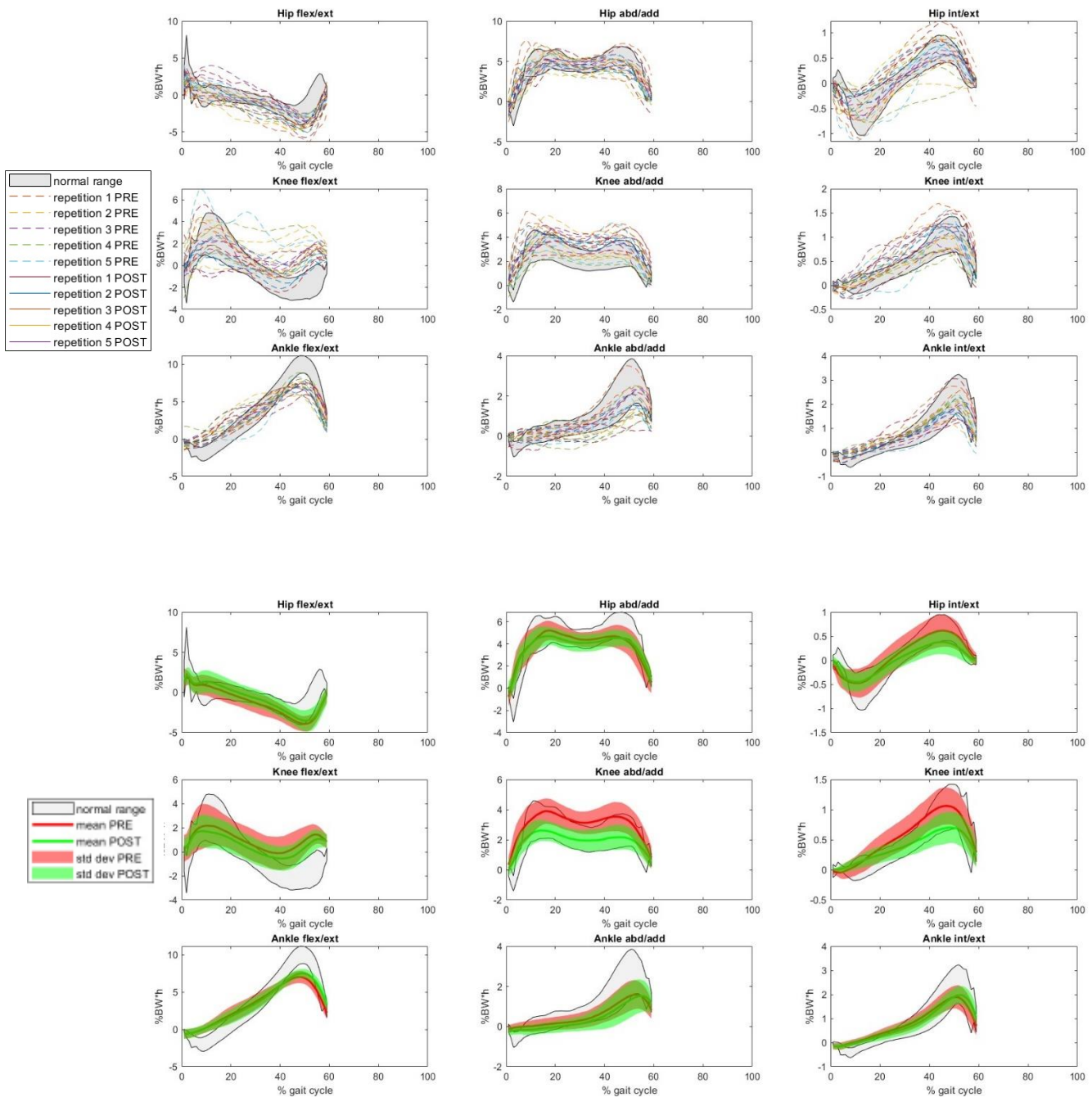


Figure 6-14: plot of the moments data for a single repetition (on the left) and with mean and standard deviation (on the right) of all patients during the gait analysis

As previously mentioned, being able to make a comparison with a normal range for the gait analysis, the variation between the two data set can be interpreted as a substantial improvement of the articular mechanics: from Figures 6-13 and 6-14 we can in fact see how the average trend shows a substantial approach to the normal range, but this data, although encouraging, must always be read

taking into account the high variability and therefore the thickness of the range. Let us now evaluate the data of the other motor tasks:

- CHAIR

- Joint Rotation

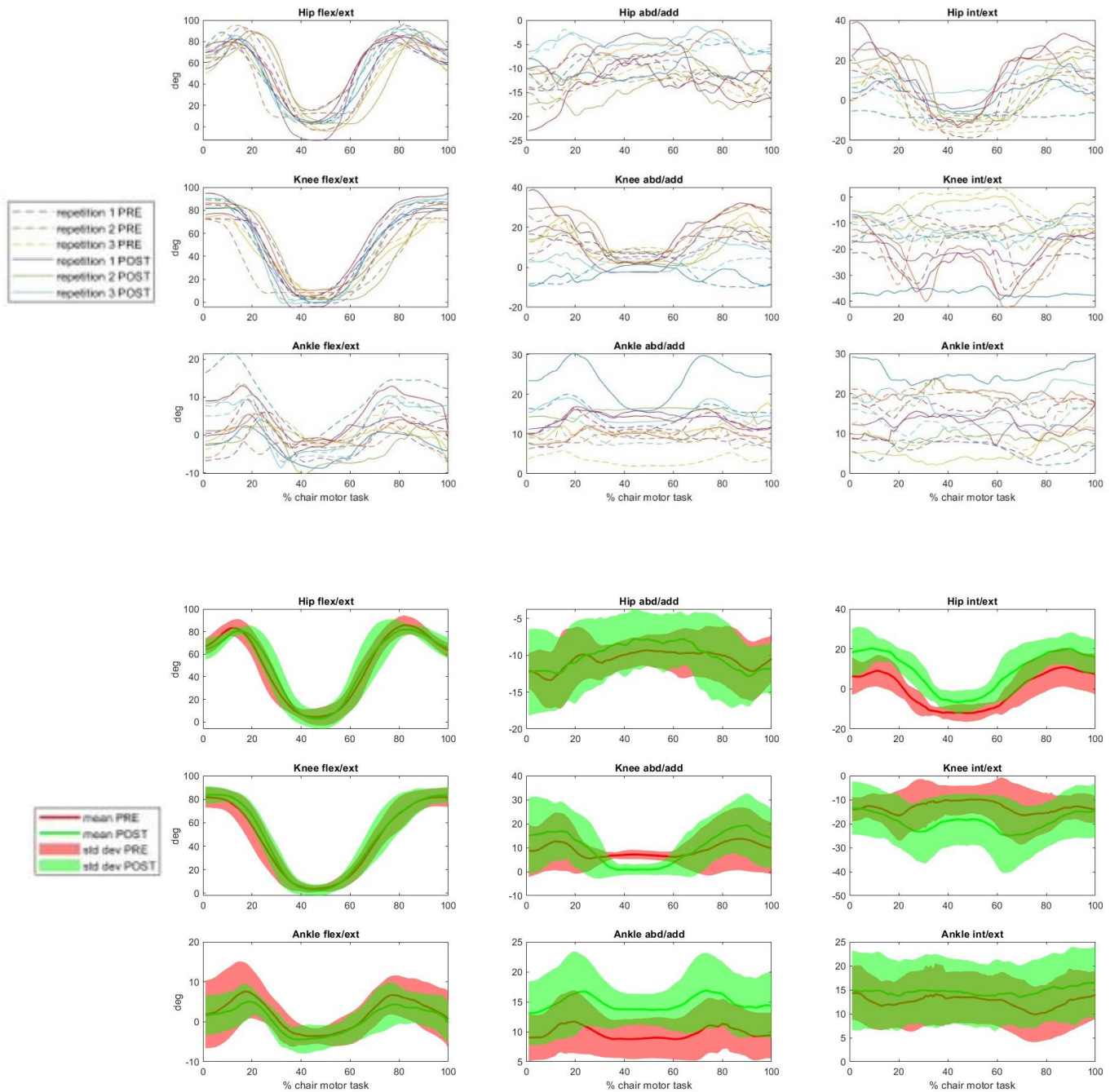


Figure 6-15: plot of the rotations data for a single repetition (on the left) and with mean and standard deviation (on the right) of all patients during the chair motor task

○ Joint Moment

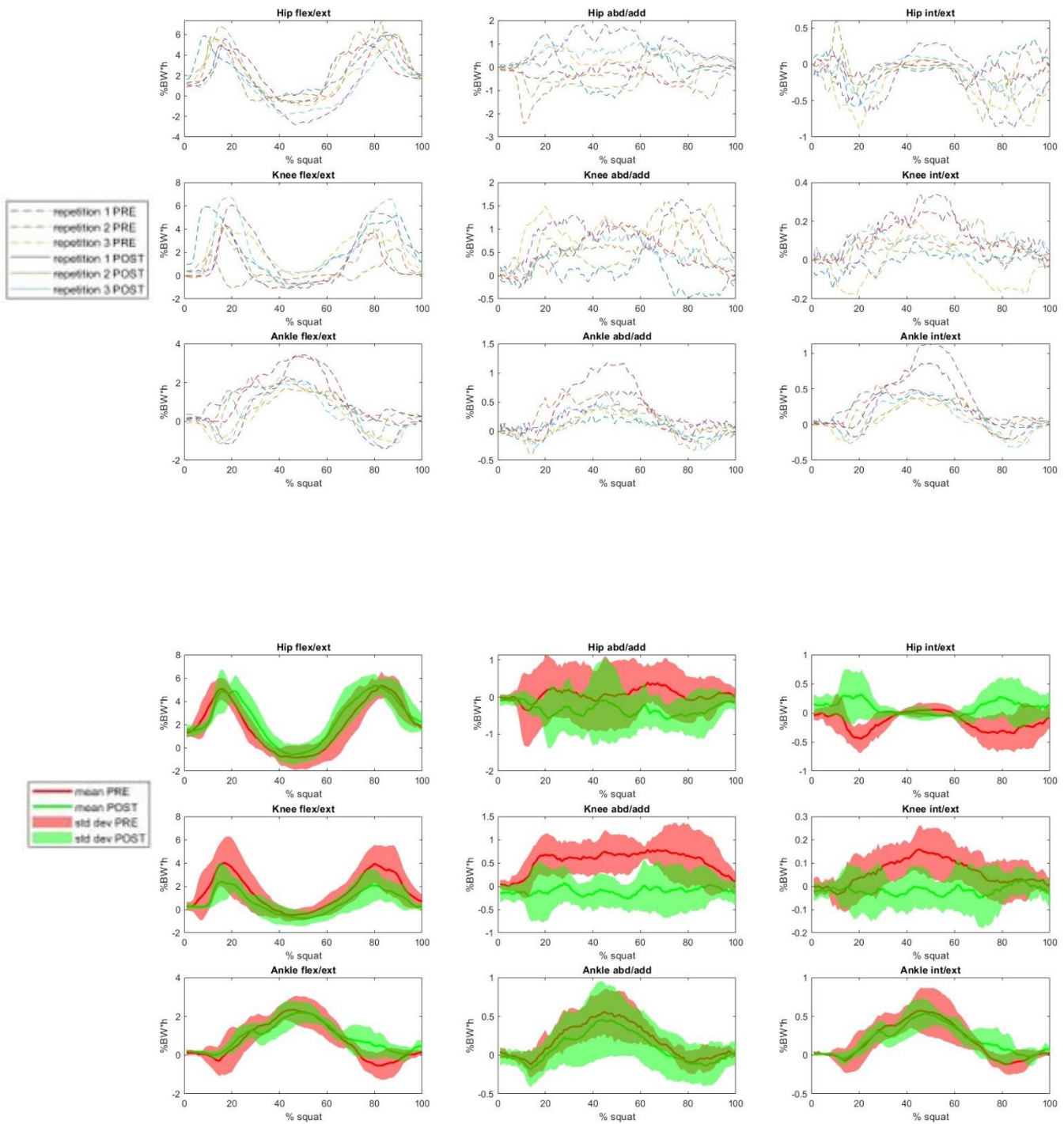


Figure 6-16: plot of the moments data for a single repetition (on the left) and with mean and standard deviation (on the right) of all patients during the chair motor task

- STRAIRS CLIMBING

- Joint Rotation

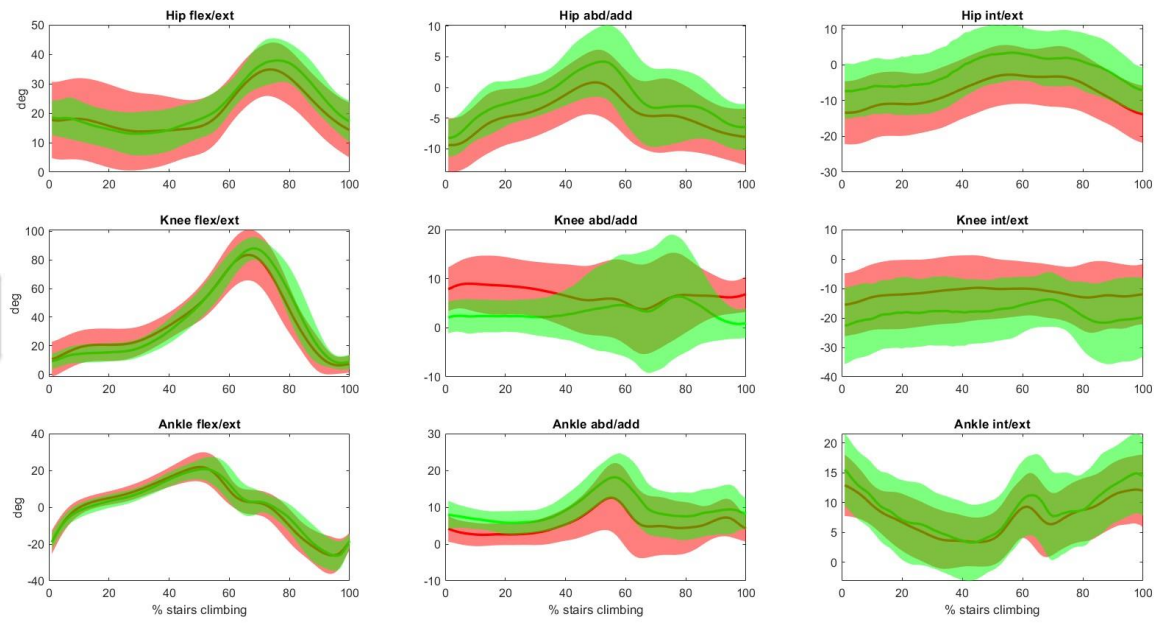
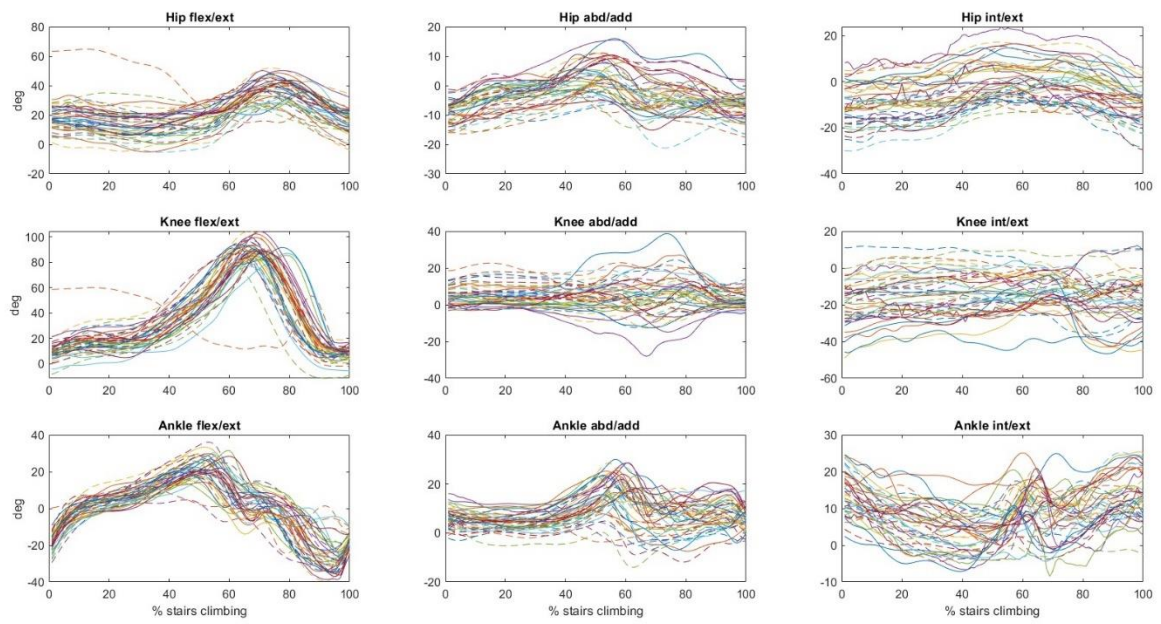


Figure 6-17: plot of the rotations data for a single repetition (on the left) and with mean and standard deviation (on the right) of all patients during stairs climbing

○ Joint Moment

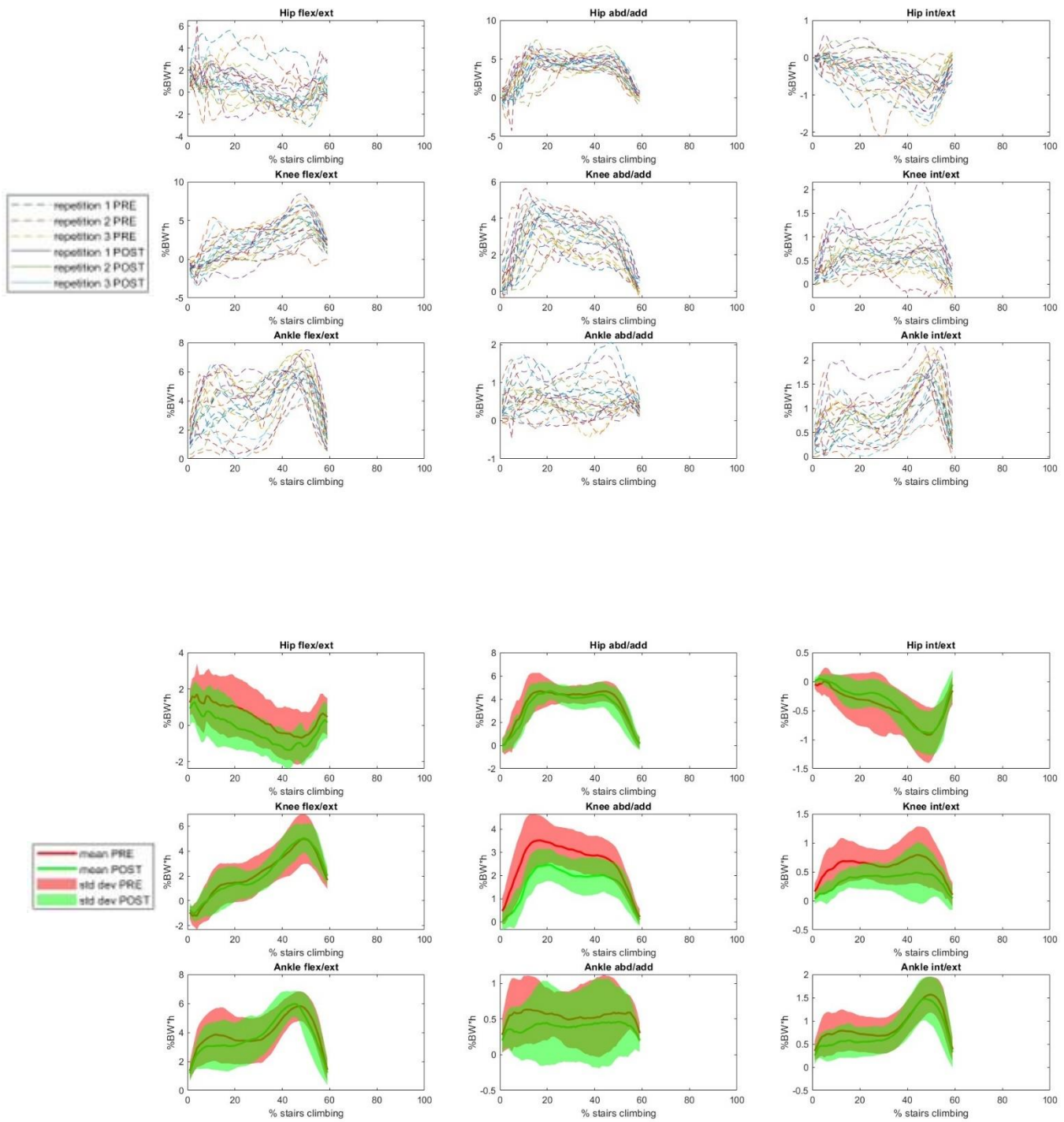


Figure 6-18: plot of the moments data for a single repetition (on the left) and with mean and standard deviation (on the right) of all patients during the stairs climbing

- STAIRS DESCENDENT

- Joint Rotation

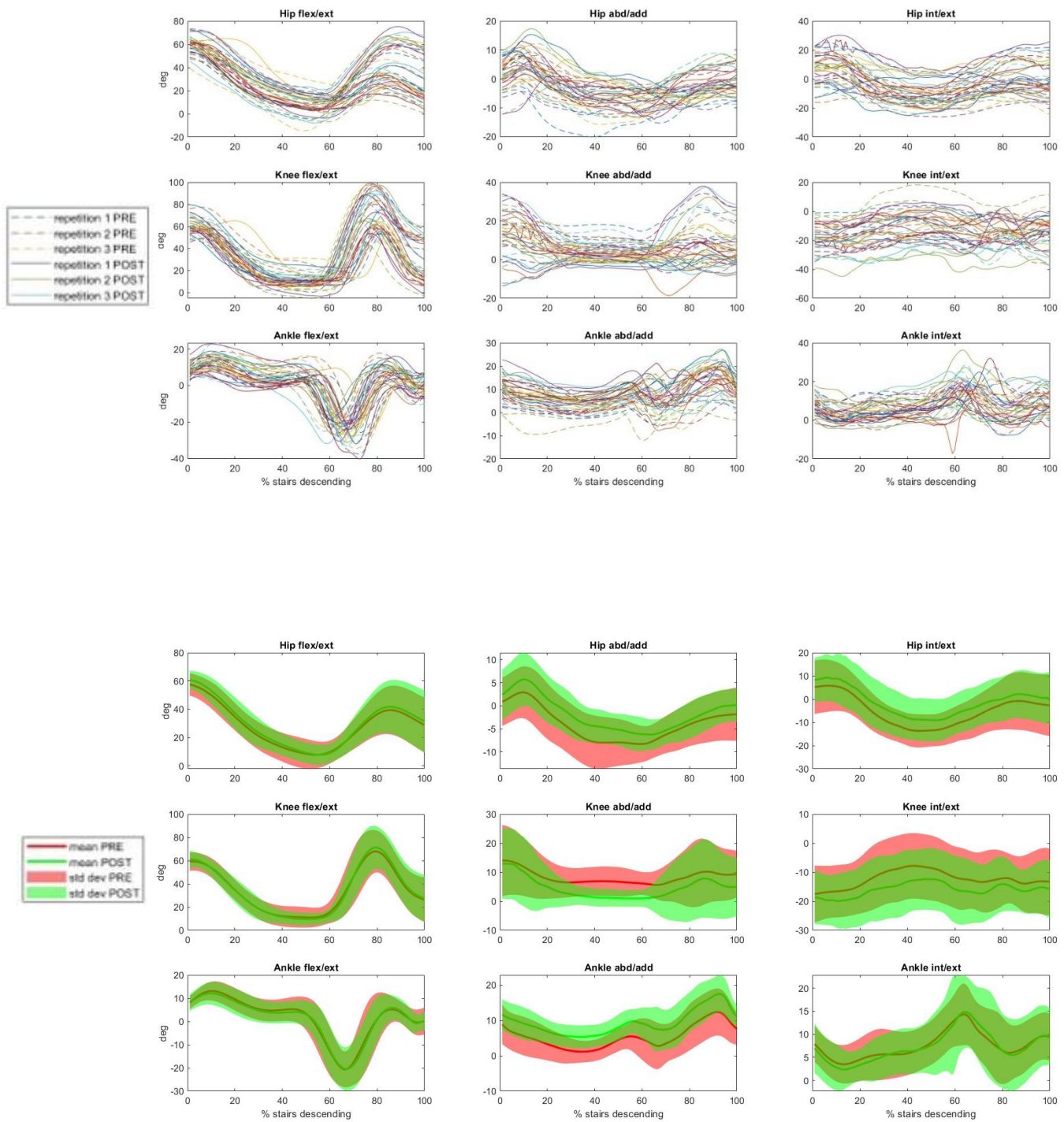


Figure 6-19: plot of the rotations data for a single repetition (on the left) and with mean and standard deviation (on the right) of all patients during the stairs descend

○ Joint Moment

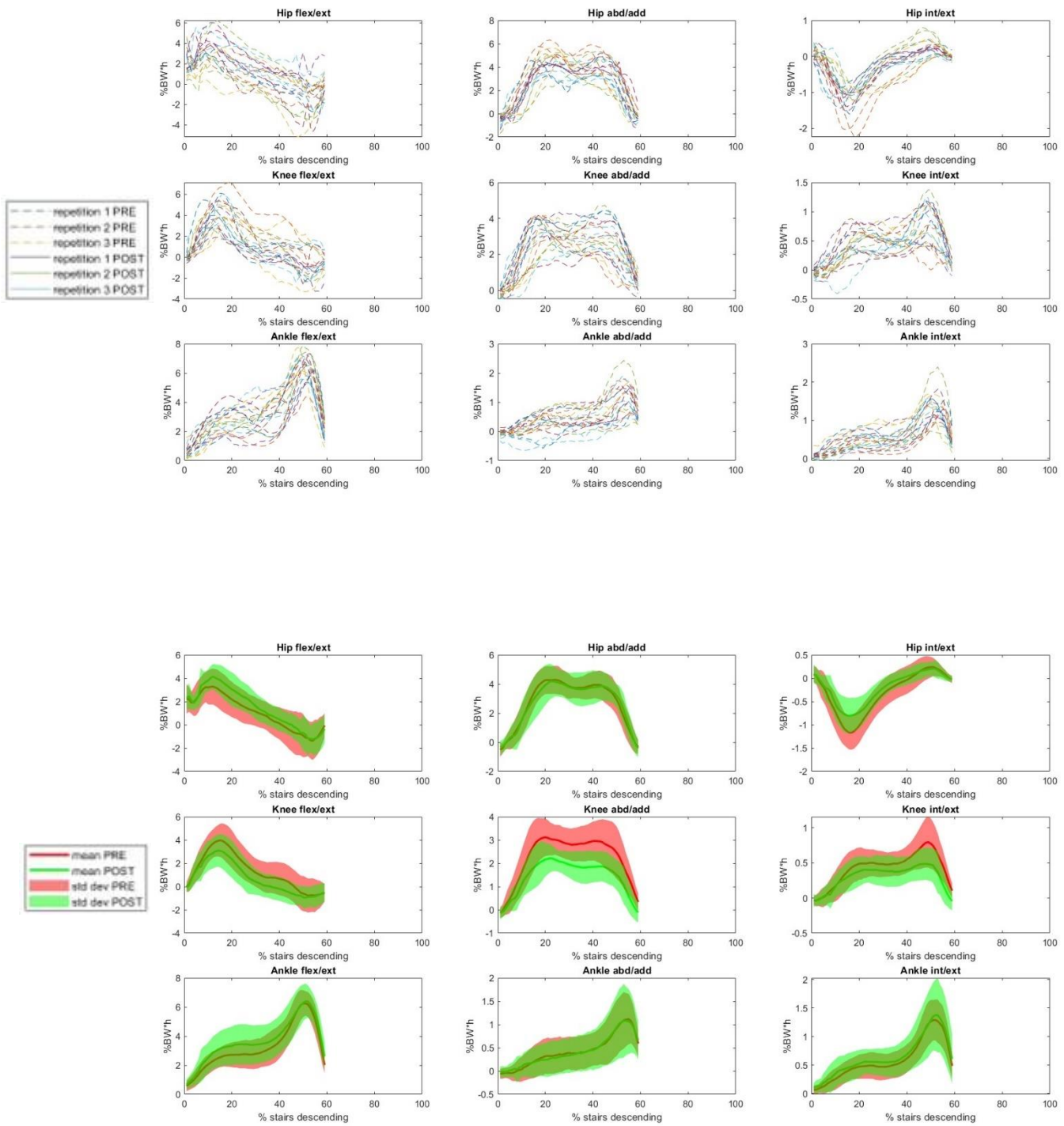


Figure 6-20: plot of the moments data for a single repetition (on the left) and with mean and standard deviation (on the right) of all patients during the stairs descendent

- SQUAT

- Joint Rotation

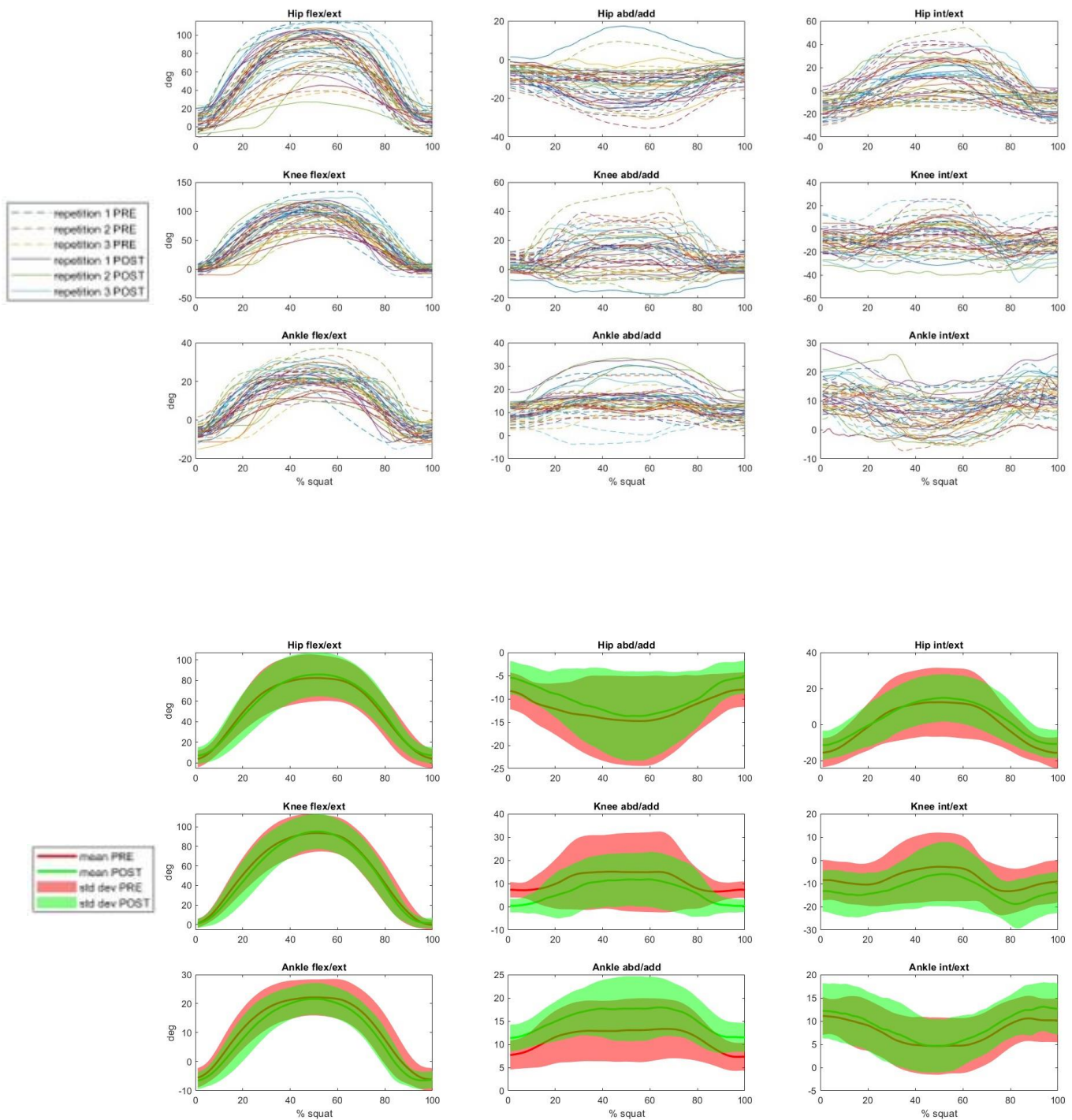


Figure 6-21: plot of the rotations data for a single repetition (on the left) and with mean and standard deviation (on the right) of all patients during the squat

○ Joint Moment

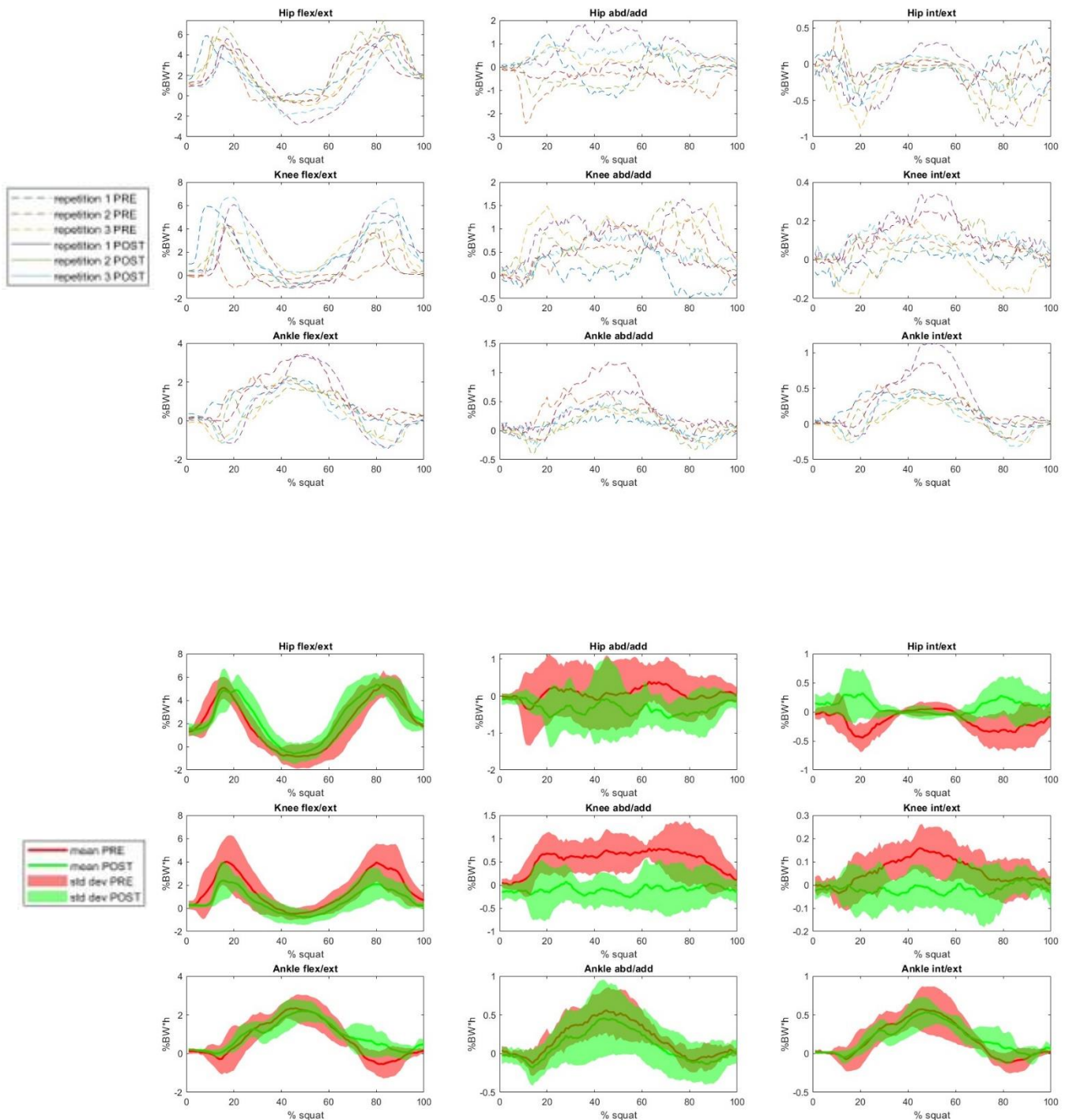
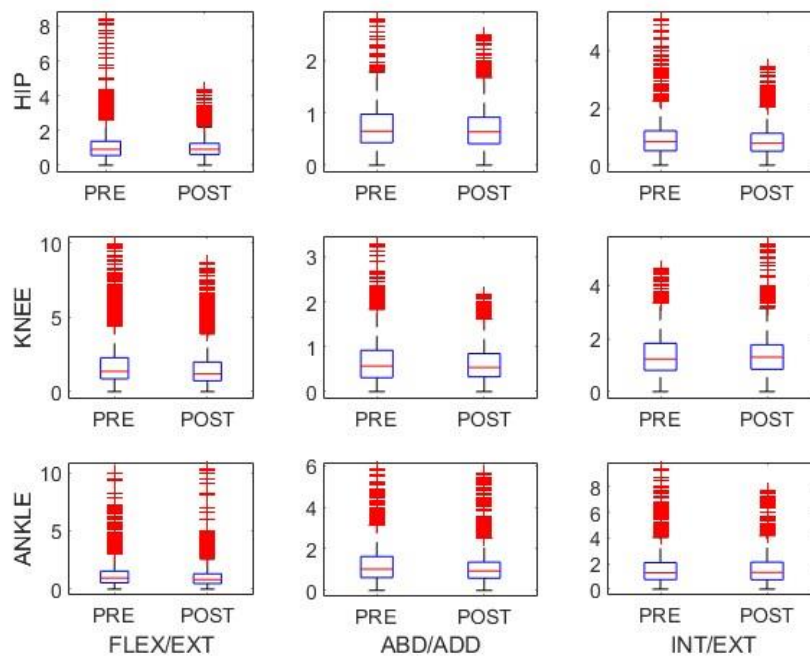


Figure 6-22: plot of the moments data for a single repetition (on the left) and with mean and standard deviation (on the right) of all patients during the squat

An analysis of the data in aggregate of the entire data set of subjects involved in the study also shows good repeatability of the data, although looking at the standard deviation values and comparing them with those obtained in the intra-patient study shows a much higher variability for

all five motor tasks. Despite this, we can still see a certain repeatability of the patterns and a substantial difference between pre- and post-surgery. Thus, despite a process aimed at normalising the data, there is still a great deal of variability between subjects and thus a dependence of the numerical data on the anatomical parameters of the subject. To complete this analysis, we can evaluate the change in standard deviation between pre- and post-surgery to see if there is a change by boxplot:



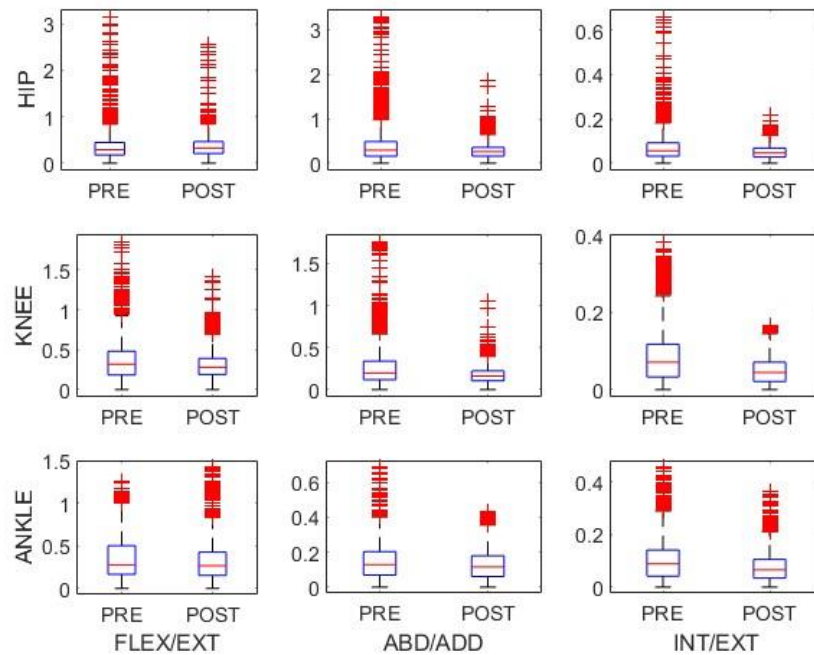


Figure 6-23: comparison of the standard deviation values between pre- and post-surgery inter-patients for the rotations and for the moments

Observing the variation in standard deviation values between the two inter-patient data sets for gait confirms the generally greater variability of the data and thus poor compliance for both rotations and moments. Exploiting the boxplots shows how many of the data are to be considered as outliers and in any case does not confirm the trend of overall decrease in variability, which can be explained by attributing these high standard deviation values to a high dependence of the data on the subject under investigation. To understand whether this variability is due to a rigid translation, or to an overall alteration of the data, please refer to the next section in which correlation calculations will be carried out.

6.1.2 Correlations

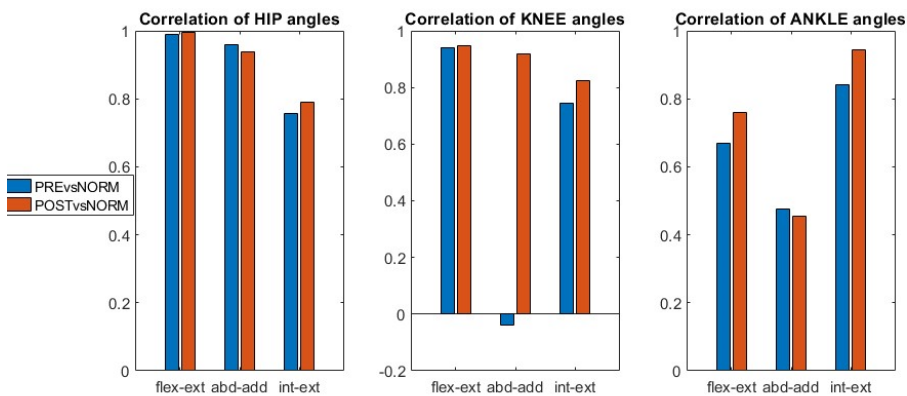
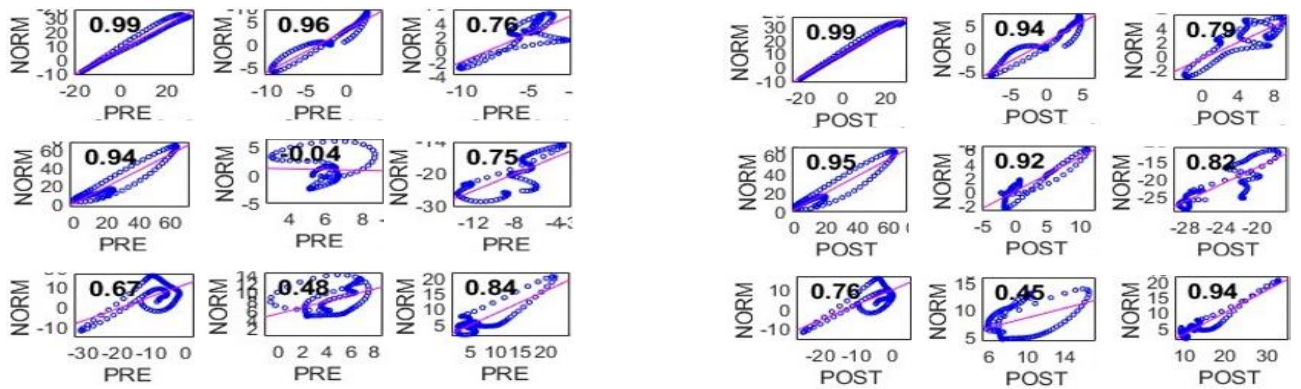
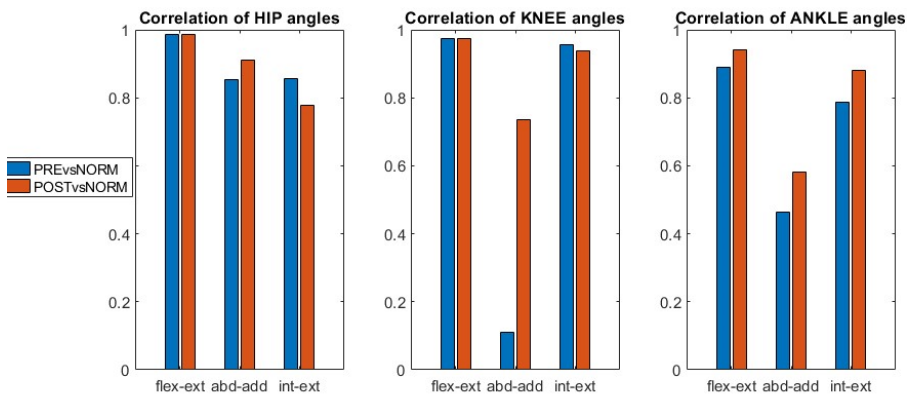
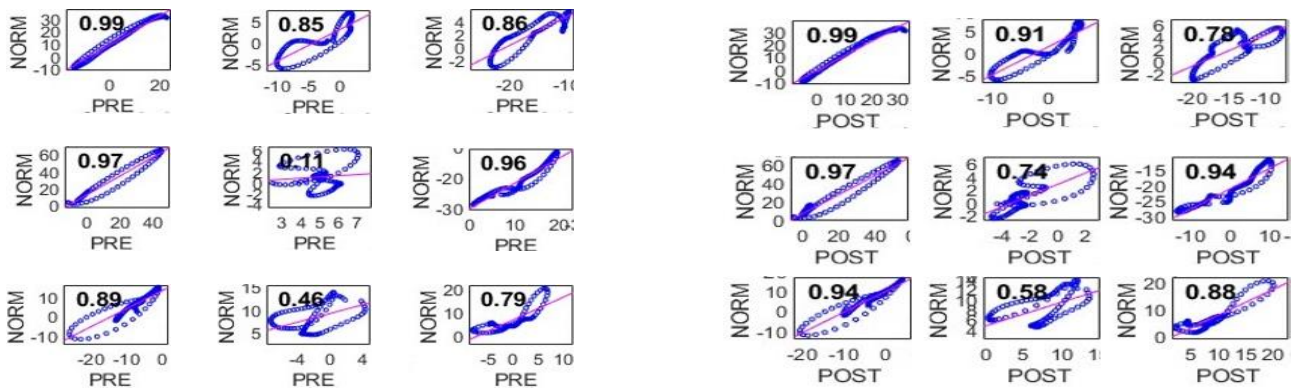
The aim of this section is to verify the existence of a link between pre, post and where present (i.e. for gait) data with normality. For this purpose, the linear correlation coefficient was chosen as an evaluation parameter; it gives an estimate of a possible link between the trends of two data sets. The limiting values are: 1 indicating that a change in the first data corresponds to the same change in the second, 0 when there is no relationship between the data trends and -1 if an increase in the first corresponds to a decrease in the second. It should be specified that a high correlation does not

imply the existence of a cause-effect relationship, but rather a conditional variability that may also be due to a common third cause, without any direct dependence between the individual variables under analysis. In the specifics of this work, the intention is to assess the correlation coefficient r , between the experimental data and the non-pathological trend and its possible variation, which is why the analysis will focus mainly on the gait data, as for the other motor tasks there is no reference. With regard to the other motor tasks, we are going to calculate the correlation coefficient between the pre- and post-surgery data in order to compare them with those obtained in gait and check whether the variations recorded between the data in the two conditions show a comparable variation (as usual, in the absence of a reference, it would be incorrect to speak of improvement). As was done with the previous data, the results obtained for three subjects that can be taken as models will be presented below, while the complete data are given in Appendix B.

6.1.2.1 Correlations of functional data in gait

In order to calculate the correlation coefficients, we used Matlab's `corrplot` function which represents the linear regression of the points and the correlation coefficient “ r ”, which we will then use for comparison. In the graphs shown, a three-by-three matrix arrangement was again chosen to simultaneously represent the data of the three joints in the three anatomical planes. Following the data on the linear regressions for each patient, the values of the r coefficients have been plotted in a bar chart to help assess its possible variation between pre and post.

○ Joint Rotation



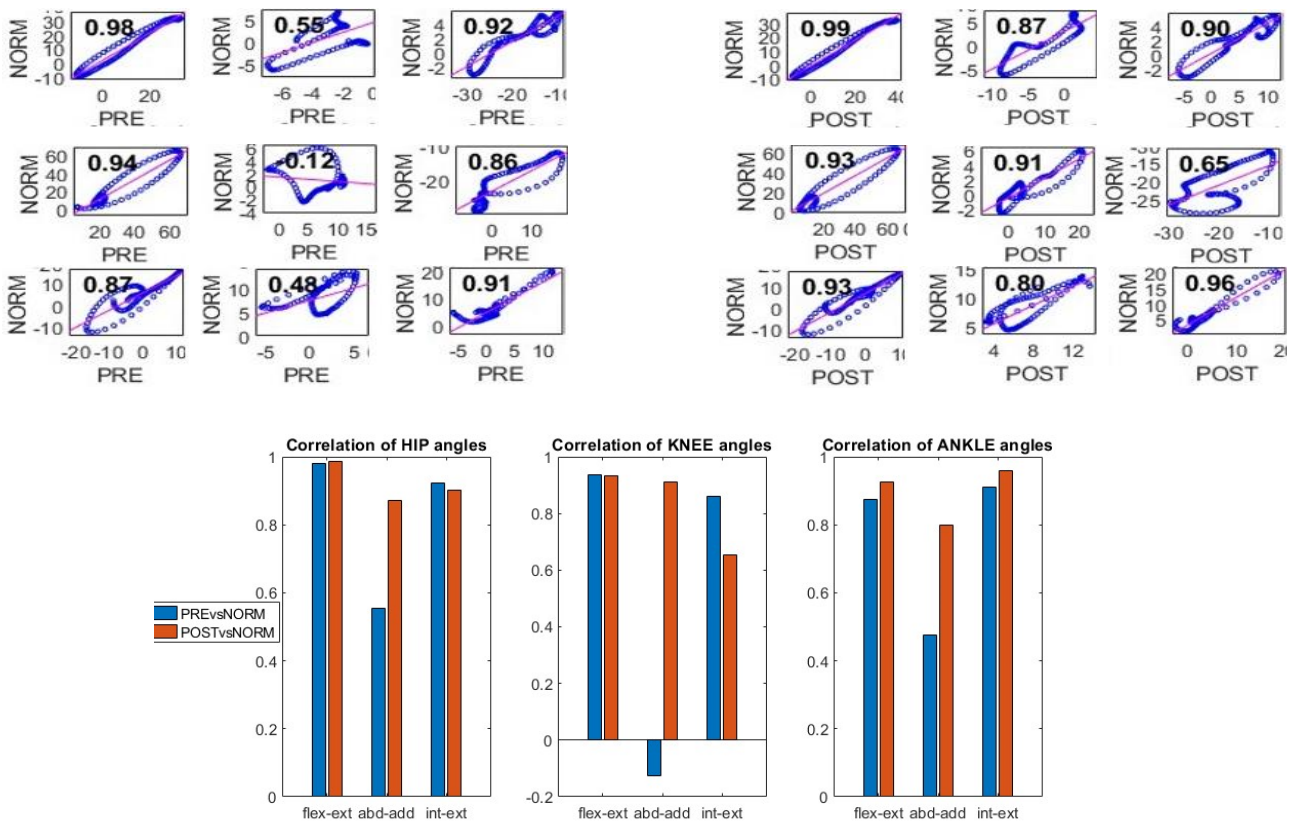
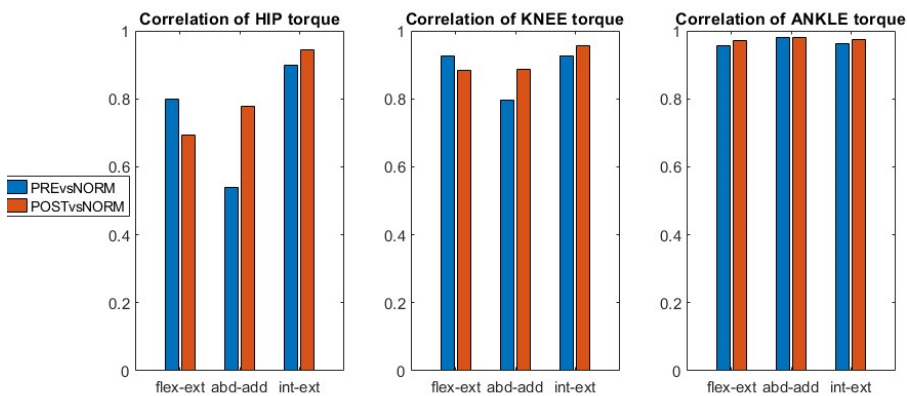
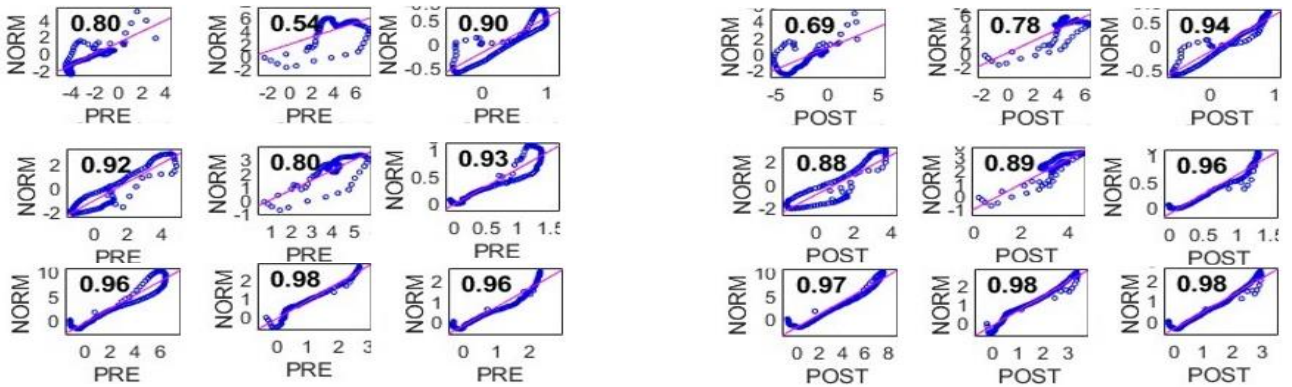
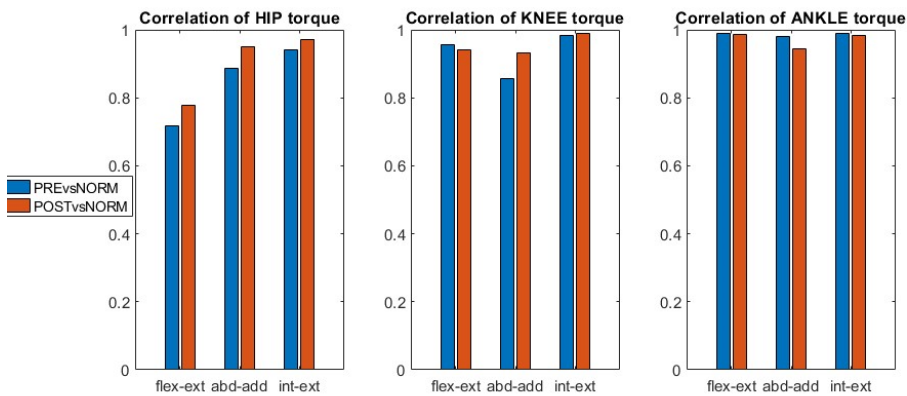
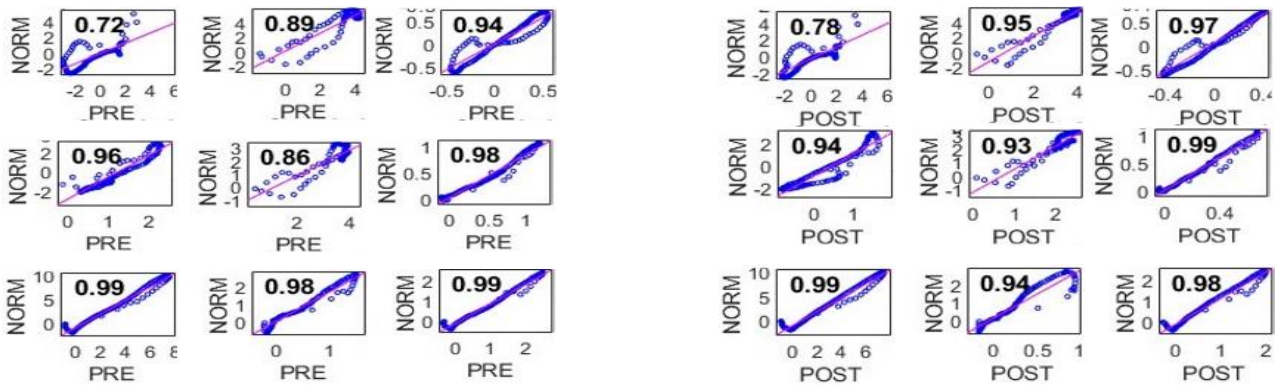


Figure 6-24: corrplot of the rotations data for three patients of PRE or POST surgery with NORMALITY and bar chart of its variation

First of all, let us note that all the correlation data reported, were accepted as statistically significant because they all registered a $p\text{-value} \ll 0.005$ (for a detailed evaluation please refer to Annex B). Observing the data on the correlation of the articular rotations we immediately notice how the three joints have a very different behaviour: in general the most significant data are those of knee abduction adduction, which in the pre-operative show an uncorrelation with the normal data, or in some cases there even seems to be an inverse proportionality relationship as there are negative r values even if they are low. This finding is in agreement with the type of anatomical disorder to be corrected by this surgical technique, knee varus, in which a mechanical axis of the femur deviated laterally (in the near-distal direction) causes abnormal rotation in the joint. It is interesting to note, however, that even in the data of the other joints, which immediately show fairly high correlation values, a good improvement in the data can be observed with a certain frequency, and no cases have been observed in which the surgical technique has caused an obvious worsening.

○ Joint Moment



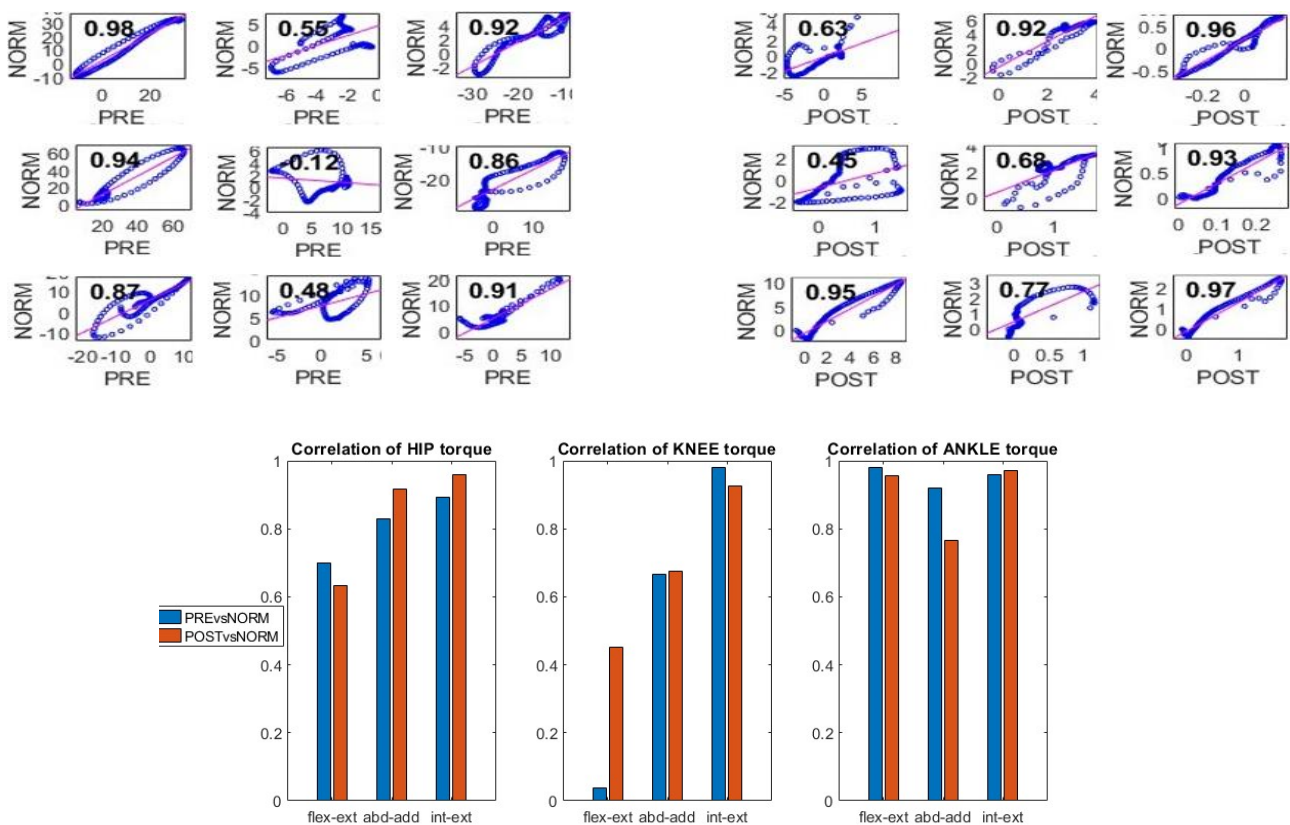


Figure 6-25: corrplot of the moments data for three patients of PRE or POST surgery with NORMALITY and bar chart of its variation

Turning to the data obtained for the correlations of the articular moments, one immediately notices how, unlike the rotations in both situations, there is no particularly critical specific articular component, which is also easy to justify if one remembers that the subjects involved in the study were selected to have a moderate pathological level, a reduced mechanical axis deviation and in general a good clinical-functional picture (for details, see section 4.1.2 on the criteria for inclusion and exclusion from the study). Correlation data are generally high and there is a good improvement in adherence with normal data following surgery.

The data comprising the entire data set is now reported for an overall assessment of the situation between pre- and post-surgery; again, for an accurate analysis of the data, taking into account any outlier variables, the use of boxplots was opted for:

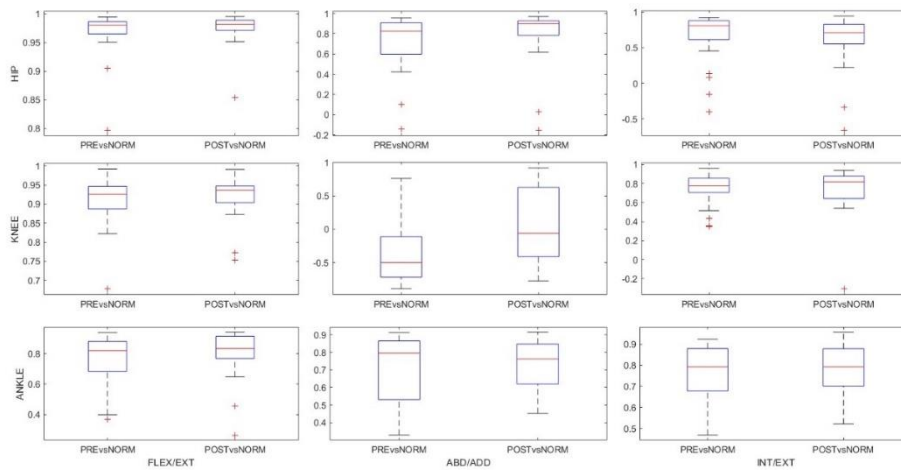


Figure 6-26: comparison of correlation coefficients of pre- and post-surgery joint rotations with normality

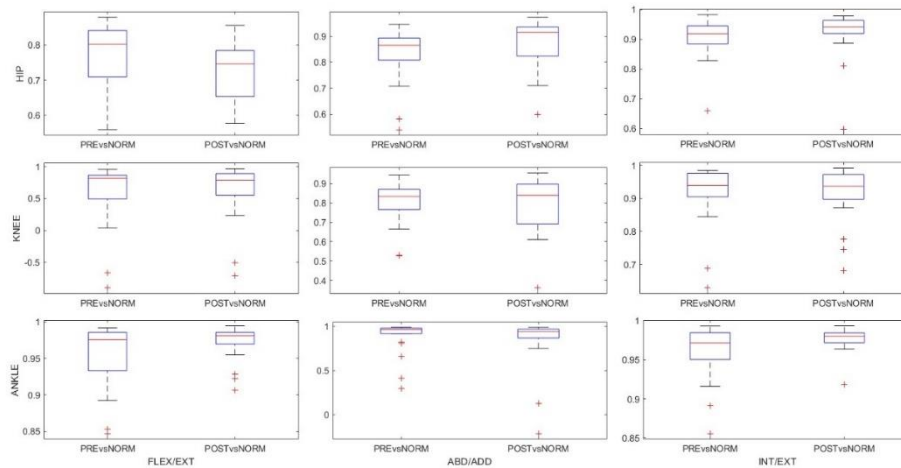


Figure 6-27: comparison of correlation coefficients of pre- and post-surgery joint moments with normality

Also from the analysis of the correlation data in aggregate of the entire data set, we can see that for the two main functional variables there is a good improvement in the data and, as assumed from the trend graphs seen for the repeatability studies, a substantial similarity between the trends. We had in fact seen how the analysis of the standard deviation of the data in aggregate had not been sufficient to show an improvement in the data, or at least a variation thereof, but by observing the overall trend we had assumed the existence of a common trend, of specific patterns that the data followed even though numerically distant, a sort of rigid translation between patients. This hypothesis is confirmed by correlation studies that have shown that both pre and post are strongly correlated with normal data and that there is a noticeable improvement following surgery. In this case, the data on the joint moments are also less affected by the dependence on the anatomical parameters of the subjects studied and in fact the standard deviation shown of the boxplot for the

moments does not show a strong increase compared to that of the joint rotations and in general stays at moderate values.

For the additional motor tasks, as there was no non-pathological reference, the same processing could not be carried out. The only correlation parameter that could be calculated was that between the pre- and post-surgery data of the various subjects, in order to verify the existence of a variation (as usual, it would be incorrect to speak of functional improvement). However, in order to have some reference to help us interpret the data, the correlation between the same data was also calculated in the gait where a positive variation was already shown. We therefore report the data obtained for gait by means of corrplot's function:

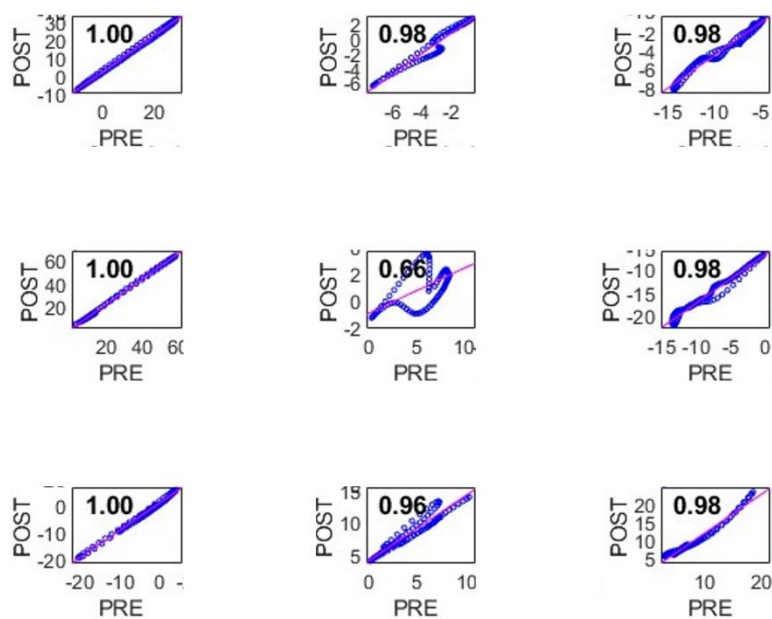


Figure 6-28: correlation indices of joint rotations between pre- and post-surgery on the entire data set in the gait analysis

From the analysis of the data on the correlations between pre- and post-surgery of the entire data set of the subjects involved, we can see that the observation on the abd-adduction component is confirmed as the one that registers the greatest change. For the other joint rotation components, the r coefficients are close to 1, which means that the data follow a similar trend.

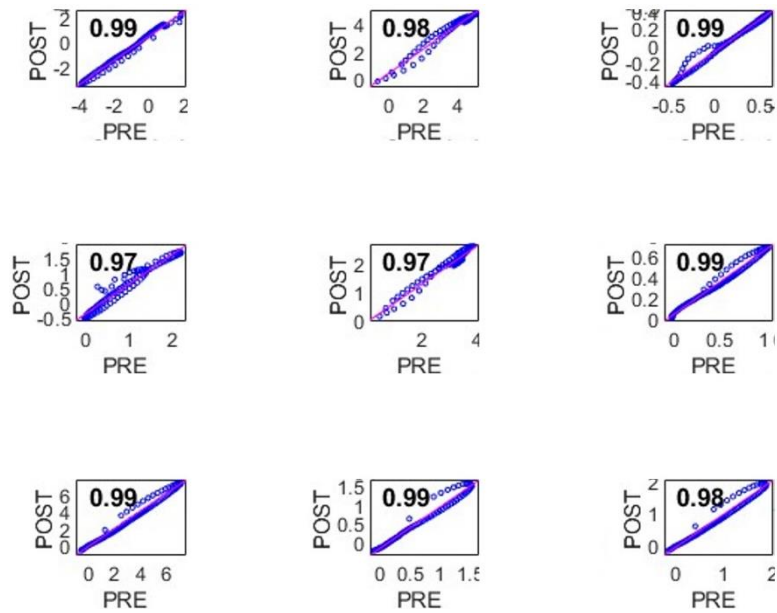
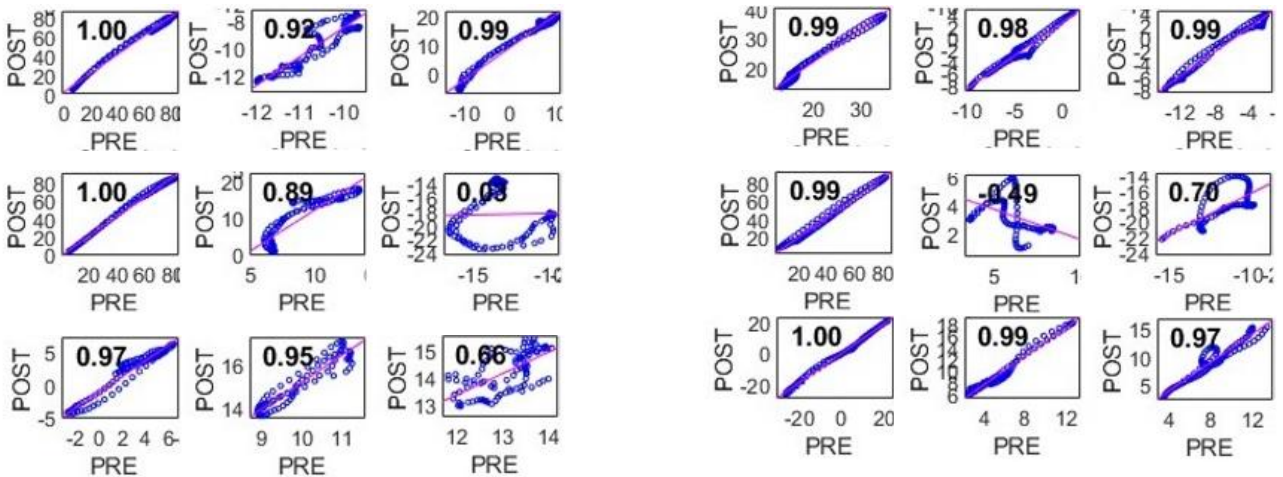


Figure 6-29: correlation indices of joint moments between pre- and post-surgery on the entire data set in the gait analysis

Also in the case of the joint moments, the data obtained from the correlations between the two moments under examination over the entire data set shows no differences from what we have already seen: there is in general a good fit of the data and the variations, although present, did not significantly alter the trajectories of the data.

6.1.2.2 Correlations of functional data in the other motor tasks

- Joint Rotation



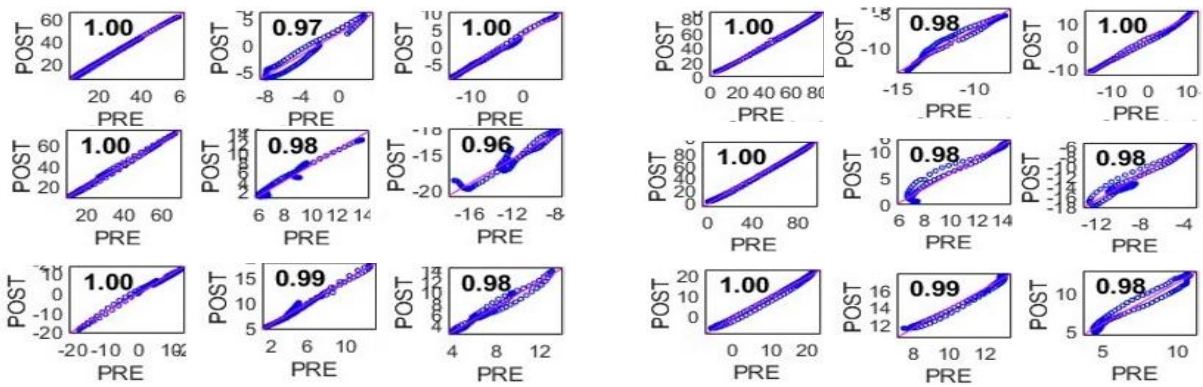


Figure 6-30: correlation indices of joint rotations between pre- and post-surgery on the entire data set in the four motor tasks, respectively: chair motor task, stairs climbing and descending and squat

Looking at the data obtained for the other four motor tasks, we can see that many of the components have significantly lower correlation coefficients than those calculated in gait, which shows that for these tasks that are more demanding, the surgery changed the patterns of rotations incisively.

- Joint Moment

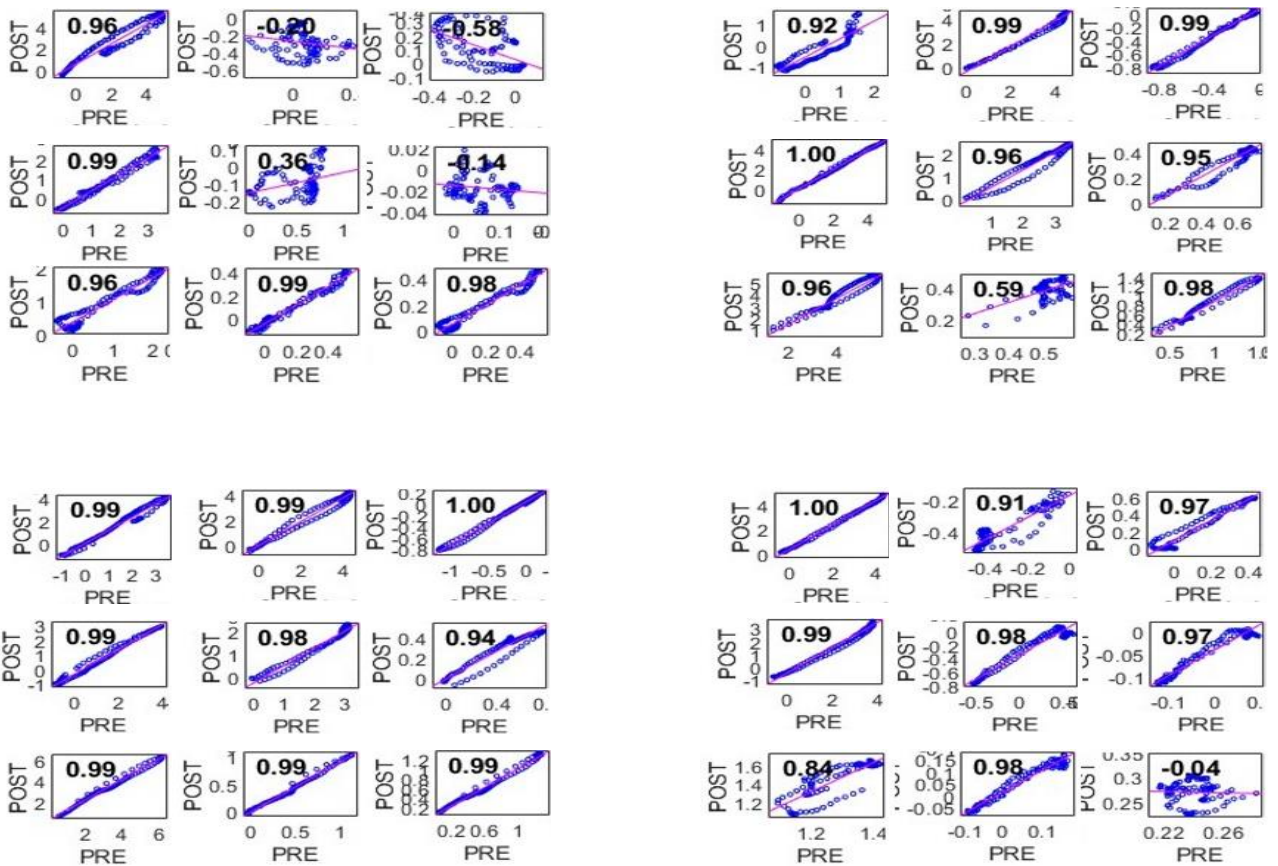


Figure 6-31: correlation indices of moment rotations between pre- and post-surgery on the entire data set in the four motor tasks

Even from the analysis of the joint moments it can be seen immediately that the correlation indices are significantly lower than those we obtained for the gait analysis.

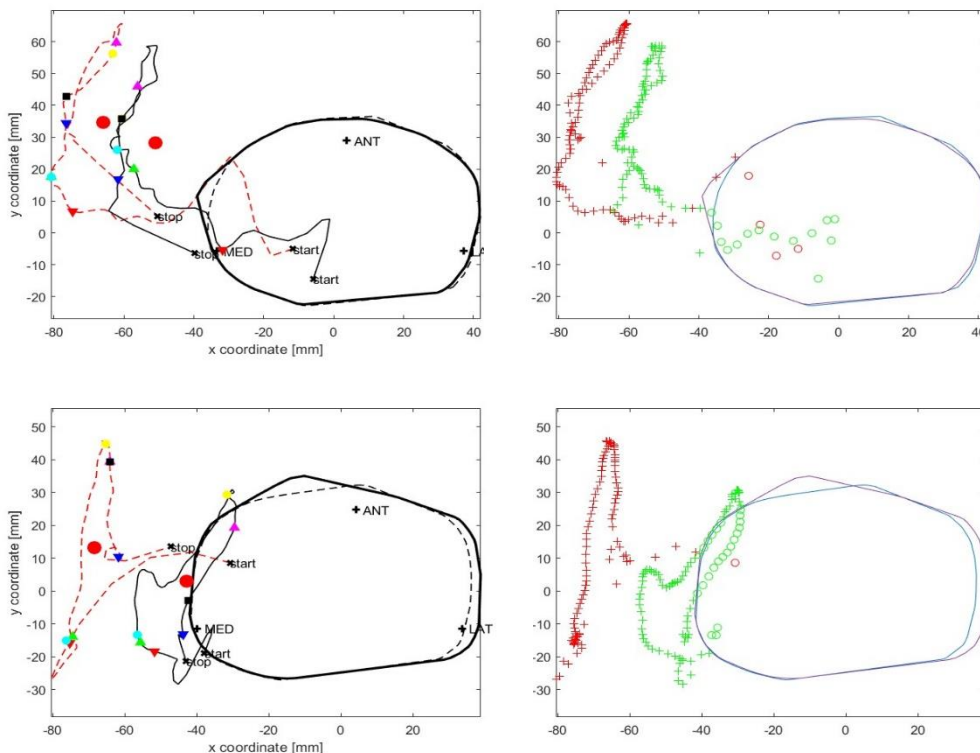
So in conclusion of this analysis, we can state that for these four motor tasks the surgery resulted in a significant change in joint stress and rotations.

6.2 Merging morphological and functional data: assessment of GRF in the tibial plateau plane

Finally, we report the results obtained on the estimation of the stress state of the tibial plateau using the method proposed in the article by Ruggeri Miriana et al. [52]. Since the validation of the method is one of the aims of this work, we report this time the data obtained for five different patients for the gait and three for the other motor tasks, followed by a series of values that summarise the results obtained for all the patients of each motor tasks. We report two graphs for each motor task:

- The first graph shows the projection of the GRF in the plane of the tibial plateau, the position of the peaks of the GRF and the components of the joint moment assessed in the knee joint (flexion/extension, abd/adduction and internal/external) and the centroid;
- The second graph evidences the fraction of time-cycle percentage during which the GRF is within the tibial plateau;

- GAIT



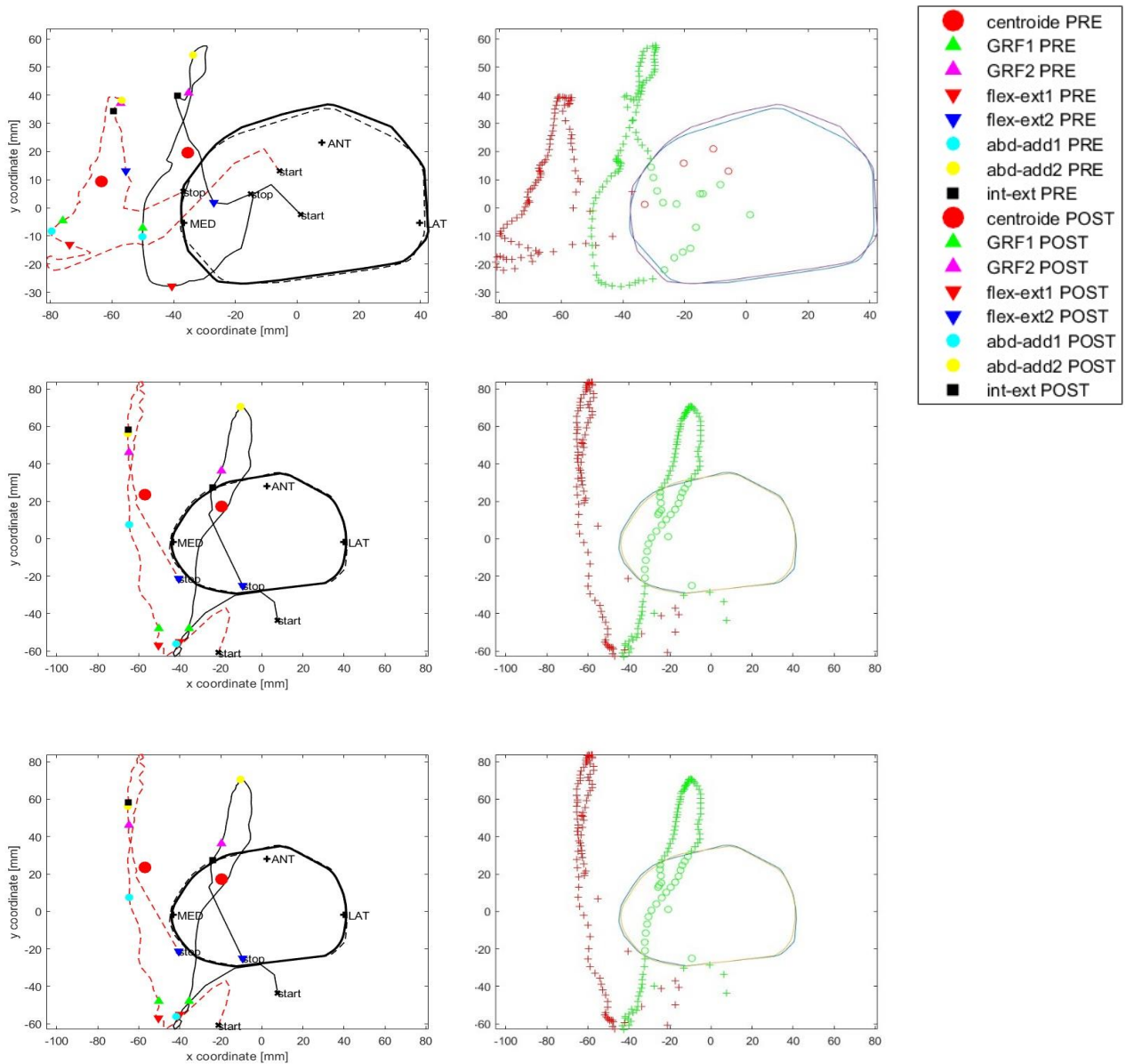


Figure 6-32: intersection of the GRF with the tibial plateau during the gait for five patients

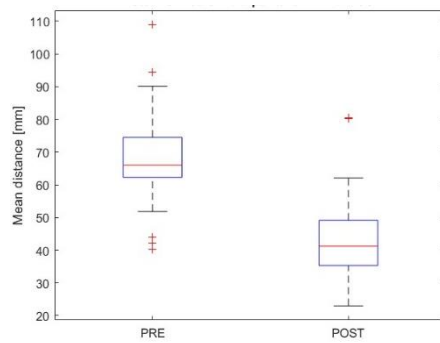


Figure 6-33: box-plot to evaluate the difference in the mean distance of the GRF between pre- and post-surgery during the gait

The table shows the data obtained from these evaluations comparing pre- and post-surgery for all the patients engaged in the study:

PATIENT	% EXT PRE	% EXT POST	DIST MEAN		PRE [mm]							POST [mm]						
			PRE [mm]	POST [mm]	1st GRF	2nd GRF	1st flex_ext	2nd flex_ext	1st abd-add	2nd abd-add	int-ext	1st GRF	2nd GRF	1st flex-ext	2nd flex-ext	1st abd-add	2nd abd-add	int-ext
1	96	86	71.4 ± 15.2	55.2 ± 16.0	78.4	78.4	71.7	78.1	78.4	77.0	81.2	55.4	65.1	31.9	59.3	61.5	63.8	63.8
2	97	73	109.0 ± 21.4	46.3 ± 10.8	133.7	103.9	102.6	101.6	133.7	103.5	110.3	58.1	48.5	36.8	40.3	59.5	50.0	49.8
3	97	95	66.0 ± 19.7	50.6 ± 10.1	93.4	42.8	93.4	55.3	92.6	43.6	51.0	55.7	46.6	62.4	47.4	48.6	24.7	49.0
4	94	74	62.2 ± 14.4	35.0 ± 10.6	64.1	73.9	64.3	57.1	64.1	77.4	71.4	46.5	32.8	45.8	19.7	48.2	38.3	33.9
5	85	78	51.8 ± 15.8	48.8 ± 13.4	71.6	46.5	72.1	40.9	71.8	46.5	46.9	62.4	41.1	62.8	38.1	62.8	40.2	42.6
6	94	47	65.6 ± 14.9	38.8 ± 8.1	53.6	82.3	55.3	64.9	57.4	79.6	84.1	35.4	45.5	38.9	42.0	37.7	40.9	40.3
7	97	36	64.8 ± 11.0	35.4 ± 11.8	78.0	66.0	75.1	62.0	80.5	64.7	65.7	48.0	28.6	47.5	34.0	53.9	27.5	27.3
8	99	78	67.7 ± 7.8	41.3 ± 6.9	70.4	69.9	71.6	56.9	72.4	73.9	69.9	52.7	30.0	50.0	40.7	52.9	38.4	37.0
9	89	70	40.3 ± 8.2	36.8 ± 11.1	47.7	37.7	50.9	37.2	45.9	38.2	35.6	43.8	36.5	52.3	6.8	52.2	48.1	30.0
10	98	43	66.4 ± 10.1	37.7 ± 11.5	73.7	68.0	68.8	54.4	74.0	63.7	68.3	44.0	25.8	20.0	23.7	55.8	27.1	28.0
11	79	32	43.9 ± 10.0	30.3 ± 8.1	58.9	41.7	62.9	34.2	62.3	47.7	46.0	38.0	31.4	36.2	12.2	39.4	37.2	38.0
12	91	87	62.2 ± 15.4	39.7 ± 8.8	71.6	79.0	72.4	35.2	71.1	68.3	74.6	44.8	42.2	47.8	40.5	48.6	42.2	40.2
13	90	91	86.6 ± 23.8	80.5 ± 19.2	99.1	83.7	103.6	86.2	100.1	63.1	80.2	88.9	64.4	37.6	43.5	92.5	77.9	76.2
14	96	86	64.4 ± 12.0	45.3 ± 12.3	73.4	65.2	72.4	54.0	77.4	65.5	65.6	48.0	51.1	47.8	24.2	48.8	61.4	52.8
15	98	94	90.1 ± 16.7	80.3 ± 15.8	104.4	86.3	121.4	75.5	115.5	85.9	89.4	94.8	84.8	103.1	61.0	102.4	84.3	88.2
16	99	95	63.4 ± 16.3	46.4 ± 10.7	85.0	54.4	83.8	58.0	83.9	52.6	55.3	54.5	43.5	72.2	17.8	62.3	50.7	49.7
17	98	96	73.8 ± 8.3	48.1 ± 9.6	78.3	69.4	74.0	72.1	80.6	78.0	76.9	60.5	40.2	59.4	42.3	67.0	53.4	41.6
18	99	53	62.3 ± 10.8	34.7 ± 7.8	81.7	56.2	81.7	56.4	81.7	59.1	54.3	40.5	36.0	41.7	23.4	39.7	36.7	36.0
19	96	0	42.2 ± 9.5	23.0 ± 5.7	42.3	44.8	45.7	45.5	45.8	46.1	43.6	26.1	24.1	30.3	18.4	31.5	24.1	23.6
20	99	91	94.5 ± 20.2	62.1 ± 18.1	127.3	85.5	127.3	99.6	107.1	59.0	85.3	97.0	49.8	99.1	41.7	64.0	43.1	52.3
21	100	76	76.4 ± 13.4	47.5 ± 16.8	70.8	75.1	77.9	45.9	62.3	81.5	82.6	61.8	36.4	70.3	30.2	72.1	66.7	31.5
22	98	85	70.0 ± 11.3	50.0 ± 14.9	71.0	79.9	63.3	47.5	77.9	82.0	79.7	41.5	66.7	35.4	27.4	42.2	71.0	67.5
23	98	35	77.8 ± 9.3	32.1 ± 9.0	85.4	74.6	83.0	72.2	86.9	77.2	73.2	51.4	26.7	51.4	28.0	50.6	29.5	25.0
24	100	4	67.8 ± 14.1	25.3 ± 6.5	83.2	51.8	87.5	54.4	89.5	57.0	51.7	27.0	25.6	39.1	11.1	30.6	29.1	30.2
25	98	81	64.6 ± 9.8	40.9 ± 9.1	71.5	62.5	85.6	55.0	71.9	61.4	59.8	46.8	42.0	61.0	30.9	48.0	42.0	39.0

MEAN CENTRALISATION	MEDIUM APPROACH OF THE GRF		AVERAGE PEAK APPROACH [%]						
	% CYCLE TIME	[mm]	[%]	1st GRF	2nd GRF	1st flex_ext	2nd flex_ext	1st abd-add	2nd abd-add
29.2	23.7	34.2	32	35	35	46	29	29	34

● CHAIR MOTOR TASK

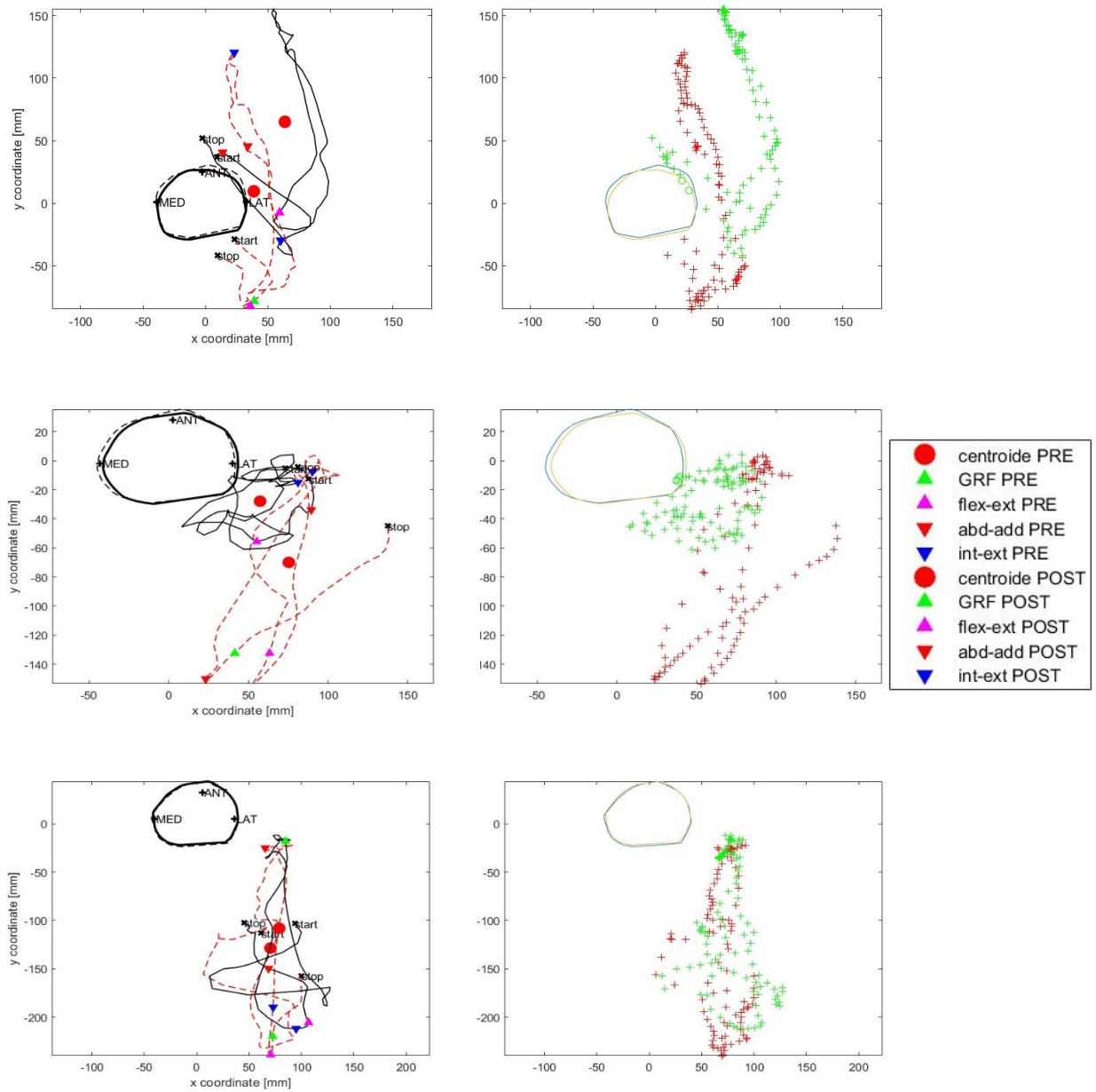


Figure 6-34: intersection of the GRF with the tibial plateau during the chair motor task for three patients

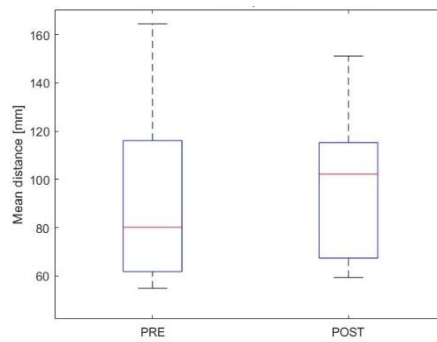


Figure 6-35: box-plot to evaluate the difference in the mean distance of the GRF between pre- and post-surgery in the chair motor task

PATIENT	% EXT PRE	% EXT POST	DIST MEAN PRE [mm]		DIST MEAN POST [mm]		PRE [mm]				POST [mm]			
							GRF	flex_ext	abd-add	int-ext	GRF	flex-ext	abd-add	int-ext
1	100	98	80.21	± 18.55	102.21	± 40.29	95.0	97.3	51.7	115.3	62.7	62.7	36.2	72.1
2	95	95	59.85	± 17.11	66.21	± 17.92	83.2	97.9	82.8	65.1	60.6	63.9	76.2	56.1
3	83	82	54.94	± 24.43	59.36	± 17.83	78.5	72.7	83.2	55.0	73.5	49.7	52.6	71.4
4	100	96	120.36	± 27.75	71.10	± 15.79	143.6	151.7	156.5	93.3	83.2	83.2	99.5	85.7
5	79	89	67.79	± 34.02	107.07	± 53.50	94.8	114.5	16.9	42.5	40.9	37.0	87.5	116.2
6	100	100	164.58	± 63.52	151.18	± 55.98	243.7	261.3	77.6	215.5	92.7	243.6	176.5	244.3
7	97	100	103.52	± 45.07	118.08	± 36.86	191.1	185.2	60.8	60.8	177.7	172.9	160.0	115.9

MEAN CENTRALISATION % CYCLE	MEDIUM APPROACH OF THE GRF		AVERAGE PEAK APPROACH [%]			
	[mm]	[%]	GRF	flex_ext	abd-add	int-ext
-1.2	-3.4	-9.9	34	33	-86	-35

• STAIRS CLIMBING

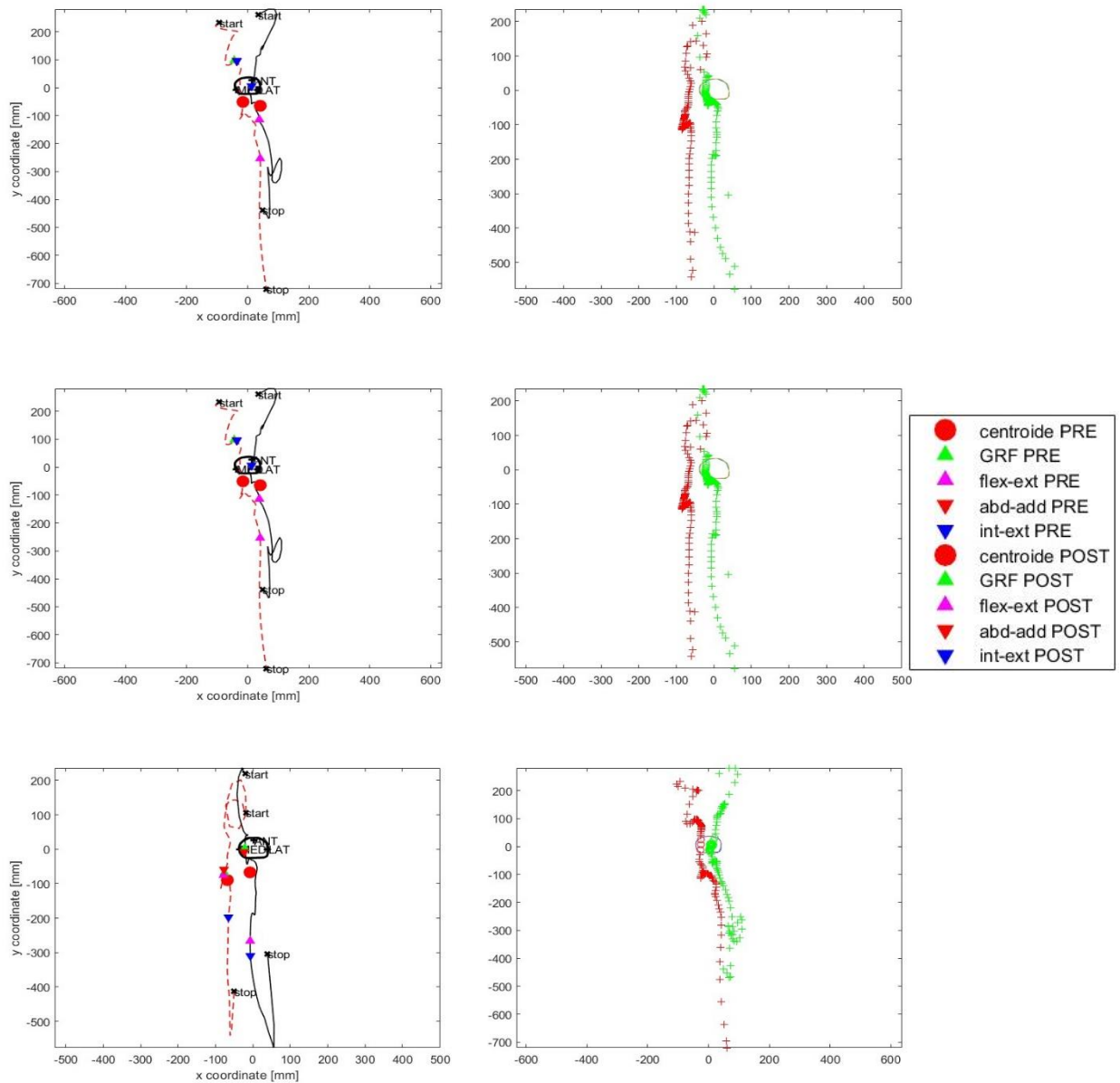


Figure 6-36: intersection of the GRF with the tibial plateau during the stairs climbing for three patients

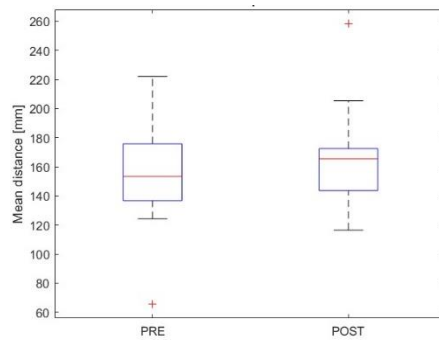


Figure 6-37: box-plot for evaluate the difference in the mean distance of the GRF between pre- and post-surgery during the stairs climbing

PATIENT	% EXT PRE	% EXT POST	DIST MEAN PRE [mm]		DIST MEAN POST [mm]		PRE [mm]				POST [mm]			
							GRF	flex_ext	abd-add	int-ext	GRF	flex-ext	abd-add	int-ext
1	100	100	203.7	± 222.4	258.5	± 328.0	136.9	325.7	63.4	207.6	174.6	302.6	60.9	249.6
2	100	80	222.1	± 160.6	173.4	± 175.7	106.9	312.8	106.4	280.3	50.0	253.6	39.8	297.6
3	87	86	149.1	± 142.3	143.5	± 121.6	103.8	161.5	74.6	117.1	44.2	165.3	24.6	133.5
4	97	75	152.2	± 131.4	151.0	± 131.8	100.3	263.3	97.2	95.5	126.8	126.8	14.3	14.3
5	84	94	130.9	± 108.8	168.9	± 150.2	96.0	129.9	88.9	94.3	145.1	132.7	145.1	145.1
6	93	80	193.4	± 194.7	173.5	± 195.3	34.6	314.0	77.6	217.0	16.4	320.8	126.9	211.7
7	83	100	130.8	± 128.4	168.4	± 170.0	119.4	203.4	101.9	101.9	124.0	212.3	123.6	441.3
8	70	90	138.8	± 152.8	158.0	± 188.6	16.6	300.8	33.7	53.4	14.1	318.6	48.7	405.6
9	84	95	65.5	± 26.3	164.1	± 120.4	89.4	93.2	90.7	52.5	140.5	315.9	160.5	140.5
10	86	98	180.7	± 147.8	166.9	± 136.4	64.6	305.9	151.3	72.9	74.9	257.4	65.0	75.4
11	91	88	145.2	± 89.9	116.4	± 107.6	117.7	239.4	120.7	120.1	72.9	191.5	40.3	80.6
12	93	80	175.8	± 141.2	170.8	± 154.7	148.1	157.8	77.6	76.6	22.2	231.8	50.8	47.7
13	62	73	124.2	± 152.7	142.1	± 160.3	64.7	184.2	65.3	65.3	36.2	353.8	69.5	183.4
14	95	73	170.9	± 169.5	205.4	± 235.9	73.0	311.5	70.7	41.1	129.3	245.1	45.0	26.6
15	100	94	156.4	± 109.5	170.8	± 161.2	75.7	263.2	70.4	61.6	70.2	253.4	125.3	43.1
16	80	75	136.7	± 132.3	150.1	± 122.4	16.3	192.7	60.8	152.1	94.6	249.3	88.2	93.3
17	94	89	154.9	± 174.2	141.8	± 152.1	38.9	216.6	38.6	54.2	65.4	213.0	63.1	199.3
18	100	95	188.3	± 153.4	180.7	± 216.0	107.3	305.3	213.9	265.9	43.9	283.0	60.4	453.5
19	88	100	125.0	± 134.3	158.2	± 102.2	45.7	232.4	67.1	60.6	62.9	207.9	79.4	75.8
20	85	84	149.6	± 133.4	172.5	± 221.2	38.5	276.5	228.7	271.7	125.7	372.3	281.6	220.7
21	100	82	154.8	± 102.0	132.7	± 139.9	103.0	109.0	97.8	209.5	20.9	268.5	24.3	311.7
22	100	86	162.1	± 97.0	141.0	± 129.7	54.6	251.3	59.7	78.5	32.3	237.7	43.9	34.7

MEAN CENTRALISATION % CYCLE	MEDIUM APPROACH OF THE GRF [mm]		AVERAGE PEAK APPROACH [%]			
			GRF	flex_ext	abd-add	int-ext
1.6	-9	-10.8	-24	-20	4	-69

● STAIRS DESCENDING

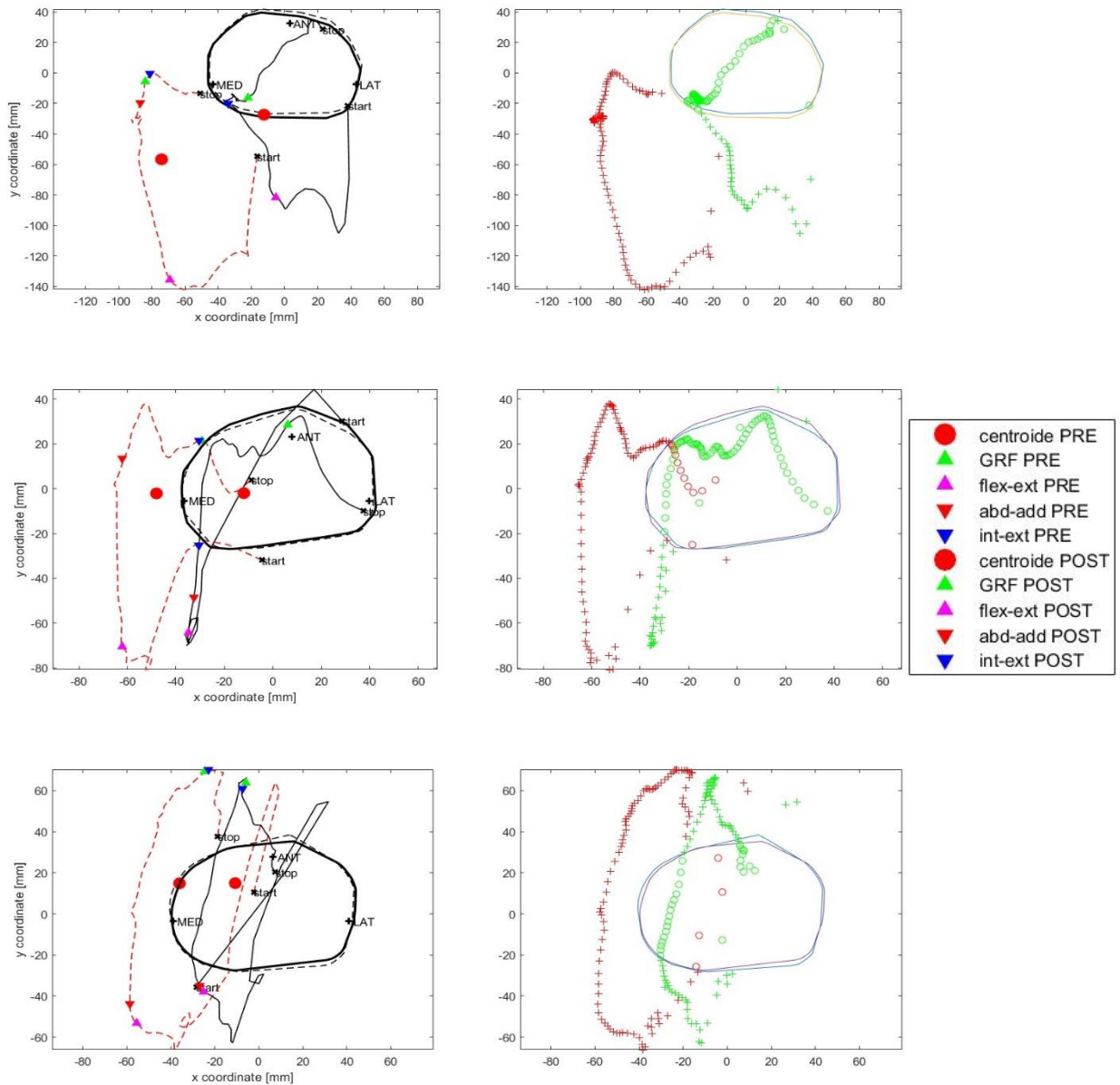


Figure 6-38: intersection of the GRF with the tibial plateau during the stairs descending for three patients

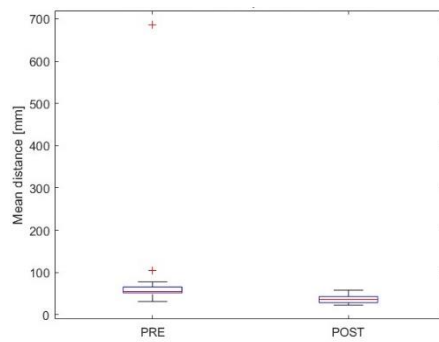


Figure 6-39: box-plot to evaluate the difference in the mean distance of the GRF between pre- and post-surgery during the stairs descending

PATIENT	% EXT PRE	% EXT POST	DIST MEAN PRE [mm]		DIST MEAN POST [mm]		PRE [mm]				POST [mm]						
							GRF	flex_ext	abd-add	int-ext	GRF	flex-ext	abd-add	int-ext			
1																	
2	100	34	105.0	± 26.9	45.7	± 23.9	85.1	154.9	90.5	82.0	29.6	84.4	41.4	41.4			
3	76	39	77.6	± 40.2	39.5	± 20.8	20.1	125.0	100.2	24.8	20.6	64.0	19.7	20.6			
4	52	48	41.6	± 29.9	28.7	± 13.9	14.2	81.9	57.6	57.6	29.4	45.7	13.1	43.5			
5	60	46	52.5	± 31.2	36.5	± 22.4	28.8	99.9	89.2	89.2	22.3	68.7	38.2	38.2			
6	100	57	62.2	± 14.4	49.9	± 28.4	65.1	86.7	84.8	67.2	20.4	86.6	80.6	98.3			
7	29	40	31.3	± 8.9	31.1	± 19.3	49.3	22.2	50.6	51.0	22.1	97.0	37.1	26.0			
8	58	42	41.6	± 26.7	31.2	± 26.5	11.1	82.9	18.8	11.1	9.8	64.4	9.8	9.8			
9	50	30	53.0	± 35.2	28.5	± 21.9	106.0	110.2	108.2	28.1	8.7	61.0	50.8	37.1			
10	100	18	686.4	± 123.0	24.1	± 8.9	800.2	814.4	803.9	734.5	18.3	47.2	18.8	20.2			
11	98	64	69.5	± 14.2	58.0	± 24.7	60.8	84.3	75.5	75.5	90.0	32.0	90.0	100.9			
12	87	28	55.8	± 21.3	35.2	± 19.3	33.2	93.2	60.6	34.2	28.7	73.0	58.1	38.5			
13	98	50	70.7	± 16.5	51.5	± 25.1	55.8	83.6	65.6	57.1	27.1	79.7	31.0	31.0			
14	71	22	53.7	± 23.7	24.4	± 10.4	36.7	106.0	42.9	37.5	9.9	35.8	33.0	13.9			
15	92	69	56.5	± 13.7	43.3	± 14.3	55.0	83.0	71.3	54.1	44.3	63.3	51.2	41.8			
16	97	17	53.4	± 14.7	23.7	± 12.3	38.3	83.6	44.3	40.4	10.1	31.6	25.5	12.7			
17	81	38	51.4	± 19.6	22.6	± 15.4	77.8	78.9	74.6	74.6	8.2	37.7	25.9	30.5			
18	96	73	61.1	± 12.6	43.0	± 13.6	69.4	77.2	73.0	69.7	60.5	46.9	45.2	57.7			
19	66	52	54.6	± 24.6	38.8	± 20.7	37.1	98.3	37.1	37.1	10.4	73.4	32.9	33.3			
20	88	57	45.6	± 11.2	36.4	± 17.7	36.4	64.2	54.5	36.7	40.2	60.2	61.8	41.3			
21	90	54	60.4	± 24.3	35.8	± 16.6	40.5	85.5	69.6	40.5	45.0	66.2	60.4	45.2			

MEAN CENTRALISATION % CYCLE	MEDIUM APPROACH OF THE GRF		AVERAGE PEAK APPROACH [%]			
	[mm]	[%]	GRF	flex_ext	abd-add	int-ext
40.1	-9.7	62.2	32	19	37	22

- SQUAT

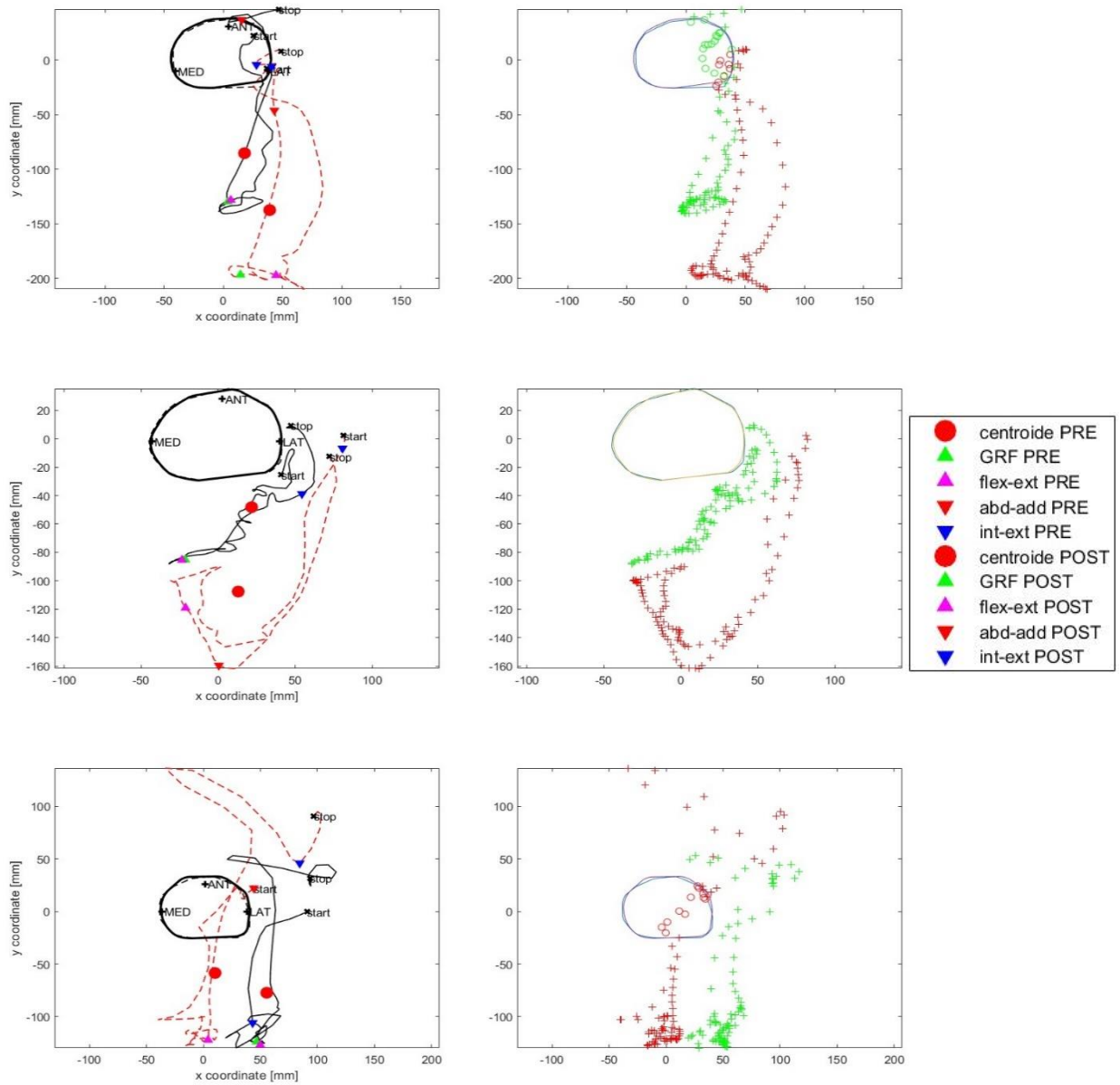


Figure 6-40: intersection of the GRF with the tibial plateau during the squat for three patients

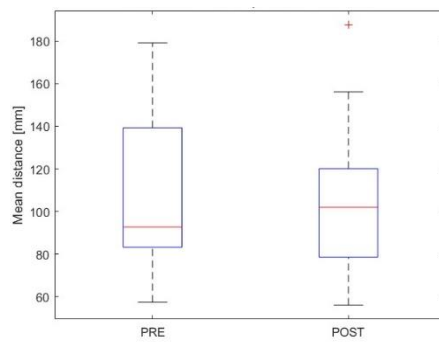


Figure 6-41: box-plot to evaluate the difference in the mean distance of the GRF between pre- and post-surgery during the squat

PATIENT	% EXT PRE	% EXT POST	DIST MEAN PRE [mm]			DIST MEAN POST [mm]			PRE [mm]				POST [mm]			
									GRF	flex_ext	abd-add	int-ext	GRF	flex-ext	abd-add	int-ext
1	90	84	108.8	±	38.3	121.5	±	52.9	134.4	134.4	80.7	38.7	177.8	177.1	47.0	177.1
2	100	100	142.7	±	57.8	132.3	±	52.6	192.2	194.2	50.5	52.2	194.4	194.4	91.1	91.1
3	92	84	157.8	±	64.9	105.7	±	43.6	204.6	210.2	72.1	35.7	136.9	135.7	36.8	48.4
4	100	100	152.9	±	49.4	128.0	±	40.2	78.3	218.6	78.4	216.8	173.9	175.2	61.4	165.8
5	88	92	84.7	±	32.8	66.2	±	22.6	113.7	90.8	32.7	114.8	68.3	71.2	32.5	88.2
6	92	92	128.1	±	57.0	115.6	±	39.4	166.8	181.0	120.6	101.4	148.8	148.8	37.9	44.4
7	97	87	145.0	±	56.8	112.1	±	50.2	182.7	194.8	76.2	76.2	180.4	183.9	52.5	52.5
8	85	80	66.1	±	38.4	73.4	±	28.4	96.0	110.0	61.3	72.2	107.7	107.7	118.9	60.7
9	100	100	179.1	±	53.0	139.8	±	53.9	228.9	227.7	88.1	139.6	197.5	197.5	69.8	119.7
10	71	92	57.4	±	29.3	92.8	±	33.6	92.4	50.1	97.5	104.2	90.0	105.1	23.4	23.4
11	93	100	75.1	±	21.1	109.1	±	20.2	88.5	90.7	88.5	88.5	117.4	117.4	92.5	118.3
12	81	88	85.7	±	50.9	74.7	±	26.3	57.2	142.4	54.5	14.1	89.4	121.2	46.1	46.1
13	78	87	86.8	±	43.6	98.2	±	52.1	121.1	134.4	134.9	134.9	138.5	169.4	121.6	138.5
14	92	87	120.2	±	52.9	82.3	±	31.4	134.8	134.8	136.4	136.4	103.9	107.6	22.2	22.2
15	93	100	88.5	±	31.2	70.4	±	24.2	95.8	115.8	74.9	105.8	109.0	82.4	122.8	121.2
16	100	100	76.5	±	26.0	94.1	±	12.0	84.4	117.1	75.3	65.6	75.0	94.9	96.9	109.7
17	75	100	86.2	±	45.7	118.8	±	39.7	133.0	133.0	118.9	30.4	71.7	163.9	111.2	63.7
18	80	72	62.0	±	30.2	56.1	±	13.5	70.2	97.1	70.2	70.2	60.9	78.6	47.4	65.6
19	87	100	82.9	±	47.3	92.5	±	18.9	131.3	135.1	137.2	97.1	115.5	115.5	114.5	77.3
20	100	100	122.5	±	25.0	67.2	±	14.6	124.9	124.9	164.0	83.9	91.4	92.1	71.3	71.3
21	87	100	83.6	±	44.0	98.1	±	24.9	129.5	129.5	34.8	9.2	113.8	112.0	57.5	76.7
22	85	100	146.8	±	69.1	156.1	±	82.2	200.6	203.6	27.9	87.2	50.8	260.0	116.3	116.3
23	89	100	96.9	±	35.7	113.8	±	23.6	124.4	124.4	49.5	96.0	134.8	138.7	116.8	116.8
24	98	100	135.9	±	64.5	187.7	±	75.7	195.6	205.6	42.0	135.0	245.0	282.6	214.2	64.1
MEAN CENTRALISATION % CYCLE		MEDIUM APPROACH OF THE GRF [mm]						AVERAGE PEAK APPROACH [%]								
		[mm]			[%]			GRF	flex_ext	abd-add	int-ext					
-4.9		2.7			-1.8			0	-1	-28	-54					

Observing the results obtained for the four additional motor tasks, a great difference is noted between the pre- and post-surgery situation, but unlike the gait, for which a substantial closeness to the centre of the tibial plateau is observed, here there is a lateralisation of the path of the GRF, but often even before the surgery it passes astride the plateau, therefore calculating the average distance from the centre there is not such a clear difference. This, however, is due to the different type of movement required in these motor tasks, but in general, when looking at the results in these cases too, improvements can be seen, in particular we can see a less variable GRF path and very good lateralisation. Looking at the values reported for the distances of the peaks from the centre there is in fact a substantial reduction, which can be interpreted as an improvement from a biomechanical point of view.

7 DISCUSSION

This paper analysed the data of all 25 patients involved in the study and the following discussion obviously refers to the analysis of the entire data set and therefore concerns all subjects involved in the study. As anticipated above, in order to facilitate the readability of the paper, a limited number of patients were chosen in the results chapter as representative, or to highlight certain aspects.

7.1 Intra-patients repeatability

To assess intra-subject repeatability, all repetitions of each subject and for each motor task were studied, after which the mean and standard deviation were calculated. The functional data under examination are all referred to one motor task and normalized to gait cycle and task cycle so as to be able to compare the data of each patient and each repetition. In view of this, it was considered appropriate to report the data obtained for the standard deviation as bands represented around the mean value, in order to evaluate the trend during the period and as a function of the mean value. In general, it can be observed that both pre- and post-operative data are characterised by a similar trend, so it makes sense to represent the range of data. An evaluation of the individual repetitions remains appropriate, as in some cases the high variability could be due to random errors that cannot be predicted and therefore avoided at the acquisition stage, as can be seen by looking at Figure 7-6 in which high standard deviation values are due to peaks in a single repetition.

Overall, however, the evaluation of the trends shows a good repeatability of the data, which remain consistent within empirical limits, confirming the goodness of the technique, as much as in the execution of the relief of the variables of interest. As shown in the legend, the pre- and post-operative ranges have been reported for each graph, and in general it can be observed that the standard deviation values in the post-operative range are significantly reduced, which is a first indication of the clinical improvement of the data. Evaluating the data in aggregate standard deviation thanks to a box-plot, it is possible to observe how there is a significant decrease and therefore a better stability of the data, especially in the abd/adduction of the knee, which, considering the nature of the pathology under examination, represents the variable of greatest interest.

7.2 Inter-patients repeatability

In the same way, it was decided to represent a single repetition of each patient (the third repetition was chosen for the gait and the second for the subsequent motor tasks) in the same graph and the mean and standard deviation were calculated in order to check for the presence of a pattern that could characterise the group under examination (pre or post). In this case, the graphs obtained from the representation of mean and standard deviation are particularly indicative. Indeed, there is a similar pattern within the same group and a significant difference between the two. Looking in particular at what happens in the frontal plane for the knee, but also for the hip and ankle, a clear distinction between the two groups of data can be seen, which demonstrates the existence of a characteristic trend as well as a variation after the surgery. It can therefore be said that the surgery caused a significant change in the functional data for all motor tasks. Of course, the analysis of the gait data remains the most significant: as these are the ones most frequently used in the functional analysis of the joints of the lower limb, for this motor task we have normality data acquired on a non-pathological sample and a better clinical evaluation is therefore possible. In the case of gait, it is possible to test whether the intervention resulted in an improvement that can be seen from the functional data, an aspect that will be further investigated by the correlation analyses. However, observing Figures 7-13, 7-14 it is evident how the post-operative data are better superimposed on the normal ranges, which highlights an improvement in joint function, not only of the knee, but also of the hip and knee, which apparently in the case of pathological knees were also altered as a compensatory mechanism.

7.3 Correlation

In order to have a qualitative estimate of the functional improvement, or at least of the change following the correction intervention, it was decided to exploit the Pearson's Correlation Coefficient "r" in order to have a quantitative estimate of the mutual variability between the data. In this context, a distinction must be made between the gait data and those obtained for the other four motor tasks: for gait, it was possible to utilise the knowledge of a non-pathological trend in order to compare the correlation with them of the pre- and post-operative data to verify the presence and level of improvement, whereas for the other motor tasks, an estimate of the change between the pre- and post-operative data had to be limited to the lack of a reference. It should therefore be underlined that in the latter case it would be improper to speak of

improvement in the functional data, so the presence and possible degree of change will be verified. It should be noted that for all correlation data, a significance value $p < 0.05$ was obtained and therefore the calculated coefficients were deemed significant.

From the data reported for the individual patients on the pre/normality and post/normality correlations, it is evident that in the knee abd-adduction there was a significant improvement in the functional data: in the pre-operative the data were either uncorrelated or poorly correlated with normality, while in the 6-month control the value of "r" indicates an excellent adherence in joint rotations and moments. This result is very evident when observing the bar graphs in which the correlation values for the three joints and in the three planes were reported, comparing pre/norm and post/norm. For the evaluation of the data in the aggregate, the "r" coefficients obtained have been reported in box plots from which it can be seen that even evaluating the entire group of subjects involved results in the confirmation of what was previously hypothesised, i.e. a good improvement in the adherence of the post-operative data with the trend of the data of the non-pathological reference sample.

Moving on to the other motor tasks in order to have a term of comparison that allows an estimate of the variation between the two data sets, it was decided to preliminarily calculate the correlation between the pre- and post-operative data in the gait, for which an improvement has already been verified. Observing the results shown in the graphs in Figures 7-28 and 7-29, we can see how for all the variables considered there is a very high correlation coefficient, almost close to 1, which is justified considering that we are considering the functional data of the same sample of subjects and moreover that in the inclusion/exclusion criteria it was decided to include only patients with a contained degree of varus and with a moderate articular pathology, therefore with limited functional disorders. Following this, the correlation between pre- and post-operative for the other motor tasks was calculated, and analysing the data we see that in some cases, such as chair exercise or even more so stairs climbing, there is a greater variation.

7.4 Superimposition of ground reaction force on tibial-plateau

Let us now evaluate the data obtained from the application of this new methodology for the evaluation of the loading state of the tibial plateau. The idea is to exploit a set of four markers to combine the CT reconstruction of the tibial plateau with the GRF in order to have an estimate of the position of this force in the plateau plane. Preliminary results showed that for all motor tasks, a lateralisation of the GRF with respect to the tibial plateau was obtained and, with the exception

of the squat, the hypothesis that the objective of the intervention would be a centralisation of the GRF so that it passes close to the tibial spine, thus giving a more homogeneous load distribution, was confirmed. Of course, not having data from a non-pathological statistical sample, it is not possible to make a certain evaluation, but considering the type of biomechanical disorder, it is legitimate to consider a centralisation, or in general a lateralisation of the load, as an objective. From the graphs shown for the gait it can be seen that there is an effective centralisation of the GRF in the post and, considering the data in aggregate, from the box-plot it can be seen that the average distance from the centre has decreased by about 34%, from an average of 68mm to 42mm. Also looking at the data reported for the position of the peaks in relation to the centre, it can be seen that on average there was an approach of more than 30% (values shown in Table 2 on page 104). In general, it was calculated for the gait that the GRF in the post is within the tibial plateau for a cycle time higher than 30%.

For the chair there is no significant difference on the residence time in the plateau of the force, even considering the type of movement already in the pre the GRF passes laterally with respect to the knee and also the average position of the GRF with respect to the centre of the tibial plateau does not undergo a great variation. Observing the peaks, it can be seen that on average the GRF and flexion-extension peaks have an approximation comparable to that seen in gait, but abd-adduction and internal-external apparently increase their distance. Looking at the data from individual patients, however, we can see that this unexpected result is in reality due to individual patients.

The motor task data on the stairs show good lateralisation, but the data are strongly influenced by the much higher antero-posterior range than the medio-lateral, which makes the improvement less evident from a numerical point of view. Similarly, when evaluating the distance of the peaks from the centre of the tibial plateau, although a discrete lateralisation is present, the component that weighs most on the distance is the antero-posterior one, which does not show a significant variation being physiological considering the movement required.

For the squat, on the other hand, a significant variation of trends can be observed in the mid-lateral component, but also less anterior-posterior oscillation. From the box-plot, it can be seen that the data between 25% and 75% in the post are at a significantly lower average distance. Turning to the analysis of the position of the peaks, it can be seen that the peaks of the GRF and that relating to the flexion-extension component do not show substantial variations, while those

of abd-adduction and internal-external on average would appear mode distant, but looking at the data of the single patients also here it can be seen that this result is due to single patients which have unusual tendency, while the trend would be to approach the peaks at the centre of the tibial plateau.

8 CONCLUSIONS AND FURURE DEVELOPMENTS

In this master's thesis work, the pre- and post-operative functional data of patients who underwent a tailored HTO, a surgical technique for knee varus correction, which restores physiological biomechanics by realigning the tibial plateau, were analysed. The main purposes of this work were two: firstly, to analyse the complete data set of acquisitions obtained from the follow-up of all the 25 patients six months after surgery, in order to demonstrate the validity of the surgical technique and to illustrate the advantages of using 3D technologies (in particular the use of an innovative custom-made fixation plate), and secondly, to use the technique proposed in a previous work carried out in the context of the same study for the assessment of the stress state of the knee joint on a larger set of patients in order to confirm its validity.

In this context, a punctual and statistical analysis of the functional data was carried out, starting with a repeatability, using mean and standard deviation, and their variation, and going on to identify common patterns within the groups (pre- and post-intervention). In order to check the degree of improvement/change in joint function, Pearson's correlation coefficient was used between the preliminary data and the six-month data, as well as with those known from the literature relating to a statistically descriptive non-pathological group of patients. By observing the linear regression values obtained, it was possible to demonstrate how the intervention led to an actual improvement in knee joint function, especially for the abd-adduction component of the knee; before the intervention, this function was uncorrelated with the normal data, while after it showed a degree of correlation close to 1. The improvement involved also hip and ankle joints, which in the case of disturbances of normal biomechanics act with a compensatory mechanism, altering their physiological function.

The data obtained for the four motor tasks predicted in terms of correlation showed that even in the execution of more demanding and complex movements, there was a change in joint behaviour, confirming that, for an accurate assessment of movement, it is useful to extend the protocol and not limit it to walking. The evaluation of the GRF in the plane of the tibial plateau confirmed how this technique can be an essential support in the clinical evaluation. In gait analysis, especially, it was able to detect a real change in the pattern data, with a rapprochement of the point of force application to the center of the tibial plateau and a centralisation of the peaks of the moment components investigated that is around 30%.

Although very promising, these functional assessment techniques are affected by a number of limitations, mainly due to the acquisition technique. First of all, it must be remembered that gait analysis has its own criticalities, mainly caused by the use of a standard osteoarticular model, which may not be perfectly coincident with the physiology of the subject under examination. Furthermore, the position of the bone segments is based on the detection of external markers which, although positioned in the more easily identifiable points, are subject to possible random errors by the operator and systematic errors due to skin movement artefacts. Talking about the new technique for the evaluation of tibial plateau stress, on the other hand, the main problem is linked to the need of measuring an external force, such as GRF, instead of the actual internal one; its measurement would require the positioning of load cells between the bone segments, an operation that is impossible to perform in vivo. However, these issues were evaluated for the purpose of this study, and it was concluded that the margin of uncertainty, although not eliminable, was acceptable.

In the comparison between pre- and post-operative data, instead, the main limitation was the evaluation of the four additional motor tasks; without a reference, it was not possible to verify if the 6 months situation showed an effective normalisation of functional data. The idea is therefore to acquire data from a population sample that is statistically descriptive and can also be used as a reference for normal function for other motor tasks requiring complex joint movements, so as to highlight any abnormalities that are not visible in gait. Having such data, it would be interesting to repeat the correlation studies to confirm our hypotheses; furthermore, the application of this technique to a combination of motor tasks and biomechanical disorders, would maybe lead to identify those movements that are most critical, and exploit them in the clinical evaluation.

Such information could help in planning orthopaedic treatment and would represent a minimally invasive and expensive analysis, operable within a reasonable period of time in accordance with diagnostic necessity. In conclusion, this work demonstrates the effective goodness of the tailored HTO proposed in the TOKA clinical study, and the proposed functional evaluation technique, and opens up the possibility of increasing the use of functional and movement analysis for clinical purposes.

LIST OF FIGURES

Figure 1-1: Anatomical planes of the human body[1]	10
Figure 1-2: Anatomical axes of the human body[2].....	11
Figure 1-3: Relative location for the anatomical parts[3]	12
Figure 1-4: Anatomical axes of the knee and relative rotation[2]	12
Figure 1-5: Articular Surfaces: patellofemoral (left side), tibiofemoral (right side)[8].....	14
Figure 1-6: Knee ligaments [9]	17
Figure 1-7: knee muscles anatomy, frontal and back view [10]	18
Figure 1-8: anatomical landmark in the pelvis and proximal femur (on the left), in the distal femur and proximal tibia and fibula (in the centre) and in the distal tibia and fibula, and in the foot (on the right) [11]	19
Figure 1-9: Bone embedded anatomical frames [11]	21
Figure 1-10: The generalized joint coordinate system composed of three axes e_1, e_2, e_3 [12]....	22
Figure 1-11: Cartesian coordinate systems defined in each bone (on the left) and joint angles defined by the rotations that occur around the three joint coordinate axe (on the right) [12] ..	23
Figure 1-12: mechanism of knee flexion (a) rolling, (b) sliding, and (c) rolling and sliding of the femoral condyles over the tibial plate.	24
Figure 2-1: mechanical axis on a full-length, standing anteroposterior radiograph [16].....	28
Figure 2-2: Illustrations of (a) varus, (b) neutral, and (c) valgus alignments [17].....	28
Figure 2-3: anatomical and mechanical axis [18].....	29
Figure 2-4: illustration of normal and osteoarthritic knee joint [17].....	30
Figure 2-5: Total Knee Arthroplasty before and after surgery [22]	32
Figure 2-6: Unicompartmental knee arthroplasty (UKA) [23]	32
Figure 2-7: LCWO. (A) Varus knee with bony cuts highlighted. (B) Removal of bony wedge from tibia and fibula. (C) Closing the gap and fixation [26]	34
Figure 2-8: (a) osteotomy saw cut. (b) progressive wedge opening to the final plate size. (c) final intra-operative fluoroscopic imaging of the definitive plate [27].....	34
Figure 2-9: (A) cutting-guide with the slot for the saw. (B) post-reduction guide with pre-defined drill holes [30].....	35
Figure 3-1: Basic scheme of the gait analysis technology, from the marker to the skeleton [32]	36
Figure 3-2: main events and periods of gait cycle [33]	37

Figure 3-3: geometrical parameters of the gait cycle [35].....	39
Figure 3-4: plot of the GRF during gait analysis [36].....	41
Figure 4-1: difference between the current standard plate (on the left) and the TOKA plate (on the right) [39]	43
Figure 4-2: In silico trial workflow [41]	46
Figure 5-1: Non-weight-bearing (a) and weight-bearing (b) posteroanterior knee radiographs [43]	50
Figure 5-2: Carestream OnSight 3D Extremity System [44] and its use for acquisition in the IOR laboratory.....	51
Figure 5-3: Technical principles of cone beam technology [45]	52
Figure 5-4: force platform in the GAIT laboratory of the IOR center and global reference frame of the analysis.....	53
Figure 5-5: locations of the anatomical landmarks (small black circles), and the reflective markers (grey circles) [46].....	55
Figure 5-6: Marker placement diagram with marker labels from (Leardini et al.,2011) [48].....	56
Figure 5-7: EMG electrodes placements	57
Figure 5-8: gait.....	58
Figure 5-9: chair motor task	58
Figure 5-10: squat.....	59
Figure 5-11: climbing steps	59
Figure 5-12: descending steps.....	60
Figure 5-13: 3D image obtained in Mimics®	61
Figure 5-14: new marker set for the matching of the data	63
Figure 5-15: TOKA inventory [51].....	64
Figure 6-1: joint rotations in the five repetition (on the left) and their mean and standard deviation (on the right) pre- and post-surgery during the gait for three patients	66
Figure 6-2: joint moments in the five repetition (on the left) and their mean and standard deviation (on the right) pre- and post-surgery during the gait for three patients	67
Figure 6-3: joint rotations in the three repetition (on the left) and their mean and standard deviation (on the right) pre- and post-surgery during the chair motor task for three patients ..	69
Figure 6-4: joint moments in the three repetition (on the left) and their mean and standard deviation (on the right) pre- and post-surgery during the chair motor task for three patients ..	70

Figure 6-5: joint rotations in the three repetition (on the left) and their mean and standard deviation (on the right) pre- and post-surgery during the stairs climbing for three patients..... 71

Figure 6-6: joint moments in the three repetition (on the left) and their mean and standard deviation (on the right) pre- and post-surgery during the stairs climbing for three patients..... 72

Figure 6-7: joint rotations in the three repetition (on the left) and their mean and standard deviation (on the right) pre- and post-surgery during the stairs descending for three patients .73

Figure 6-8: joint moments in the three repetition (on the left) and their mean and standard deviation (on the right) pre- and post-surgery during the stairs descending for three patients .74

Figure 6-9: joint rotations in the three repetition (on the left) and their mean and standard deviation (on the right) pre- and post-surgery during the squat for three patients 75

Figure 6-10: joint moments in the three repetition (on the left) and their mean and standard deviation (on the right) pre- and post-surgery during the squat for three patients 76

Figure 6-11: comparison of the rotation standard deviation values of three patients to assess their variation..... 79

Figure 6-12: comparison of the moment standard deviation values of three patients to assess their variation..... 80

Figure 6-13: plot of the rotations data for a single repetition (in the upper figure) and with mean and standard deviation (in the bottom figure) of all patients during the gait analysis..... 82

Figure 6-14: plot of the moments data for a single repetition (on the left) and with mean and standard deviation (on the right) of all patients during the gait analysis..... 83

Figure 6-15: plot of the rotations data for a single repetition (on the left) and with mean and standard deviation (on the right) of all patients during the chair motor task..... 84

Figure 6-16: plot of the moments data for a single repetition (on the left) and with mean and standard deviation (on the right) of all patients during the chair motor task..... 85

Figure 6-17: plot of the rotations data for a single repetition (on the left) and with mean and standard deviation (on the right) of all patients during stairs climbing 86

Figure 6-18: plot of the moments data for a single repetition (on the left) and with mean and standard deviation (on the right) of all patients during the stairs climbing 87

Figure 6-19: plot of the rotations data for a single repetition (on the left) and with mean and standard deviation (on the right) of all patients during the stairs descendent..... 88

Figure 6-20: plot of the moments data for a single repetition (on the left) and with mean and standard deviation (on the right) of all patients during the stairs descendent..... 89

Figure 6-21: plot of the rotations data for a single repetition (on the left) and with mean and standard deviation (on the right) of all patients during the squat	90
Figure 6-22: plot of the moments data for a single repetition (on the left) and with mean and standard deviation (on the right) of all patients during the squat	91
Figure 6-23: comparison of the standard deviation values between pre- and post-surgery inter-patients for the rotations and for the moments.....	93
Figure 6-24: corrplot of the rotations data for three patients of PRE or POST surgery with NORMALITY and bar chart of its variation	96
Figure 6-25: corrplot of the moments data for three patients of PRE or POST surgery with NORMALITY and bar chart of its variation	98
Figure 6-26: comparison of correlation coefficients of pre- and post-surgery joint rotations with normality	99
Figure 6-27: comparison of correlation coefficients of pre- and post-surgery joint moments with normality	99
Figure 6-28: correlation indices of joint rotations between pre- and post-surgery on the entire data set in the gait analysis	100
Figure 6-29: correlation indices of joint moments between pre- and post-surgery on the entire data set in the gait analysis	101
Figure 6-30: correlation indices of joint rotations between pre- and post-surgery on the entire data set in the four motor tasks, respectively: chair motor task, stairs climbing and descending and squat.....	102
Figure 6-31: correlation indices of moment rotations between pre- and post-surgery on the entire data set in the four motor tasks.....	102
Figure 6-32: intersection of the GRF with the tibial plateau during the gait for five patients ...	104
Figure 6-33: box-plot to evaluate the difference in the mean distance of the GRF between pre- and post-surgery during the gait.....	104
Figure 6-34: intersection of the GRF with the tibial plateau during the chair motor task for three patients.....	106
Figure 6-35: box-plot to evaluate the difference in the mean distance of the GRF between pre- and post-surgery in the chair motor task.....	106
Figure 6-36: intersection of the GRF with the tibial plateau during the stairs climbing for three patients.....	108

Figure 6-37: box-plot for evaluate the difference in the mean distance of the GRF between pre- and post-surgery during the stairs climbing	108
Figure 6-38: intersection of the GRF with the tibial plateau during the stairs descending for three patients.....	110
Figure 6-39: box-plot to evaluate the difference in the mean distance of the GRF between pre- and post-surgery during the stairs descending.....	110
Figure 6-40: intersection of the GRF with the tibial plateau during the squat for three patients	112
Figure 6-41: box-plot to evaluate the difference in the mean distance of the GRF between pre- and post-surgery during the squat.....	112

Bibliography

- [1] R. Tang, X.-D. Yang, S. Bateman, J. Jorge, and A. Tang, *Physio@Home*. 2015. doi: 10.1145/2702123.2702401.
- [2] C. Ferraresi, "Meccanica applicata ai sistemi biomedici."
- [3] lumen, "Anatomical Orientation and Directions | Human Anatomy and Physiology Lab (BSB 141)." 2020.
- [4] K. Davis, "The knee: Anatomy, injuries, treatment, and rehabilitation," *Medical News Today*. 2017. [Online]. Available: <https://www.medicalnewstoday.com/articles/299204><https://www.medicalnewstoday.com/articles/299204#knee-anatomy>
- [5] "Some_Aspects_of_Functional_Anatomy_of_the_Human_Knee_Joint.pdf."
- [6] G. Hierholzer, W. Platzer, S. Weller, and O. Trent, *Grande Atlante di Tecnica Chirurgica - Arti Inferiori*, Italian Ed. USES, 2000.
- [7] G. Sendic, "Knee Joint: anatomy, ligaments and movements," *Kenhub*. 2020. [Online]. Available: <https://www.kenhub.com/en/library/anatomy/the-knee-joint>
- [8] "understanding-the-mechanics-of-the-knee."
- [9] Stanford Health Care, "Types of Knee Ligaments | Stanford Health Care." 2020. [Online]. Available: <https://stanfordhealthcare.org/medical-conditions/bones-joints-and-muscles/knee-ligament-injury/types.html>
- [10] "Knee muscle anatomy - Archview Physiotherapy _ Massage _ Dry Needling _ Pilates."
- [11] a Cappozzo, F. Catani, U. Della Croce, and a Leardini, "Position and orientation in space of bones during movement," *Clin. Biomech.*, vol. 10, no. 4, pp. 171–178, 1995, [Online]. Available: pdf AHa
- [12] E. S. Grood and W. J. Suntay, "A joint coordinate system for the clinical description of 3D Motions: Applications to the Knee," *Journal of biomechanical engineering*, vol. 105. pp.

136–144, 1983.

- [13] G. R. Scuderi, D. R. Hedden, J. A. Maltry, S. M. Traina, M. B. Sheinkop, and M. A. Hartzband, “Early Clinical Results of a High-Flexion, Posterior-Stabilized, Mobile-Bearing Total Knee Arthroplasty. A US Investigational Device Exemption Trial.,” *J. Arthroplasty*, vol. 27, no. 3, pp. 421–429, 2012, doi: 10.1016/j.arth.2011.06.011.
- [14] D. B. Kettelkamp, R. J. Johnson, G. L. Smidt, E. Y. Chao, and M. Walker, “An Electrogoniometric Motion in Normal of Knee Gait,” *J. Bone Jt. Surg.*, vol. 52-A, no. 4, pp. 775–790, 1970.
- [15] K. L. Bennell, D. J. Hunter, and R. S. Hinman, “Management of osteoarthritis of the knee,” *BMJ*, vol. 345, no. 7868, pp. 1–8, 2012, doi: 10.1136/bmj.e4934.
- [16] M. Day and B. R. Wolf, “Medial Opening-Wedge High Tibial Osteotomy for Medial Compartment Arthrosis/Overload,” *Clin. Sports Med.*, vol. 38, no. 3, pp. 331–349, 2019, doi: 10.1016/j.csm.2019.02.003.
- [17] N. Chantarapanich, P. Nanakorn, B. Chernchujit, and K. Sittthiseripratip, “A finite element study of stress distributions in normal and osteoarthritic knee joints.,” *J. Med. Assoc. Thai.*, vol. 92 Suppl 6, no. December, 2009.
- [18] X. Liu, Z. Chen, Y. Gao, J. Zhang, and Z. Jin, “High Tibial Osteotomy: Review of Techniques and Biomechanics,” *J. Healthc. Eng.*, vol. 2019, no. January 2008, 2019, doi: 10.1155/2019/8363128.
- [19] L. Sharma *et al.*, “Varus and valgus alignment and incident and progressive knee osteoarthritis,” *Ann. Rheum. Dis.*, vol. 69, no. 11, pp. 1940–1945, 2010, doi: 10.1136/ard.2010.129742.
- [20] Hcup, “Healthcare Cost and Utilization Project, Agency for Healthcare Research and Quality.” pp. 1–5, 2006.
- [21] J. N. (MD) Insall and W. N. S. (MD), *Surgery of the Knee*, Third edit. Churchill Livingstone, 2001.
- [22] C. Benjamin, “Knee joint replacement - discharge : MedlinePlus Medical Encyclopedia,” *MedlinePlus*. 2021. [Online]. Available:

<https://medlineplus.gov/ency/patientinstructions/000170.htm>

- [23] K. T. Kim, "Unicompartmental knee arthroplasty," *Knee Surgery and Related Research*, vol. 30, no. 1. 2018. doi: 10.5792/ksrr.18.014.
- [24] F. MAR and M. G, *Aging and degeneration: Adult Articular Cartilage*, 2nd editio. England, 1979.
- [25] S. Sabzevari, A. Ebrahimpour, M. K. Roudi, and A. R. Kachooei, "High tibial osteotomy: A systematic review and current concept," *Arch. Bone Jt. Surg.*, vol. 4, no. 3, pp. 204–212, 2016.
- [26] G. M. Marcheggiani Muccioli *et al.*, "Lateral Closing Wedge High Tibial Osteotomy for Medial Compartment Arthrosis or Overload," *Clin. Sports Med.*, vol. 38, no. 3, pp. 375–386, 2019, doi: 10.1016/j.csm.2019.02.002.
- [27] M. Orrego *et al.*, "Medial opening wedge high tibial osteotomy: more than ten years of experience with Puddu plate technique supports its indication," *Int. Orthop.*, vol. 44, no. 10, pp. 2021–2026, 2020, doi: 10.1007/s00264-020-04614-w.
- [28] J. M. Brinkman, P. Lobenhoffer, J. D. Agneskirchner, A. E. Staubli, A. B. Wymenga, and R. J. Van Heerwaarden, "Osteotomies around the knee: Patient selection, stability of fixation and bone healing in high tibial osteotomies," *J. Bone Jt. Surg. - Ser. B*, vol. 90, no. 12, pp. 1548–1557, 2008, doi: 10.1302/0301-620X.90B12.21198.
- [29] K. W. Nha, H. J. Kim, H. S. Ahn, and D. H. Lee, "Change in Posterior Tibial Slope after Open-Wedge and Closed-Wedge High Tibial Osteotomy," *Am. J. Sports Med.*, vol. 44, no. 11, pp. 3006–3013, 2016, doi: 10.1177/0363546515626172.
- [30] S. F. Fucentese *et al.*, "Accuracy of 3D-planned patient specific instrumentation in high tibial open wedge valgisation osteotomy," *J. Exp. Orthop.*, vol. 7, no. 1, 2020, doi: 10.1186/s40634-020-00224-y.
- [31] V. Cimolin and M. Galli, "Summary measures for clinical gait analysis: A literature review," *Gait Posture*, vol. 39, no. 4, pp. 1005–1010, 2014, doi: 10.1016/j.gaitpost.2014.02.001.
- [32] "Clinical Analysis of Instrumented Gait course in Costa Rica."
- [33] R. Di Gregorio and L. Vocenas, "Identification of gait-cycle phases for prosthesis control,"

Biomimetics, vol. 6, no. 2, 2021, doi: 10.3390/biomimetics6020022.

- [34] N. Stergiou, *Biomechanics and Gait Analysis*, AP-Edito. 2020.
- [35] “The Gait Cycle: Phases, Parameters to Evaluate & Technology | Gait Cycle Analysis | Tekscan.” [Online]. Available: <https://www.tekscan.com/blog/medical/gait-cycle-phases-parameters-evaluate-technology>
- [36] “Mokka: Mokka Documentation.” [Online]. Available: <http://biomechanical-toolkit.github.io/docs/Mokka/index.html>
- [37] A. Manuscript, H. T. Alignment, C. L. Affect, L. Tibiofemoral, and C. Forces, “NIH Public Access,” vol. 48, no. 4, pp. 644–650, 2016, doi: 10.1016/j.jbiomech.2014.12.049.How.
- [38] T. Nagura *et al.*, “Increased medially oriented ground reaction force during gait in patients with varus knee osteoarthritis can be treat target to reduce medial compartment loads,” *Osteoarthr. Cartil.*, vol. 22, no. 2014, pp. S122–S123, 2014, doi: 10.1016/j.joca.2014.02.223.
- [39] “TOKA website.”
- [40] “Protocollo di ricerca clinica come da Comitato Etico Area Vasta Emilia Centro Cod. CE AVEC: 623/2019/Disp/IOR.”
- [41] “TOKA Protocol – Appendix 9.”
- [42] M. Ruggeri, “‘Combination of Gait Analysis and Imaging in Knee Biomechanics : the case of HTO.’ Tesi di Laurea Magistrale in Ingegneria Biomedica.,” no. March, p. 135, 2021.
- [43] E. S. Levin, J. C. Mandell, and S. E. Smith, “Do non-weight-bearing knee radiographs for chronic knee pain result in increased follow-up imaging?,” *Skeletal Radiol.*, vol. 50, no. 3, pp. 515–519, 2021, doi: 10.1007/s00256-020-03585-8.
- [44] “Why Weightbearing CT for Orthopaedic Diagnosis_ - Everything Rad.”
- [45] F. Lintz, C. de C. Netto, A. Barg, A. Burssens, and M. Richter, “Weight-bearing cone beam CT scans in the foot and ankle,” *EFORT Open Rev.*, vol. 3, no. 5, pp. 278–286, 2018, doi: 10.1302/2058-5241.3.170066.
- [46] A. Leardini, Z. Sawacha, G. Paolini, S. Ingrosso, R. Nativo, and M. G. Benedetti, “A new

- anatomically based protocol for gait analysis in children," *Gait Posture*, vol. 26, no. 4, pp. 560–571, 2007, doi: 10.1016/j.gaitpost.2006.12.018.
- [47] C. Belvedere *et al.*, "Experimental evaluation of current and novel approximations of articular surfaces of the ankle joint," *J. Biomech.*, vol. 75, pp. 159–163, 2018, doi: 10.1016/j.jbiomech.2018.04.024.
- [48] I. Rizzoli Orthopedics, "Rizzoli Markersets - NaturalPoint Product Documentation Ver 2.1." [Online]. Available: https://v22.wiki.optitrack.com/index.php?title=Rizzoli_Markersets%0Ahttps://v21.wiki.optitrack.com/index.php?title=Rizzoli_Markersets
- [49] V. Agostini, M. Ghislieri, S. Rosati, G. Balestra, and M. Knaflitz, "Surface Electromyography Applied to Gait Analysis: How to Improve Its Impact in Clinics?," *Front. Neurol.*, vol. 11, no. September, 2020, doi: 10.3389/fneur.2020.00994.
- [50] G. S. (Politecnico di Milano), "Foot positioning parameters derived from weight-bearing CT scans : comparison of two segmentation methods and correlation with baropodometric measures," 2022.
- [51] "Protocollo TOKA_V.02_07-10-19 (Clean) - LETTO.pdf."
- [52] M. Ruggeri *et al.*, "Superimposition of Ground Reaction Force on Tibial-plateau Supporting Diagnostics and Post-operative Evaluations in High-tibial Osteotomy. A Novel Methodology," *Gait Posture*, vol. 94, no. February, pp. 144–152, 2022, doi: 10.1016/j.gaitpost.2022.02.028.